2010

Magmatic processes in the Jurassic Bonanza arc: insights from the Alberni region of Vancouver Island, Canada

Benjamin D. (Benjamin David) Paulson
Western Washington University

MAGMATIC PROCESSES IN THE JURASSIC BONANZA ARC: INSIGHTS FROM THE ALBERNI REGION OF VANCOUVER ISLAND, CANADA

by

Benjamin D. Paulson

Accepted in Partial Completion
of the Requirements for the Degree
Master of Science

Moheb A. Ghali, Dean of the Graduate School

ADVISORY COMMITTEE

Chair, Dr. Susan M. DeBari

Dr. Bernard A. Housen

Dr. R. Scott Babcock

MASTER'S THESIS

In presenting this thesis in partial fulfillment of the requirements for a master's degree at Western Washington University, I grant to Western Washington University the non-exclusive royalty-free right to archive, reproduce, distribute, and display the thesis in any and all forms, including electronic format, via any digital library mechanisms maintained by WWU.

I represent and warrant this is my original work, and does not infringe or violate any rights of others. I warrant that I have obtained written permissions from the owner of any third party copyrighted material included in these files.

I acknowledge that I retain ownership rights to the copyright of this work, including but not limited to the right to use all or part of this work in future works, such as articles or books.

Library users are granted permission for individual, research and non-commercial reproduction of this work for educational purposes only. Any further digital posting of this document requires specific permission from the author.

Any copying or publication of this thesis for commercial purposes, or for financial gain, is not allowed without my written permission.

Benjamin D. Paulson

February 23rd, 2010

MAGMATIC PROCESSES IN THE JURASSIC BONANZA ARC: INSIGHTS FROM THE ALBERNI REGION OF VANCOUVER ISLAND, CANADA

A Thesis

Presented to

The Faculty of

Western Washington University

Accepted in Partial Completion

of the Requirements for the Degree

Master of Science

by

Benjamin D. Paulson

February 2010

ABSTRACT

The Early to Middle Jurassic Bonanza island arc on Vancouver Island, Canada, exposes the middle and upper crust of an ancient arc crustal section. The arc is exposed for a length of ~500 km along the west coast of Vancouver Island. The three components of the Bonanza arc represent different crustal levels of magmatism. The deepest level of magmatism is represented by the Westcoast Crystalline Complex, the intermediate level is represented by the Island Intrusions Suite, and the surficial level is the represented by Bonanza Group volcanics. Samples of the volcanic section were collected in the Pemberton Hills region of northern Vancouver Island, the Nootka Sound region in central Vancouver Island, and the Alberni region of southern Vancouver Island. These three localities represent ~400 km of strike length.

The Bonanza volcanics are medium K and calc-alkaline. They range from high-alumina basalt (Al_2O_3 >15 wt.%) to dacite, with 48.5-72.5 wt.% SiO_2 and 4.0-8.7 wt.% MgO. They have a moderate enrichment in the light rare earth elements (LREEs), with abundances 25-90x chondrite with chondrite-normalized $(La/Yb)_n$ values from 4.0 to 14.

Geochemistry of the volcanics was analyzed to document along-strike variations that occur within the Bonanza arc. Examination of specific trace elements and trace element ratios suggests that the Bonanza Arc was influenced by the addition of a sediment component during magma generation, with the greatest influence in the Alberni and Pemberton Hills region. While an altered oceanic basaltic slab fluid signature is present in all portions of the arc, it is less pronounced than the sediment component. However, some of the slab fluid component signature may have been modified by alteration.

Geochemical modeling of fractionation processes (least squares calculations for major elements and Rayleigh fractionation of the REE) and magma mixing were undertaken to evaluate processes that diversify parental melts in the arc. In the Alberni region, where this analysis was focused, the volcanic stratigraphy is divided into two distinct facies: The Red Bed Creek facies and the Klanawa facies. A model that combines both crystal fractionation and magma mixing has moderate success for reproducing compositions in the Klanawa facies, while compositions in the Red Bed Creek facies requires assimilation of country rock, crystal fractionation and magma mixing between primitive melts and silicic melts derived from the Westcoast Crystalline Complex.

ACKNOWLEDGEMENTS

I would like to thank my advisor, Dr. Susan DeBari, for her guidance, assistance and patience over the duration of this study. I would also like to acknowledge the rest of my committee, Dr. Bernard Housen and Dr. R. Scott Babcock for their comments and suggestions that helped to improve this study.

Funding for this study was provided in part by Western Washington University, including support from the Geology Department and the Office of Research and Sponsored Programs (formerly the Bureau for Faculty Research). Additional funding was provided by the Geological Society of America's Graduate Student Research Grant.

Finally I would like to thank Sarah Larson and Tovah Bayer Karl for their assistance in the field.

TABLE OF CONTENTS

LIST OF FIGURES

Appendix Figures

LIST OF TABLES

Appendix Figures

INTRODUCTION

Continental crust is thought to form primarily through the continued accretion of island arc crustal sections (Reymer and Schubert, 1984; Rudnick, 1995). Studies of active island arcs have determined that the magmatic flux derived from the mantle wedge is basaltic (e.g. Kay, 1985; Kay and Kay, 1985), but the bulk composition of continental crust is andesitic (Rudnick and Fountain, 1995). Thus it is important to understand how intermediate and felsic rocks that eventually become continental crust form and evolve within an island arc setting.

The first step in understanding magma evolution is to know the composition of the magmatic flux derived from the mantle wedge (the parental magmas). Island arc subduction zones have four major chemical reservoirs that are tapped as parental magmas are generated: 1) the mantle lithosphere, 2) the subducted basaltic oceanic crust and associated fluids, 3) subducted oceanic sediments, and 4) the upper-plate crust that is assimilated during magma transport (Elliott, 2003).

Trace elements can yield information about the relative contributions of each chemical reservoir (Elliott, 2003). In modern arcs, this technique is employed with the benefit of unaltered glasses and lavas (e.g. Aleutians, Japan, Izu-Bonin) (Kelemen et al., 2001; Kimura et al., 2002; Hochstaedter et al., 2001), but with the limitation that only the uppermost, volcanic portion of island arc crust is accessible. The downside of this approach is that the compositions of volcanic products from island arcs are likely influenced by magmatic differentiation of the original parental source magmas at deeper crustal levels.

To fully understand how basaltic parental magmas diversify, it is imperative that we use not only the volcanic upper island arc crust, but also the associated plutonic rocks that represent the residual magmas from which the volcanic products evolved. In active modern arcs, we generally have no access to the underlying plutonic material. In contrast, in many ancient island arc settings the deeper-seated plutonic sections of the arc have been preserved and are exposed at the surface (e.g. Talkeetna section, Alaska; Kohistan section, Pakistan) (Greene et al., 2006; Clift et al., 2005; and Dhuime et al., 2009, respectively). Thus, examination of ancient island arcs can allow access to products of all levels of arc magmatism. This benefit of access can yield significant insight into the processes responsible for the diversification of parental melts.

The Jurassic Bonanza arc is an excellent example of an exposed island arc crustal section (DeBari et al., 1999; Larocque and Canil, 2009). The mid to upper crust of the arc is exposed, allowing a rare opportunity to study the plutonic crustal roots of the arc and the associated erupted volcanics. The Bonanza arc is located on the west coast of Vancouver Island, with north to south along-strike exposure of over 500 km (Muller, 1977; Carson, 1973). The arc formed from presumed eastward-dipping subduction during the Early to Middle Jurassic (Late Sinemurian to Bajocian) (Armstrong, 1998). The resulting explosive volcanism and comagmatic plutonism formed the Bonanza volcanics (uppermost crust), the Island Intrusions (mid to upper crust), and the Westcoast Crystalline Complex (mid crust) (Isachsen, 1987, DeBari et al., 1999). DeBari et al. (1999) studied the plutonic portions of the Bonanza arc; however, the geochemistry of the volcanics has not been characterized other than in a generalized way to correlate with deeper units in the arc (DeBari et al., 1999).

The primary goals of this study are: 1) to document the range of magma compositions along strike of the arc; and 2) to elucidate the mid-crustal level processes responsible for diversification of parental magmas. To achieve these goals, samples were collected in three localities along the strike of the arc and analyzed for their major and trace element chemistry. Analysis of specific trace element systems in the most mafic rocks provides an opportunity to examine the relative contributions from the four chemical reservoirs and how they vary along the strike of the arc during the generation of the parental melts. Secondly, a thorough analysis of the geochemistry of samples from the southern portion of the arc, coupled with mineral chemistry, is used to elucidate the processes responsible for diversification of magmas in that locality. Given the similarity of differentiated composition throughout the arc, the diversification processes active in the southern part of the arc are likely representative of the entire arc.

GEOLOGIC SETTING

Geologic Setting and Stratigraphy of the Bonanza Arc

The major tectonostratigraphic terranes of Vancouver Island consist of Wrangellia, the Crescent terrane, and the Pacific Rim terrane (Yorath et al., 1999) (Figure 1). Wrangellia comprises the majority of the island, with the Pacific Rim terrane and Crescent terrane representing narrow bands on the west and southern coasts, respectively. The Pacific Rim terrane and the Crescent terrane have been interpreted to be disrupted accretionary wedges (Yorath et al., 1999). This interpretation disputes the conclusion of Brandon (1989) who interpreted the Pacific Rim terrane to be olistostromal mélange. Regardless, both terranes are bordered by, or separated from the Bonanza Arc portion of Wrangellia by crustal penetrative faults which straddle different tectonic and temporal settings (Yorath et al., 1999).

Wrangellia consists of Paleozoic to Mesozoic volcanic, plutonic, and sedimentary rocks. Their stratigraphy is important, given that they form the basement to the Bonanza arc. The Sicker Group is the oldest component of Wrangellia. It has been interpreted as an island arc system (Massey, 1992). The basal member of the Sicker Group marks the Devonian initiation of the Sicker arc. This member consists of pillowed basalts and basaltic andesites, which grade upward into basalt and basaltic andesite flows and pyroclastic flows, suggesting a sub-marine to subaerial progression (Yorath et al., 1999). The upper Devonian member of the Sicker Group and the lower Permian member represent siliciclastic and carbonate sedimentation, indicating a cessation of arc magmatism by the upper Devonian (Yorath et al., 1999). Mississippian to Early Permian

siliciclastic and carbonate rocks of the Buttle Lake Group (Muller, 1980, Sutherland-Brown et al., 1986). Paleozoic units have a total thickness of ~2-5 km.

Overlying the Buttle Lake Group is an ~7 km thick package of tholeiitic basalts (Karmutsen Formation), interpreted most recently as flood basalts from an oceanic plateau (see Greene et al., 2009 and references therein). These basalts occur as a tripartite association of basal pillow lavas overlain by volcaniclastic rocks and capped by subaerial lavas. The Karmutsen Formation is conformably overlain by 650 to 1400 m of upper Triassic carbonates and shales of the Quatsino, Parson Bay, and Sutton members of the Vancouver Group (Yorath et al., 1999).

The Vancouver Group rocks are intercalated with and overlain by the Bonanza arc volcanics and are intruded by Bonanza arc plutons. DeBari et al. (1999) interpret the Bonanza volcanism and comagmatic plutonism during the Early Jurassic (Late Sinemurian) to be due to eastward (west to east) subduction (in present day coordinates) of the paleo-Pacific oceanic lithosphere. Clift et al. (2005) suggests that the Bonanza arc and the Jurassic Talkeetna arc (in Alaska) may represent a continuous subduction zone or the Bonanza arc represents a southern coeval arc.

Jurassic aged plutons (190.3 +/- 1.0 to 186.6 +/- 5.3 Ma) of the Westcoast Crystalline Complex intrude the deepest exposed level of the arc (DeBari et al., 1999) (Figure 2). This unit consists of gabbroic to dioritic plutonic rocks, migmatites, amphibolites, and metasedimentary rocks (DeBari et al., 1999). The Westcoast Crystalline Complex shows assimilation of the Paleozoic Sicker arc rocks and the associated sediments, but there are no clear intrusive contacts with the Karmutsen Formation (DeBari et al., l999). The contacts of the plutonic rocks and the country rock

are typically gradational and concordant to the foliation in the country rock (DeBari et al., 1999).

The Island Intrusions, whose ages overlap those of the Westcoast Crystalline Complex, comprise the middle section of the arc (DeBari et al., 1999) (Figure 2). The Island Intrusions consist of northwesterly aligned batholiths and stocks of hornblende diorite, quartz diorite, tonalite, and granodiorite (DeBari et al., 1999). As reported by Muller et al. (1981) and summarized by DeBari et al. (1999) the lack of gneissic foliation as well as the contact relationships of the Island Intrusions makes them distinguishable from the Westcoast Crystalline Complex. The Island Intrusions have sharp contacts with the Bonanza Group and the Karmutsen Formation (DeBari et al., 1999).

The Bonanza Group volcanic rocks (202-165 Ma) represent the surficial expression of arc magmatism. The Bonanza volcanics are a thick sequence (up to 2,500 meters) (Muller, 1974a; Nixon et al., 1994; Nixon et al., 2005) of lava flows, pyroclastic deposits, and thin interbedded sedimentary rocks and are the focus of this study. The composition of the lava flows ranges from mafic to intermediate, while the tuffs tend to be intermediate to felsic (DeBari et al., 1999, Nixon et al., 1994). Sedimentary rocks are mainly restricted to the lower sections of the Bonanza Group and are fine-grained, marine shales with thin interbedded carbonates. Sedimentary rocks are essentially absent in the higher portions of the Bonanza group suggesting a submarine to subaerial progression (Massey, 1992, Nixon et al., 1994, Nixon et al., 1995, Yorath et al., 1999).

The Bonanza volcanics are unconformably overlain by the Kyuquot Group in the south and the Longarm Group in the north. These units are middle to upper Jurassic sediments with maximum thickness of nearly 800 meters that unconformably overlie the

Bonanza Group (Yorath et al., 1999; Nixon et al., 1994). The Kyuquot Group and the Longarm Group are mostly siliciclastic sediments with variable lithology, including coarse-grained conglomerate, cross-bedded sandy limestone, non-laminated marine shales, siltstone, and fine grained sandstone (Muller et al., 1981). Clastic material was interpreted to be derived from emergent rocks of the Bonanza Arc and transported and deposited in a shallow, near-shore marine setting (Muller et al., 1981).

Deposition of the Nanaimo Group began during the Santonian and continued until the Maastrichtian (85-66 Ma, according to the IUGS) on the eastern side of Vancouver Island (Pacht, 1984). The Nanaimo Group is a thick sequence of marine and nonmarine sediments that Brandon et al. (1988) suggest were deposited in a syn-orogenic forearc basin. The Nanaimo Group contains clasts of quartz diorite that are interpreted (Pacht, 1984) to be derived from the Island Intrusions. These clasts signify that unroofing and exhumation of the Bonanza arc was occurring by 85-66 Ma (Pacht, 1984). Moreover, the Nanaimo Group has sediment derived from Wrangellia, the San Juan and Cascade nappes, and Coast Plutonic Complex which Brandon et al. (1988) has interpreted that these units were together by the Late Cretaceous.

Regional stratigraphic variations within the Bonanza volcanics

The stratigraphic relationships of the Bonanza volcanics vary from south to north. In the following sections, those relationships are described for Southern Vancouver Island (Alberni region), Central Vancouver Island (Nootka Sound region), and Northern Vancouver Island (Pemberton Hills).

Southern Vancouver Island – Alberni Region

In southern Vancouver Island (Figure 3), Yorath et al. (1999) informally divided the Bonanza group volcanics into two stratigraphic members: the basal 'Red Bed Creek facies' and the 'Klanawa facies' (Figure 4). The Red Bed Creek facies appears conformable with the Triassic Parson Bay Formation and consists of a homogenous maroon tuff. Maximum thickness of the Red Bed Creek facies is approximately 750 m (Yorath et al., 1999). The dark maroon tuffs are composed primarily of a coarse ash and tend to form massive, structureless features. Minor interbeds of coarser lapilli tuff consist of 50% well sorted, clast supported, angular to rounded lapilli of dominantly non-vesicular red or green plagiophyric porphyries (Yorath et al., 1999).

Overlying the Red Bed Creek facies is the Klanawa facies. Due to limited exposure, the stratigraphy of the Klanawa facies is poorly understood, although the lithologic variations are well known (Yorath et al., 1999). The Klanawa facies is characterized by plagiophyric pyroclastic deposits and lesser flows of intermediate to felsic compositions. Basalts occur mainly in the northern parts of southern Vancouver Island whereas rhyolites are more abundant in the south, west and upper parts of the succession (Yorath et al., 1999).

Central Vancouver Island – Nootka Sound Region

In the Nootka Sound area on Vancouver Island (Figure 5), Muller (1981) reports that the Bonanza Group volcanics are conformable with the underlying Triassic sediments and consist of maroon and green colored amygdaloidal lava, volcanic breccia, crystal tuff and tuffaceous siltstone. On the shorelines of the Tahsis and Zeballos inlets and the Hecate Channel, there are exposures of dark green and maroon, massive to

agglomeratic lava, with common plagioclase phenocrysts as well as plagioclase-pyroxene crystal tuff, breccia, and rare ignimbrite (Muller et al., 1981). The thickness in this region has been estimated by Jeletzky (1954) to be approximately 600 m, although Muller (1981) suggests that this could be excessive due to faulting in the area. In the Nootka Sound area, the maroon color of the Bonanza group is thought to signify subaerial deposition (Tipper and Richards, 1976), but the presence of interbedded near-shore sedimentary rocks suggests a fluctuation between subaerial and submarine deposition (Muller et al., 1981). The proportion of sedimentary rocks diminishes up section, but more detailed stratigraphy is needed to report any other variations.

Northern Vancouver Island – Pemberton Hills

In northern Vancouver Island (Figure 6), a basal, predominantly subaqueous epiclastic-pyroclastic succession is overlain by a predominantly subaerial succession of mafic to felsic flows and pyroclastic units. The basal units can be correlated laterally, whereas the upper units are more restricted with total thickness estimated to be near 3.5 kilometers (Nixon et al., 1994).

The basal succession is dominated by a sediment-tuff unit and appears to be gradational with the underlying upper Triassic to lower Jurassic siliciclastic siltstones and shales. Distinctions can be drawn between the basal sediment-tuff unit of the Bonanza Group and the underlying sediments based on the increased grain size of the Bonanza Group and the pyroclastic component (Nixon et al., 1994). The basal sediment-tuff unit in the Pemberton Hills is very heterogeneous and the lithology varies widely. Coarse–grained lithologies include heterolithic volcanic conglomerates, thick to medium bedded monolithic volcanic breccias, tuff breccias, and lithic lapilli tuffs. Interbedded finer-

grained lithologies include thinly bedded to laminated tuffaceous sandstone and siltstone, crystal and crystal-vitric tuff, and siliceous siltstones (Nixon et al., 1994).

The middle to upper Bonanza stratigraphy in the Pemberton Hills was described by Nixon et al. (1994) as follows: 400 m of porphyritic to aphanitic mafic to intermediate flows with minor interbedded lithic lapilli-tuffs tuffs which are overlain by 400 m of felsic, welded to non-welded pumice lapilli-tuffs and vitric tuffs. Minor aphanitic to finely porphyritic flows are also present as well as coarse-grained volcanic breccia. 700 m of porphyritic to aphanitic flows with minor lithic lapilli-tuffs, tuff breccias, volcanic conglomerates and sandstones with rare laharic breccias represent the next stratigraphic package. Next a sequence of welded to non-welded lithic lapilli-tuff and tuff-breccias, vitric tuffs (which are locally pumiceous), aphanitic flows and pyroclastic flow deposits are estimated to have a thickness greater than 250 m and less than 600 m. Finally the upper portions of the Bonanza stratigraphy in the Pemberton Hills are represented by greater than 900 m of porphyritic to aphanitic mafic to intermediate flows, which are interbedded with minor lithic lapilli-tuffs, crystal tuffs, tuff-breccias, and volcanic clastic sandstones.

The middle to upper Bonanza stratigraphy in the Pemberton Hills area include mafic to intermediate flows near the top of the aforementioned sediment-tuff unit which Nixon et al. (1994) suggest marks the transition from a predominantly submarine to subaerial transition.

Age of the Bonanza Arc

The age of the Bonanza arc is fairly well constrained through both paleontologic and isotopic techniques (Table 1). The Bonanza arc was long-lived, active between 202 – 165 Ma (DeBari et al., 1999). Whether volcanism was persistent throughout this time or was episodic is open to debate, but the earliest and youngest ages of the Bonanza arc are well known. Muller et al., (1981) report many fossil localities (bivalves and ammonites) from the interbedded sedimentary units of the lower Bonanza strata that yield an age of Early Jurassic (Pliensbachian, 189 Ma to 183 Ma, according to the IUGS). Poulton and Tipper (1991) describe Aalenian (176 Ma to 172 Ma, according to the IUGS) ammonites found in northern Vancouver Island. The oldest radiometric age comes from Friedman and Nixon (1995), who report a (U-Pb, Pb-Pb age of 202 ± 3 Ma for zircon from a rhyolite flow in the Bonanza Volcanics. The Westcoast Crystalline Complex and the Island Intrusions yield zircon ages ranging from 190.3 +/- 0.7 Ma to 168 +/- 5.3 Ma with the majority of the ages between 175 Ma to 168 Ma (DeBari et al., 1999).

PETROGRAPHY OF UNITS WITHIN THE ARC

Samples were collected along the length of the Bonanza arc from the Alberni Region in southern Vancouver Island, the Nootka Sound Region in central Vancouver Island, and the Pemberton Hills in northern Vancouver Island.

Volcanic rocks

A total of 82 volcanic samples were sectioned and analyzed to investigate alteration, phenocryst relationships, textural characteristics, and modal abundance of phases present. Of the 82 samples, 21 are from the Alberni Region in southern Vancouver Island, 16 are from the Nootka Sound Region in central Vancouver Island, and 45 are from the Pemberton Hills in northern Vancouver Island. Table 2 shows a summary of petrographic observations.

As mentioned earlier, Yorath et al. (1999) informally divided the Bonanza Group volcanics in the Alberni Region into two stratigraphic members: the Red Bed Creek facies and the overlying Klanawa facies. The Red Bed Creek facies are petrographically homogenous. They are typically massive, maroon-colored crystal lithic tuffs composed of fine lithic clasts, phenocrysts, and matrix. Euhedral to subhedral phenocrysts of plagioclase (≤ 1mm) average, by volume, about 10-14% of the tuffs. Some of these phenocrysts are fresh, but most show substantial alteration to both calcite and sericite. Mafic phenocrysts are rare, but where they do occur they are pyroxene altered to chlorite, ± biotite altered to chlorite. Potassium feldspar and quartz are also rare <1-1mm subhedral phenocryst phases. Lithic clasts consist mostly of 0.2-0.6 mm angular lithic

(altered andesite) fragments and devitrified volcanic glass. The matrix is mostly ash with opaque disseminated hematite.

The Klanawa facies consists of plagioclase-phyric, basalts, basaltic andesite and andesite lava flows. These flows contain, on average, 60-80% groundmass with phenocrysts of plagioclase, pyroxene, and rare potassium feldspar. Angular lithic (andesitic) fragments (<1-5mm), calcite filled amygdules, and semi-opaque devitrified glass is also present. The majority of the plagioclase in the Klanawa facies occurs as 0.3-1.5 mm tabular, euhedral to subhedral laths, both as phenocrysts and microlites in the groundmass. Some of the plagioclase is altered to sericite and some of the grains are completely replaced by calcite. The majority of plagioclase lacks zoning; however, some of the larger crystals show slight oscillatory zoning. Subhedral to euhedral phenocrysts of pyroxene are typically ≤1mm, but rare, larger crystals (up to 1.5 mm) are present that may contain inclusions of plagioclase. The majority of the mafic phases are altered to chlorite. The rare unaltered pyroxene occurs as a fresh portion or core of pyroxene surrounded by abundant oxides and rims of chlorite. Common accessory minerals for both the Red Bed Creek and Klanawa facies include pyrite, chalcopyrite, apatite, and hematite.

Bonanza volcanic rocks from the Nootka Sound Region in central Vancouver Island do not display the two distinct facies so characteristic of southern Vancouver Island. The unit consists of basalts, basaltic andesites, and andesite porphyries, crystal lithic tuffs, lapilli tuffs, and block and ash flows. As in the Alberni region, many of the rocks have experienced substantial alteration.

Phenocrysts in the porphyries are dominated by plagioclase and less pyroxene, with rare amphibole, +/- biotite, quartz, and potassium feldspar. Plagioclase phenocrysts can be as large as 6-8mm and represent 80% (by volume) of the phenocrysts present. Plagioclase lacks zoning, except in rare cases. Plagioclase alters to sericite, zeolite minerals, clay minerals and calcite. Some plagioclase has been completely replaced by calcite. Plagioclase also occurs as 1-2mm subhedral to euhedral crystals within the groundmass.

The most common mafic phase is pyroxene (0.5-1.5 mm) that makes up at most 15% (by volume) of the phenocryst phases. Other mafic minerals include rare amphibole and biotite that never exceed more than 5% of the phenocrysts. Amphibole occurs as (<1 mm) isolated euhedral crystals. Biotite occurs as 1-2 mm anhedral, elongate crystals that have jagged diffuse edges and are often broken and warped. These mafic minerals are commonly altered to chlorite. Rare metamorphic epidote occurs as partial rims on some of the phenocrysts. Common accessory and alteration minerals for lava flows include pyrite, apatite, zeolites and hematite.

Pyroclastic deposits in the Nootka Sound region contain crystal lithic tuffs, lapilli tuffs, and block and ash flows. Lithic fragments in the pyroclastic rocks are monolithic plagioclase phyric porphyries as described above. The lithic fragments in block and ash flows can be greater than 10 cm in hand sample, but are less than 5mm in the lithic tuffs and are sub-rounded to sub-angular clasts with less than 1mm plagioclase phenocrysts set in an aphanitic ground mass. The phenocrysts in the pyroclastic rocks are less than 1mm broken and angular crystals of plagioclase +/- quartz, potassium feldspar, pyroxene and rare amphibole.

Samples from the Pemberton Hills in northern Vancouver Island are variable in their lithology. They include flows of basalt, basaltic andesite, andesite and rhyolite as well as air-fall tuffs, lapilli tuffs and block and ash flows. Phenocrysts are 20-50% (by volume) of the lava flows. Typical phenocryst assemblages are dominated by plagioclase with less pyroxene and rare biotite, amphibole, and potassium feldspar. Plagioclase is ubiquitous. Plagioclase phenocrysts are 0.3mm to 1.2mm subhedral to euhedral tabular crystals that are typically homogenous, but some larger crystals have oscillatory zoning. Alteration to sericite is common as well as replacement by calcite. Plagioclase is also common as microlites in the groundmass and in some samples plagioclase show a noticeable alignment.

Pyroxene crystals range from 0.3 mm to 1.2 mm subhedral to euhedral crystals. The vast majority of pyroxene is rimmed by chlorite and contains patches of chlorite within the crystal. In some samples, pyroxene is very fresh. Biotite is rare and found in just a few samples. Much of the biotite is altered to chlorite and only some "cores" of biotite can be found. Common accessory minerals include apatite, pyrite, chalcopyrite, hematite and titanite.

Lithic fragments in the block and ash flows and the lithic tuffs are typically plagioclase-rich, sub-rounded to sub-angular, 1mm to 2mm clasts that can reach up to 4cm in the block and ash flows. The plagioclase in the clasts is fresh and make up about 20 to 30% (by volume) of the clasts. In some cases, the clasts have alteration rinds that are characterized by narrow bands which have a reddish tint in plain light and are opaque in polarized light. The matrix of the clasts is aphanitic with plagioclase microlites barely visible.

The felsic flows are often substantially altered. In many cases, the alteration is so great that original mineralogy is unrecognizable under the microscope. Substantial alteration to zeolite and clay minerals is common. Plagioclase, quartz, calcite and zeolite filled amygdaloids dominate the felsic flows.

Intrusive rocks

The intrusive rocks of the Bonanza arc are heterolithic (see DeBari et al., 1999 for full petrographic descriptions). Two representative samples were sectioned for this study, one from the Island Intrusions and one from the Westcoast Crystalline Complex. Island Intrusions sample 91-082 is dominated by feldspar (35% plagioclase, 10% k-spar) and quartz (10%) with mafic phases consisting of biotite (10%), amphibole (15%), pyroxene (15%) and oxide phases (5%). The Westcoast Crystalline Complex sample 93-388 has a similar mineralogy but with a greater proportion of k-spar in the feldspar phases (20%), less quartz (5%) and a slight increase in the mafic phases (biotite (10%), amphibole (20%), and pyroxene (15%).

The majority of the feldspar in the intrusive rocks is plagioclase. Plagioclase occurs as 1-4 mm subhedral to euhedral tabular laths that often display minor oscillatory zoning as well as albite twining. There is a second distribution of plagioclase within the Island Intrusion sample of sub-millimeter euhedral micro-laths. In both occurrences of plagioclase there is some minor alteration of the plagioclase to clay minerals as well as some inter-grown oxide minerals. K-spar in the intrusive rocks (10-20%) occurs as 1-2 mm anhedral to subhedral blocky crystals that are inter-grown between and around plagioclase and the mafic minerals. Biotite (10-15%) is typically altered to chlorite and forms <1-2 mm thin, elongate crystals. Some biotite has grown on rims of amphibole.

Pyroxene (10-15%) is typically unaltered, 1-3 mm subhedral to euhedral crystals, or occurs as anhedral cores of amphibole. Submillimeter crystals of pyroxene are occasionally surrounded by plagioclase. Amphibole crystals (10-15%) are subhedral and often show alteration. The crystals range from 2-4 mm and have abundant oxides within them.

Quartz, apatite, and titanite are also present in the intrusive rocks. The quartz (~5% of the Westcoast Crystalline Complex sample and 10% o f the Island Intrusion sample) occurs as <1 mm-2 mm anhedral blebs that have crystallized between the feldspar and mafic phases. Apatite and titanite both comprise less than 2% of the samples. Apatite occurs as inclusions within other phases, whereas titanite can be seen growing between the dominant phases.

The oxide minerals represent ~5% of the sample and occur as <1 mm-2 mm anhedral clots within the ground mass as well as within and on the edges of the mafic phases.

PETROLOGY AND GEOCHEMISTRY

Analytical Techniques

Mineral compositions were obtained using a 4 wavelength dispersive spectrometer (WDS) JEOL Superprobe 733 electron microprobe at the University of Washington. Energy dispersive spectrometry (EDS) was used in mineral identification before full probe analyses. Compositions were measured from polished slides with a 15 kV accelerating voltage and 3μm beam diameter for the analyses of the feldspar phases and 2μm beam diameter for the analyses of the other phases. A beam current of 10nA was used for feldspar and a 15nA beam current was used for olivine, amphibole, pyroxene and oxide minerals. Peak counting time was concentration dependent, with a 20 sec minimum, 40 sec maximum time, or when 0.4% statistical error was obtained (1 sigma). Analytical error is < 3% relative for major elements and <8% relative for minor elements.

Whole-rock samples were analyzed at the Washington State University (WSU) GeoAnalytical Laboratory by X-ray fluorescence (XRF) for 10 major element oxides and 13 minor elements; and for 19 trace elements by inductively-coupled plasma mass spectrometry (ICP-MS). Preparation techniques and analytical methods for XRF (Johnson et al., 1999) and ICP-MS (Knaack et al., 1994) are available on-line from the WSU GeoAnalytical Lab (http://www.wsu.edu/~geology/geolab/note.html).

Mineral Chemistry of units within the Bonanza Arc

Mineral chemistry (pyroxene, plagioclase, and amphibole) analyzed by microprobe from eight polished samples is reported in Tables 3-5. The samples include three volcanic rocks from the Pemberton Hills in northern Vancouver Island (04-024-A, 04-027-A and 04-034-A), three volcanic rocks from the Alberni Region in southern Vancouver Island (04-004-A, 04-005-A and 04-007-A), a sample of a Westcoast Crystalline Complex diorite and a sample of an Island Intrusions tonalite, both from the Alberni Region (91-082 and 93-338 respectively). Samples from the Alberni region were chosen to represent all levels of the arc crust and results are used in modeling. The volcanic samples represent the shallow levels of arc crust while the Island Intrusion represents the intermediate levels of arc crust and the Westcoast Crystalline Complex represents the deepest level of arc (DeBari et al., 1999). The least-altered samples possible were chosen for analysis.

Pyroxene

Both clinopyroxene and orthopyroxene grains were analyzed, with the majority of orthopyroxene in the intrusive rocks, while the clinopyroxene was found in the volcanic rocks. The clinopyroxenes are dominantly augite (Table 3) and orthopyroxene are iron-rich enstatite. Clinopyroxenes have an average composition of $Wo_{44}En_{42}Fs_{14}$ while Orthopyroxene grains have compositions averaging $Wo_8En_{54}Fs_{38}$.

In the volcanic rocks, the Mg#s (100Mg/[Mg+Fe]) of the clinopyroxene have little variability ranging between 74 and 77. The concentration of Al_2O_3 is restricted between 2.8 and 2.9 wt.%, while the TiO_2 contents are between 0.5 and 0.6 wt.%. Elevated CaO contents also show little variability with concentrations between 21.1 and

21.7 wt.%. The clinopyroxenes have moderate amounts of FeOt (8.0 to 9.2 wt.%), elevated MgO (14.5 to 15.0 wt.%) and low Na_20 (0.3 to 0.4 wt.%) and MnO (0.2 to 0.3 wt.%).

In the intrusive rocks, the Mg#s of the orthopyroxene are lower than that of the volcanic rocks and are in the range 55-61. The concentration of Al_2O_3 is slightly lower than the clinopyroxene of the volcanics with concentrations from 1.6 to 2.2 wt.% with the exception of one sample that has an Al_2O_3 concentration of 3.4 wt.%. The orthopyroxene of the intrusive rocks have lower CaO contents (1.5 to 9.5 wt.%) but much greater amounts of FeOt (16.5 to 22.5 wt.%) compared to the pyroxene of the volcanic rocks.

Plagioclase

Plagioclase is ubiquitous in every sample. Anorthite contents ranged from almost pure albite to An_{70} (Table 4). The pure albite phase can be found in almost all the volcanic samples from the Alberni region and is probably a result of the low grade metamorphism that many of the volcanics have experienced. Anorthic plagioclase was more common in the Klanawa facies, the Pemberton Hills region of northern Vancouver Island, as well as within the intrusive samples. The compositional variation of the plagioclase feldspars can be seen in Figure 7.

Minor amounts of SrO were present in all plagioclase grains, with concentrations below 0.25 wt.%. One plagioclase from 04-004-A had 0.45 wt.% SrO, almost twice as much as any other plagioclase. The concentration of FeOt was predominantly low in all samples; typically less than 2.13 wt.% with the exception of one plagioclase in 04-034-A that was anomalously enriched with 8.80 wt.% FeOt.

Amphibole

Amphibole (Edenite) was analyzed in both the volcanic and intrusive rocks. Amphibole has similar chemistry regardless of being an intrusive amphibole or a volcanic amphibole (Table 5).

The Mg#s of amphiboles range from 55 to 75 while the majority of samples have Mg#s from 60 to 64. Amphiboles from the Bonanza arc have moderate Al_2O_3 contents (4.1 to 7.3 wt.%), low Na_2O (0.4 to 1.4 wt.%), low K_2O (0.3 to 0.7 wt.%) and elevated CaO (10.3 to 21.3 wt.%). Amphibole has a fairly restricted range of MgO (9.3 to 14.3 wt.%) with greater variability in FeOt contents (8.0 to 20.2 wt.%).

Whole-Rock Geochemistry

The Bonanza volcanics range from basalt to dacite with SiO_2 contents from 48.5 to 72.5 wt.% (Table 6). The majority of the samples (>60%) fall within the medium-K series with a smaller subset in the high-K field. Based on petrographic observations (e.g. 04-003-F), the high-K samples probably have excess K as a result of alteration (Figure 8). The majority of samples are calc-alkaline on an AFM diagram (Figure 9).

In both the north and the south, basalt, andesite and dacite were present, but the range of composition was more restricted in the central portion of the island (Figure 10). The SiO_2 contents from the central portion of Vancouver Island range from 52-55 wt.% compared to the north and south where the SiO_2 contents range from 48.5-73 wt.%.

The basaltic end members of the Bonanza volcanics are high-alumina basalts (Al_2O_3 >15 wt.%) with MgO contents from 4.0 to 8.7 wt.%. Harker diagrams (Figure 10) show that the basalts have decreasing Al_2O_3, CaO, MgO, FeO_t and TiO_2 with increasing SiO_2, whereas K_2O and Na_2O are more scattered. The Mg#s (100Mg/[Mg+Fet]) are moderate (44-62) and generally decrease with increasing SiO_2. The most primitive sample (04-036-A) was collected in northern Vancouver Island and has 8.7 wt.% MgO, 136 ppm Ni and 338 ppm Cr and Mg# of 62.

Basalts from the different regions of the Bonanza arc show little difference in major elements for a given SiO_2 content; however some of the samples from the central portion of the arc are slightly more primitive, with elevated Mg#s, MgO contents, and concentrations of Ni and Cr compared to the north and south.

Whole-rock chemistry of andesite and dacite in the Bonanza arc show trends similar to the basalt. Andesite and dacite range from 0.5 to 7.0 wt.% MgO. As with the

basalts, the andesite and dacite of the Bonanza volcanics show decreasing Al_2O_3, CaO, MgO, FeO_t and TiO_2 with increasing SiO_2. The K_2O content increases with increasing SiO_2, while the Na_2O contents don't show a discernable trend. The Mg#s in the andesites and dacites are typically lower than the basalt (6-40). The majority of the andesites have Mg#s that range from 42-55 while the dacites have Mg#s between 27 and 55. Andesite and dacite analyzed from the northern and southern portions of the Bonanza arc are indistinguishable with respect to major element chemistry.

Trace elements of the Bonanza volcanics are plotted against wt.% SiO_2 in Figure 11. There is much more scatter in trace elements than major elements, but some trends are still clearly visible. The concentrations of Ni and Cr are generally low for all samples (< 50 ppm and <100 ppm, respectively), although some samples have elevated Ni and Cr contents (e.g. 04-036-A) There is a general decrease of Ni and Cr contents with increasing SiO_2. Incompatible elements such as Rb, Th, Ta, U, and Zr all increase with increasing SiO_2; but mobile elements such as K_2O and Ba do not show reliable trends due to extensive alteration. The trace element Sr shows a systematic decrease with SiO_2 from 670 ppm to 62 ppm which is likely related to Ca-rich plagioclase fractionation. The trace element V and also has a systematic decrease with SiO_2 from 375 ppm to 98 ppm.

On a Mid Ocean Ridge Basalt (MORB) normalized multi-element spider diagram (Figure 12), the Bonanza volcanics are characterized by high concentrations of large ion lithophile elements (LILE) Cs, Rb, Ba, Th, Pb, and Sr, with lower concentrations of the high field strength elements (HFSE) Nb, Ta, Zr, Hf, and Y. Concentrations of the trace elements, in general, tend to be indistinguishable for samples from the northern and

southern regions of the Vancouver Island; but samples from the central region tend to have lower incompatible trace element concentrations.

The rare earth element (REE) chemistry of the Bonanza volcanics is shown in chondrite normalized multi-element diagrams (Figure 12). The majority of the trends show moderate enrichment in the light rare earth elements (LREE's), with abundances 25-90x chondrite with chondrite-normalized $(La/Yb)_n$ values from 4.0 to 14.0. La/Yb is not correlated with SiO_2.

Samples from the northern and southern part of the arc are indistinguishable. The chondrite-normalized $(La/Yb)_n$ for samples in the north range from 4.1-14.0 and samples from the south have values between 4.3-12.9 with the majority of the samples greater than 6.0. The LREEs are represented by chondrite-normalized $(La/Sm)_n$ and range from 1.6-4.0 in the north and from 1.6-2.9 in the south. The HREEs are represented by chondrite-normalized $(Dy/Yb)_n$ with values from 0.5-2.6 in the north and 0.6-2.7 in the south.

Samples from the central part of the arc show lower total REE abundances than in the north or south, as well as flatter REE patterns, with chondrite-normalized $(La/Yb)_n$ below 6.0 in all but one sample. The lower $(La/Yb)_n$ is a result of lower light REE abundances with $(La/Sm)_n$ = 1.4-2.1. Heavy REE element ratios are similar to the north and the south with chondrite-normalized $(Dy/Yb)_n$ values from 0.7-2.0.

DeBari et al. (1999) report that the geochemistry of volcanic rocks of the Bonanza arc are indistinguishable from the plutonic rocks of the Island Intrusions. However, new observations from this study suggest that some of the volcanic rocks have different REE characteristics and modal mineralogy than the Island Intrusions. In the Alberni region in

the south, the Island Intrusions tend to have a more concave down pattern in the REEs (Figure 13) as well as lower concentrations of REEs compared to the volcanic rocks of the Klanawa Facies of the Bonanza volcanics. Moreover, the Island Intrusions and the Westcoast Crystalline Complex are amphibole-rich and the volcanics are amphibole-poor.

DISCUSSION

Along-strike variations in major and trace elements

Samples were collected in the southern, central, and northern portions of the arc (~400 km) in an effort to document any along-strike variations in geochemistry. Careful examination of the specific major and trace elements will allow for insights into the relative contribution of the subduction components within the Bonanza arc. Major elements, trace elements and trace element ratios are plotted against latitude in Figure 14.

In the central portion of the arc (Nootka Sound region) there is very little major element compositional variation. Samples were collected over many kilometers and represent more than 200 m of volcanic stratigraphy (Figure 5), so sampling bias is not likely. Conversely, there is wide variation in the major elements for both the Pemberton Hills region in the north and the Alberni region in the south, although much of this variation correlates with varying SiO_2 contents.

For all regions of the arc, the most mafic samples have Al_2O_3 and MgO concentrations between 18-21.5 wt.% and 3.5-8.6 wt.%, respectively. There is little variation in concentrations of CaO, Na_2O and K_2O; while FeO_t tends to be slightly

elevated in the southern region (up to 11.3 wt.%) compared to the north and the central regions (8.2 – 9.7 wt.%).

As with the major elements, the trace elements and trace element ratios show very little variation in the central portion of the arc. Behavior of the trace elements, in general, is similar for the northern and southern portions of the arc and is mostly indistinguishable from either region. However, some of the trace elements in the central portion of the arc show trends distinct from the northern and southern region. For example, Cr and Ni concentrations are higher in the central part of the arc, suggesting more primitive compositions than in the north or south (except for the primitive northern sample 04-036-A) (Figure 14). Additionally, samples in the central region have a lower enrichment in the LREEs and have lower Zr and Hf. Concentrations of Nb, Ta, Th, and U are also lower compared to rocks from the north and the south with comparable SiO_2 values, including the most mafic samples.

Relative variations in the subduction component

Differentiation, assimilation, and alteration can affect the geochemical signatures of arc derived rocks, so it is important to pay careful attention to the most mafic, least altered samples. To limit the effects of differentiation and assimilation only the most mafic samples (SiO_2 <54 wt.%, MgO >4 wt.%) are examined. Examination of alteration is shown in Figure 15.

Trace elements can be broadly classified as being either mobile or immobile in fluids. The trace element Nb is very immobile in fluids and is used to examine alteration. Both K and Ba are mobile in fluids. Plots of K and Ba against Nb (Figure 15) show

mostly scatter with no clear pattern. Thus, they cannot reliably be used to interpret subduction input. Conversely, Ta and Zr are fluid immobile. When they are plotted against Nb (Figure 15), a clearly defined linear pattern emerges. Both La and Th are plotted against Nb to examine the alteration and a linear trend is clearly visible. Samples that deviate too far from this trend were considered unreliable and were eliminated from further consideration.

Keeping this trace element reliability in mind, we have compared trace element ratios in the most mafic rocks that are proxies for particular geochemical reservoirs. Both Th/La and Th/Nd can be used as proxies to trace sediment melt incorporated in the arc lavas (Singer et al., 2007; Class et al., 2000). In depleted MORB mantle, Th/La is 0.042 and Th/Nd is 0.013 (Workman and Hart, 2005) and is used as a baseline of what samples would be if there were no involvement of sediments during melting (Figure 16).

To evaluate the contribution from a slab fluid (hydrous fluid due to dehydration subducted sediment and altered oceanic MORB), trace element ratios of both Pb/Ce and Ba/La can be used (Singer et al., 2007; Elliott, 2003; Class et al., 2000). As with the previous ratios, the Pb/Ce and Ba/La values from the arc are compared to the depleted MORB mantle source values (Figure 16) (0.03 for Pb/Ce and 2.93 for Ba/La) (Workman and Hart, 2005).

In Figure 16, only samples with less than 54 wt.% SiO_2 and greater than 4 wt.% MgO are plotted. As Figure 16 shows, the values for all the ratios are above the depleted mantle base-line. This indicates that varying amounts of slab fluid and sediment melt must be a factor in all regions of the Bonanza arc, with considerable over lap with the samples from the northern and southern regions of Vancouver Island.

Figure 17 shows four plots that further evaluate the contribution of slab fluid and sediment melt component to volcanic rocks of the Bonanza Arc. In Figure 17, Th/Nb ratios that represent the sediment melt component are plotted on the X-axis while the trace element ratios that represent the slab fluid component (Ba/Th, Cs/Th, Pb/Ce, and U/Th) are plotted on the Y-axis. The Bonanza volcanic samples utilized in this plot all have <58 wt.% SiO_2.

The tan and purple regions superimposed on Figure 17 were created using data from Bryant et al. (2003) and references therein. The tan region represents data from the Izu arc system, while the purple region represents data from the Mariana arc system. The Izu arc system has been interpreted to have a strongly enriched slab fluid signature (Bryant et al., 2003; Bryant, 1999; Elliot et al., 1997) while the Mariana arc system has been interpreted to have a strongly enriched sediment melt signature (Bryant, 1999).

As shown in Figure 17, the vast majority of samples from the Bonanza volcanics fall in the same field defined by the Mariana data. The trace element ratios that represent slab fluid signature are low for the most of the samples from the Bonanza Arc. Ba/Th values are less than 400 for all but two samples and ranges between 102 and 322 in the northern and southern regions of Vancouver Island. Ba/Th is much more variable in the central region with values as low as 76 and as high as 1166. Values of Cs/Th display little variability for the southern region and range between 0.2 and 0.8. The values of Cs/Th for the northern and central regions are much more variable and range from 0.1 to 2.5 in the north and 0.1 to 5.2 in the central regions. Values for both Pb/Ce and U/Th show moderate variability for all regions of the arc. In the south, Pb/Ce ranges from 0.07 to 0.17 while U/Th ranges from 0.27 to 0.30. In the central region Pb/Ce ranges from

0.05 to 0.40 and values of U/Th are between 0.29 and 0.50. The northern region has values of Pb/Ce between 0.08 and 0.13 and values of U/Th between 0.29 and 0.46.

The low values of Ba/Th, Cs/Th, Pb/Ce and U/Th for most samples suggest that the hydrous slab fluid component had only a minor influence on the Bonanza volcanics regardless of region. The sediment melt component seems to have the greater influence on the chemistry of the Bonanza volcanics with the greatest influence from the sediment melt component in the Pemberton Hills. However, as shown with Ba, the trace element ratios used as tracers of the fluid component have likely been affected by alteration.

Volcanic samples from the Bonanza arc are compared to samples from other major arc systems in Figures 18 and 19. In both figures, La/Sm is normalized to chondrite and plotted against Ba/Th (in Figure 18) and Th/Nb (in Figure 19). Data used to define the fields for other major arc systems comes from Elliot (2003) and references therein. Elevated Ba/Th, like those in the Izu arc system, would suggest that the slab fluid component contributes to the generation of arc magmas. As in Figure 17, samples from the Bonanza arc have a relatively low Ba/Th value which, as seen in figure 16 suggests that the role of the slab fluid component in the Bonanza volcanics was minor.

Both $(La/Sm)_n$ and Th/Nb are tracers of a sediment melt component. Volcanic samples that have a sediment melt signature would define a linear array on Figure 19 that would have a varying slope depending on the amount of sediment melt involved; the further the values are from the origin, the greater the contribution from the sediment melt component. Samples with low amounts of the sediment component would plot near the MORB field in Figure 19. Volcanic samples from the Bonanza arc define a linear field

with values that have a moderate distance from the origin. This suggests a limited, but important role, of the sediment melt component.

In summary, the sediment melt component has a greater influence on the compositions of the Bonanza volcanics than the slab fluid component, but some of the slab fluid signature may have been lost due to alteration. While the sediment melt component has only a moderate contribution, it was a factor in all regions of the Bonanza arc and is most pronounced in the Alberni and Pemberton Hills regions. While it is possible that the variations observed could be due to a lack of continuity in the arc system, it does not seem likely. Varying degrees of a sediment melt component would be reasonable over 500 km and is observed in modern arcs (e.g. Aleutians, Jicha et al., 2004).

Diversification of magmas in the Bonanza arc

The previous section describes sources that contributed to generation of parental magmas in the Bonanza arc, whereas this section describes how those magmas diversified within the arc crust.

Field evidence described by Muller and Carson (1969), Muller et al. (1974a), Muller et al. (1981), Isachsen (1987), and DeBari et al. (1999) suggests that partial melting of the mid to deep crust, as represented by the migmatized parts of the Westcoast Crystalline Complex, was ubiquitous in the Bonanza arc. Observations of abundant leucosomes within the migmatized amphibolite-rich country rock of the Westcoast Crystalline Complex suggest that melting of the country rock played an important role in the evolution of the magmas that fed the Island Intrusions and the Bonanza volcanics.

Features include tonalitic to trondhjemitic leucosomes with gneissic to agmatitic textures mixed with amphibolite melanosomes (DeBari et al., 1999).

As described above, the northern and southern regions of the Bonanza arc show a wider range of volcanic compositions than the central region (greater diversification, Table 6), and there are no significant compositional differences between the north and the south. Given this similarity, magmatic processes responsible for differentiation of mafic to felsic lavas was investigated using magma compositions from the Alberni region in the south. There is better stratigraphic control in the volcanic rocks of the Alberni region compared to the Pemberton Hills area in northern Vancouver Island.

There are several models used to understand magmatic processes responsible for the diversification of parental magmas. This study specifically evaluates three models: (1) Simple crystal fractionation of a primitive, mantle-derived magma to a more differentiated composition, (2) magma mixing between primitive, mantle-derived mafic magmas and felsic leucocratic phases derived by partial melting of the Westcoast Crystalline Complex, and (3) crystal fractionation coupled with mixing of leucocratic phases derived from the Westcoast Crystalline Complex.

Crystal fractionation in the volcanic rocks can be examined by use of least-squares calculations for major elements, and Rayleigh fractionation models for trace elements. In the Alberni region of Vancouver Island, the goal was to use least-squares calculations to examine the relationship of more primitive compositions and compare those to more evolved compositions. Moreover, least-squares calculations quantify and constrain the relative proportions of crystal and liquid phases that can be compared to observed modal abundances.

Inputs to the least squares calculations include major element compositions of parent and daughter magmas and composition of fractionating minerals observed (Tables 7-10). The most primitive sample analyzed in the Alberni region was chosen as the parent magma (48.45 wt.% SiO_2, 6.49 wt.% MgO, 50.7 Mg#). Daughter compositions selected for the least-squares analysis have lower wt.% MgO, lower Mg#, higher wt.% SiO_2, compared to the parent composition and are representative of other evolved samples from this segment of the arc.

Mineral compositions used in least-squares calculations of fractionated pyroxene, plagioclase and oxide phases were obtained by electron microprobe analysis. No fresh olivine samples were analyzed, thus the composition used was based on expected compositions for calculated Mg#.

Least-square solution outputs include the total percent crystallized, proportions of fractionated minerals, and residuals for each major element oxide. Outcomes of least-squares calculations can be seen in Tables 7-10.

Step 1: basalt to basaltic andesite

Both the parent and the daughter are from the Klanawa Facies of the Alberni region and are representative of other samples from this facies (Figure 20). Sample 04-005-A, a basalt, was chosen as the parent composition based on its relatively high Mg# (50.6), low SiO_2 content (48.45 wt.%) and lower REE abundances. Sample 04-007-A, a basaltic andesite, was chosen as the daughter composition because of its lower Mg# (46.0), higher SiO_2 content (52.58 wt.%) and higher abundances of REE relative to 04-005-A (the parent).

Possible fractionating minerals include cpx + plag + sp + ol + amph (abbreviations defined in Table 7). Least-squares solutions for Step 1 (Table 7) indicate 53.3% crystallization with crystallizing proportions as follows: 17.2% pyroxene, 54.8% plagioclase, 5.2% amphibole, 9.4% spinel, and 13.5% olivine. This calculated modal abundance of crystallizing phases does not correspond to the observed modal abundances of the volcanic rocks. The volcanics from the Alberni region tend to lack olivine and typically have only pyroxene and amphibole as their major mafic phase. A value of 53.3% crystallization is large amount of crystallization for evolution of a basalt to basaltic andesite, suggesting that more processes than fractional crystallization are responsible for diversification of the volcanics.

A validity test for the least-squares calculations of major elements is Rayleigh modeling of trace element fractionation. The Rayleigh equation is $C_L/C_o=F^{(D-1)}$ where C_L is the concentration of a trace element in the fractionated melt, C_o is concentration in the parent melt, F is melt fraction, and D is bulk distribution coefficient. The Rayleigh fractionation equation is effective in predicting trace element behavior in co-magmatic systems by relating the modal mineralogy, associated crystal/liquid partition coefficients, and degree of crystallization.

As shown in Figure 21, the Rayleigh fractionation equation is used to model progressive crystal fractionation of the parent (04-005-A). To see how the REE concentrations change with progressive crystallization, the modeled REE concentrations are compared to observed REE concentrations of the daughter (04-007-A). The crystallizing phases used are cpx + plag + sp + ol + amph, which are the outputs from the

least-squares calculations. The distribution coefficients used are from Rollinson (1993) shown in Appendix Table 11.

For the Rayleigh fractionation model, the values of *F* (melt fraction remaining) are step-wise and happen in 20% crystallization increments with the percentage of crystallizing phases set as 17.2% pyroxene, 54.8% plagioclase, 5.2% amphibole, 9.4% spinel, and 13.5% olivine. The Rayleigh fractionation model consistently produces increasing REE concentrations with increasing values of *F* while REE pattern slopes remain nearly parallel (Figure 21).

By 40% crystallization, the modeled concentrations of the REEs are already higher than the observed daughter, and with progressive crystallization are well above the observed abundances of the daughter by 50% crystallization. Thus, the 53.3% crystallization predicted by least squares cannot be realistic. Differentiation processes must be more complex than simple crystal fractionation.

To satisfy the constraints of major and trace elements, an alternative hypothesis to simple crystal fractionation was tested. This hypothesis incorporates a combination of crystal fractionation and magma mixing. To test this hypothesis, a leucosome from the Westcoast Crystalline Complex (91-039d), and interpreted as a partial melt of pre-existing crust, is mixed with the parent basalt composition (04-005-A). This leucosome is a leuco-granite with a mineralogy consisting of dominantly quartz, plagioclase, and lesser amounts of biotite, amphibole and k-spar. The leucosome has a Mg# of 30.4, 71.6 wt.% SiO_2, and a LREE-enriched and depleted concave up HREE pattern (Figure 22) (DeBari et al., 1999).

A hybrid liquid of comprised of a mix between 15% of the leucosome 91-039d and 85% of the parent 04-005-A was progressively crystallized. Figure 22 shows the REE concentrations of the residual liquid after 40% crystallization of the hybrid magma. The leucosome mixing is effective at lowering the over all concentration of the REE and the modeled concentrations of the REEs match very closely with the observed concentrations of the REEs from the daughter.

Comparisons of the major elements for the various models are shown in Figure 23. Major element concentrations in the residual liquid after 53.3% crystallization of the parent basalt match closely with the observed concentrations of the daughter (Figure 23). However, as discussed above, the concentration of the REEs are far too high to be explained solely by progressive crystallization. Major element concentrations of the hybrid liquid after 40% crystallization are also compared to the daughter in Figure 23. This crystallized hybrid magma is produced when 15% of leucosome 91-039d is mixed with 85% of mafic parent 04-005-A and then crystallized 40%. As shown in both Figure 22 and 23, the crystallized hybrid does a better job approximating both major element and REE concentrations of the observed daughter than just fractional crystallization.

There are some major elements that do not match well in either scenario. In the mixing scenarios, the concentrations of MnO and P_2O_5 are problematic. Modeled concentrations are higher than the observed concentrations for P_2O_5 and lower for the observed concentrations of MnO. In the case of P_2O_5, the increase in concentration is a consequence of the incompatibility of P_2O_5 with the phases modeled. The presence of apatite as an accessory phase is fairly common in the volcanics, and is likely the host for excess P_2O_5. The concentration of MnO is modeled to be zero by 40% crystallization and

has negative concentrations with increased fractionation. Mixing these negative concentrations produce artificially lower concentrations in the various mixing scenarios.

Step 2: basaltic andesite to andesite

Many of the volcanics sampled are of more evolved compositions than just basalt and basaltic andesites. In an effort to understand the processes responsible for the most evolved compositions, it is important to look at various compositional steps along the way.

Sample 04-007-A, a basaltic andesite from the Klanawa Facies and the daughter composition from step 1 above, is the parent composition for step 2. Sample 04-003-E, an andesite from the Red Bed Creek facies, was chosen as the daughter composition because of its lower Mg# (40.76) and increased SiO_2 content (59.9 wt.%). However, unlike the previous step, REE abundances are *lower* in the daughter relative to the parent, a typical feature (although not ubiquitous) in the Red Bed Creek facies.

Mineral assemblages used in the calculations include cpx + plag + sp + amph. Least-squares solutions are shown in Table 8 and predict 79.1% crystallization with the proportions of crystallizing phases as: -12.1% pyroxene, 55.3% plagioclase, 51.9% amphibole and 5.0% spinel. A negative pyroxene is problematic and is indicative of a failed fractionation model. A less likely scenario would be that pyroxene is being resorbed by the magma.

As in the previous step, the Rayleigh fractionation model was again used to examine the behavior of the trace elements. Figure 24 shows that with increasing fractionation of 04-007-A, the trace element concentration increases rather than

decreases. Clearly, crystal fractionation cannot be solely responsible for this second stage of differentiation.

In an effort to produce the daughter composition, magma mixing was also employed. The leucosome phase, 91-039-d was mixed in various proportions with the parent 04-007-A and the results are shown in Figure 25. In all mixing scenarios, the concentrations of the trace elements decrease with increasing proportions of the leucosome phase. However, even when the proportion of the leucosome phase is increased to 40% of the hybrid composition, the trace element concentrations are not low enough to match the observed concentrations of the daughter.

Clearly neither fractional crystallization nor magma mixing are sufficient to explain the production of the Red Bed Creek facies from the Klanawa facies. The results from these models suggest that two distinct processes are at work, or two different sources exist for the Red Bed Creek facies and the Klanawa facies of the Bonanza Volcanics. A closer examination of the Red Bed Creek facies is discussed in a later section.

2nd Try, Step 2: basaltic andesite to andesite

Decreased REE with increased SiO_2 was the factor that caused failure in modeling Step 2 above (basaltic andesite of the Klanawa facies to the andesite of the Red Bed Creek facies). However, as seen above, not all samples within the Red Bed Creek facies have such low REE abundances. More felsic samples with higher REE abundances as modeled in Step 3 (below) also exist (type 2). This step models differentiation of sample 04-007-A, the same basaltic andesite from the Klanawa Facies used in Step 2, to produce sample 04-004-A, a higher REE dacite from the Red Bed Creek facies, and the same

sample used in Step 3. Sample 04-004-A also has a lower Mg# (27.4) and increased SiO_2 content (65.41 wt.%) compared to 04-007-A. As in Step 2, the REE abundances of the daughter are lower relative to the parent, but not as low as the daughter in Step 2.

Mineral assemblages used in the calculations are cpx + plag + sp + amph. Least-squares solutions are shown in Table 9 and predict 79.5% crystallization with the proportions of crystallizing phases as: 9.2% pyroxene, 62.1% plagioclase, 23.4% amphibole and 5.3% spinel. The calculated modal abundance of crystallizing phases are reasonable for the more felsic plutonic rocks of the Bonanza arc, but again as in step 1, do not correspond to the observed modal abundances of the volcanic rocks.

As shown in Figure 26, the Rayleigh fractionation equation is used to model progressive crystal fractionation of the parent (04-007-A). The modeled REE concentrations are compared to observed REE concentrations of the daughter (04-004-A). The phases used are the same as the solutions to least squares model. The Rayleigh fractionation model consistently produces increasing REE concentrations with increasing values of *F* while REE pattern slopes remain nearly parallel (Figure 26), in contrast to the observed daughter.

As before, in an effort to produce a more evolved composition with lower REE abundance, magma mixing was tested. Leucosome phase (91-039d) was mixed with the parent basaltic andesite composition with the results shown in Figure 27. A hybrid liquid from a mix of 75% basaltic andesite (04-007-A) with 25% leucosome (91-039d) has acceptable results for the middle and heavy REEs, but there is divergence between the LREEs. Moreover, the major elements of the calculated hybrid liquid are dissimilar to the observed daughter composition (Figure 28).

As in step 1, a combination of mixing and fractional crystallization was employed but with limited success. Figure 29 shows the results of a combination of 50% leucosome 91-039d with 50% basaltic andesite parent 04-007-A, which was progressively crystallized. There is some agreement in the REEs between the calculated hybrid liquid and the observed daughter composition. However, mixing of 50% leucosome and 50% basaltic andesite is physically difficult and decreasing the proportions of leucosome phase will produce REE abundances that are all too high.

Step 3: andesite to dacite

Although production of basaltic andesite from the Klanawa facies to the low REE andesite from the Red Bed Creek facies was not successful, it is appropriate to model differentiation within the felsic Red Bed Creek facies as Step 3. Sample 04-003-E, an andesite from the Red Bed Creek facies (the daughter composition from step 2 above), is the parent composition for step 3. Sample 04-004-A, a typical dacite from the Red Bed Creek facies, was chosen as the daughter composition because of its lower Mg# (27.3) and increased SiO_2 content (65.41 wt.%).

Phase assemblages include cpx + plag + sp + amph. Least-squares solutions are shown in Table 10 and predict 43.3% crystallization with the proportions of crystallizing phases as 36.7% pyroxene, 57.0% plagioclase, 2.8% amphibole, and 3.5% spinel. It should be noted that there is a very large R^2 (7.47) associated with these solutions, but the majority of the error is associated with the big difference in the amount of Na_2O between the parent (0.2 wt.% Na_2O) and the daughter (3.1 wt.% Na_2O). The difference in the amount of Na_2O is likely associated with alteration. However, ignoring the errors associated with the Na_2O, the predicted crystallization of 42.9% is reasonable.

As in previous steps, the Rayleigh fractionation equation was used to examine the behavior of the trace elements. As shown in Figure 30, at 40% crystallization there is nice agreement in the middle REEs, but some divergence in both the heavy and light REEs.

Assimilation in the Red Bed Creek Facies

As seen in Step 2 above, the more felsic Red Bed Creek facies could not be produced from the Klanawa facies by fractional crystallization and/or magma mixing of primitive melts and leucosomes. The Klanawa facies tend to be porphyritic flows while the Red Bed Creek facies are more pyroclastic. It is reasonable to assume that different processes are at work to produce the different facies. As discussed in a previous section and shown in Figure 2, the Red Bed Creek facies represents the initial volcanic activity in the Alberni region of the Bonanza arc. The Klanawa facies represents a transition from the pyroclastic nature of the Red Bed Creek facies to a series of porphyritic flows.

Examination of the REE patterns of the Red Bed Creek facies shows considerable variability, unlike the Klanawa facies, which tend to have similar patterns with varying concentrations. The variability of the REE concentrations in the Red Bed Creek facies is comparable to the variability of the REEs of the leucosomes in the Westcoast Crystalline Complex (Figure 31). It is reasonable to assume that the leucosomes (as partial melts within the crust) played an important role in the generation of the magmas from the Red Bed Creek facies. Magma mixing, fractional crystallization and assimilation were all examined in an effort to produce the observed compositions of the Red Bed Creek facies.

The least felsic sample from the Red Bed Creek facies is an andesite (sample 04-003-E), with 59.9 wt.% SiO_2. Fractional crystallization of the most primitive sample from the Klanawa facies (04-005-A) could not produce this Red Bed Creek andesite, nor could magma mixing between the primitive sample and a leucosome composition from the Westcoast Crystalline Complex (91-039d). Fractional crystallization of the most evolved sample from the Klanawa facies (sample 04-007-A) also did not successfully reproduce the Red Bed Creek andesite.

A combination of magma mixing between the most primitive sample of the Klanawa facies (04-005-A) and the leucosome phase (91-039d), coupled with assimilation of a basaltic andestie from the Sicker Group (92-284) produced results that are close to the observed composition of the Red Bed Creek facies andesite (04-003-E) as show in Figure 32. While the light REEs and the heavy REEs have nice alignment, there is some divergence with respect to the middle REEs.

A model for diversification of magmas within the Bonanza arc

A time-integrated, petrogenetic model (Figure 33) for the generation of the volcanic rocks in the Alberni region of Vancouver Island requires different processes to produce the two distinct facies of the Bonanza volcanics. The Red Bed Creek facies are a series of pyroclastic flows deposited conformably on the Vancouver Group. Over-lying the Red Bed Creek facies are a series of porphyritic flows of the Klanawa facies (Figure 4).

As discussed above, some component of crustal melt is required to replicate the observed intermediate compositions for volcanic rocks. A reasonable hypothesis is that

mantle derived magmas stalled and interacted with the preexisting Sicker arc crust to produce the Westcoast Crystalline Complex. During this interaction, migmatization of the Westcoast Crystalline Complex produced abundant leucosomes which then ascended upwards. These leucocratic crustal partial melts mixed with some of the primitive mantle derived magmas and erupted to produce a series of pyroclastic flows which would become the Red Bed Creek facies. Due to the heterogenic nature of the preexisting crust, as well as the variation in the leucosomes being produces, the resulting Red Bed Creek facies has considerable variability in its composition with both the major elements as well as the rare earth elements.

As mantle-derived magmas continued their ascent, they stalled at shallower levels and begin to crystallize to form the Island Intrusions. As fractionation occurs, periodic injections of minor amounts of leucosomes from the Westcoast Crystalline Complex mixed with these shallower intrusions, which in turn cause an eruption and the formation of a flow now represented by the Klanawa facies.

SUMMARY

The Jurassic Bonanza arc is an exposed island arc crustal section on the west coast of Vancouver Island, with north to south along-strike exposure of over 500 km. Explosive volcanism and comagmatic plutonism formed the Bonanza volcanics, the Island Intrusions, and the Westcoast Crystalline Complex. The three components of the Bonanza arc represent different crustal levels of magmatism with the deepest level of magmatism represented by the Westcoast Crystalline Complex, the intermediate level represented by the Island Intrusions and the surficial level represented by Bonanza Group Volcanics.

The Bonanza volcanics range from high-alumina basalt (Al_2O_3 >15 wt.%) to dacites with SiO_2 contents from 48.5 to 72.5 wt.%. They are calc-alkaline with MgO contents from 4.0 to 8.7 wt.%. The Bonanza Volcanics have a moderate enrichment in the light rare earth elements (LREE's), with abundances 25-90x chondrite with chondrite-normalized $(La/Yb)_n$ values from 4.0 to 14.

Values of Th/La and Th/Nd have moderate variability in the Alberni region and in the Pemberton Hills and less variability in the Nootka Sound region. Values for Pb/Ce and Ba/La show a greater range of variability for the Bonanza volcanics in all regions on Vancouver Island. These values indicate the sediment melt component has a greater influence on the chemistry of the Bonanza volcanics. The Pemberton Hills region has the greatest influence from the sediment component while the Alberni region has a moderate influence from the sediment signature. The Nootka Sound region has the least amount of influence from the sediment signature but is most affected by the slab fluid component.

The slab fluid component has little influence on the Pemberton Hills and Alberni region, although some of the slab fluid component may be lost due to alteration.

While simple crystal fractionation can produce a daughter composition that matches closely with the observed concentrations of the major elements in the Klanawa facies, simple crystal fractionation alone can not produce the concentrations of REE observed in the more evolved rocks in the Alberni region of the Bonanza arc. Rather, a model that is a combination of both crystal fractionation and magma mixing is much more successful in producing results that fit both the observed concentrations of the REEs as well as the major elements of intermediate compositions of the Klanawa facies.

Processes are more complex in the Red Bed Creek facies and require assimilation of country rock as well as magma mixing between primitive melts and leucosome phases to approximate the observed compositions in the Red Bed Creek facies.

Thus, in summary, the volcanic rocks of the Bonanza arc all have a contribution of a sediment melt component. The greatest influence of the sediment melt component is in the Alberni region and the Pemberton hills. Additionally, many open system crustal processes were at work to diversify parental melts into the more evolved compositions observed today.

REFERENCES

Anderson R.G. and Greig, C.J. 1989. Jurassic and Tertiary plutonism in the Queen Charlotte Islands, British Columbia. In Current research, part H. Geological Survey of Canada, paper 89-1H, pp. 95-104.

Anderson, R.G. and Reichenbach, I. 1991. U-Pb and K-Ar framework for Middle to Late Jurassic (172 - >158 Ma) and tertiary (46-27 Ma) plutons in the Queen Charlotte Island, Queen Charlotte Islands, British Columbia. In: Current Research. Geological Survey of Canada, Paper 95-A, pp. 91-96.

Archibald, D.A., and Nixon, G.T. 1995. 40Ar/39Ar geochronometry of igneous rocks in the Quatsino – Port McNeill map area, northern Vancouver Island (92L/12, 11). B.C. Geological Survey, Geological Fieldwork 1994, Paper 1995-1, pp. 49–59.

Armstrong, R.L.A. 1988. Mesozoic and early Cenozoic magmatic evolution of the Canadian Cordillera. Geological Society of America, Special Paper 218, pp. 55-91.

Brandon, M.T., Cowan, D.S., and Vance, J.A. 1988. The Late Cretaceous San Juan thrust system, San Juan Islands, Washington: Geological Society of America Special Paper, 222, pp. 81

Brandon, M.T. 1989. Deformational styles in a sequence of olistostromal mélanges, Pacific Rim Complex, western Vancouver Island, Canada. Geological Society of America Bulletin, v. 101, pp. 1520-1542.

Burns, L.E. 1985. The Border Ranges ultramafic and mafic complex, south-central Alaska: Cumulate fractionates of island arc volcanics. Canadian Journal of Earth Sciences, v. 22, pp. 1020-1038.

Bryant, C.J., Arculus, R.J., and Eggins, S.M. 1999. Laser ablation inductively coupled plasma–mass spectrometry and tephras; a new approach to understanding arc-magmas genesis. Geology, v. 27, pp. 1119–1122.

Bryant, C.J., Arculus, R.J., and Eggins, S.M. 2003. The geochemical evolution of the Izu-Bonin arc system: a perspective from tephras recovered by deep-sea drilling. Geochemistry, Geophysics, Geosystems, v. 4(11), pp. 1094.

Carson, D.J.T. 1973. The plutonic rocks of Vancouver Island, British Columbia: their petrography, chemistry, age and emplacement. Geological Survey of Canada, Paper 72-44, pp 1-70.

Castillo, P.R., Newhall, C.G. 2004. Geochemical constraints on possible subduction components in lavas of Mayon and Taal volcanoes, southern Luzon, Philippines. Journal of Petrology, v. 45, pp. 1089-1108.

Class, C., Miller, D.L., Goldstein, S.L., and Langmuir, C.H. 2000. Distinguishing melt and fluid components in Umnak Volcanics, Aleutian Arc, Geochemistry, Geophysics, Geosystems v. 1. Paper number 1999GC000010.

Clift, P.D., Pavlis, T., DeBari, S.M., Draut, A.E., Rioux, M., and Kelemen, P.K. 2005. Subduction erosion of the Jurassic Talkeetna-Bonanza arc and the Mesozoic accretionary tectonics of western North America, Geology, v. 33, pp. 881–884.

Clift, P.D., Draut, A.E., Kelemen, P.B., Blusztajn, J., and Greene, A. 2005. Stratigraphic and Geochemical Evolution of an arc upper crustal section; the Jurassic Talkeetna Volcanic Formation, South Central Alaska, Geological Society of America Bulletin, v. 117 (7/8), pp. 902–925.

Crickmay, C.H. 1928. The Stratigraphy of Parson Bay, British Columbia; University of California, Department of Geological Sciences Bulletin, v. 18 (2), pp. 51-70.

Davidson, J., Turner, S., Handley, H., Macpherson, C., and Dosseto, A. 2007. Amphibole "sponge" in arc crust? Geology, v. 35 (9), pp. 787-790.

DeBari, S.M., and Sleep, N.H. 1991. High-Mg, low-Al bulk composition of the Talkeetna island arc, Alaska; Implications for primary magmas and the nature of arc crust. Geological Society of America Bulletin, v. 103, pp. 37-47

DeBari, S.M., Anderson, R.G., Mortensen, J.K. 1999. Correlation among lower to upper crustal components in an island arc: the Jurassic Bonanza Arc, Vancouver Island, Canada. Canadian Journal of Earth Sciences, v. 36, pp. 1371-1413.

Dhuime, B., Bosch, D., Garrido, C.J., Bodinier, J.L., Bruguier, O., Hussain, S.S., and Dawood, H. 2009. Geochemical Architecture of the Lower- to Middle-crustal Section of a Paleo-island Arc (Kohistan Complex, Jijal–Kamila Area, Northern Pakistan): Implications for the Evolution of an Oceanic Subduction Zone. Journal of Petrology, v. 50(3), pp. 531-569

Elliott, T. 2003. Tracers of the Slab. In: Inside the Subduction Factory. (Eds. J. M. Eiler. Washington, DC, American Geophysical Union), pp. 23-45

England, T.D.J. 1989. Late Cretaceous to Paleogene Evolution of the Georgia Basin, Southwestern British Columbia; Memorial University of Newfoundland, unpublished Ph.D. thesis.

Friedman, R.M., and Armstrong, R.L. 1995. Jurassic and Cretaceous geochronology of the southern Coast Belt, B.C., 49°–51°N. In Jurassic magmatism and tectonics of the North American Cordillera. Edited by D.M. Miller and C. Busby. Geological Society of America, Special Paper 299, pp. 95–139.

Friedman, R.M., and Nixon, G.T. 1995. U–Pb zircon dating of Jurassic porphyry Cu(–Au) and associated acid sulphate systems, northern Vancouver Island, British Columbia, Geological Association of Canada – Mineralogical Association of Canada Annual Meeting, Victoria, B.C., pp. A-34.

Gehrels, G.E. and Greig, C.J. 1991. Late Jurassic detrital zircon link between the Alexander-Wrangellia terrane and Stikine and Yukon-Tanana terranes. Geological Society of America, Abstracts with Programs, 23: pp. 434.

Greene, A.R., DeBari, S.M., Kelemen, P.B., Blusztajn, J., and Clift P.D. 2006. A detailed geochemical study of island arc crust: The Talkeetna Arc section, south-central Alaska, Journal of Petrology, v. 47, pp. 1051–1093.

Greene, A.R., Scoates, J.S., Weis, D., Nixon, G.T., and Kieffer, B. 2009. Melting history and magmatic evolution of basalts and picrites from the accreted Wrangellia oceanic plateau, Vancouver Island, Canada. Journal of Petrology, v. 50(3), pp. 467-505, doi:10.1093/petrology/egp008.

Gunning, H.C. 1930. Geology and Mineral Deposits of the Quatsino-Nimpkish Area, Vancouver Island. British Columbia; Geological Survey of Canada, Summary Report 1929. Part A. pp. 94-143.

Gunning, H.C. 1932. Zeballos River Area, Vancouver Island B.C.; Geological Survey of Canada, Summary Report 1932, Part A II, pp. 29-50.

Hildreth, W., MoorBath, S. 1988. Crustal contributions to arc magmatism in the Andes of Central Chile. Contributions to Mineralogy and Petrology, v. 98, pp. 455-489

Hirshmann. M., Wiens, D., Peacock, S. 2000. Subduction Factory Science Plan, http://www.margins.wustl.edu/SubFac/SubFac_sciplan.html

Hoadley, J.W. 1953. Geology and Mineral Deposits of the Zeballos-Nimpkish Area, Vancouver Island, British Columbia; Geological Survey of Canada, Memoir 272.

Hochstaedter, A., Gill, J., Peters, R., Broughton, P., Holden, P., and Taylor, B. 2001. Across-arc geochemical trends in the Izu-Bonin arc: Contributions from the subducting slab, Geochemistry, Geophysics, Geosystems, vol. 2, Paper number 2000GC000105

Isachsen, C.E. 1984. Geology, geochemistry, and geochronology of the Westcoast Crystalline Complex and related rocks, Vancouver Island, British Columbia. M.Sc. thesis, University of British Columbia, Vancouver.

Isachsen, C.E. 1987. Geology, geochemistry, and cooling history of the Westcoast Crystalline Complex and related rocks, Meares Island and vicinity, Vancouver Island, British Columbia. Canadian Journal of Earth Sciences, v. 24, pp. 2047–2064.

Irving, E., Yole, R.W. 1987. Tectonic rotations and translations in Western Canada; new evidence from Jurassic rocks of Vancouver Island. Geophysical Journal of the Royal Astronomical Society, v. 91(3), pp. 1025-1048.

International Commission on Stratigraphy. 2004. International Stratigraphic Chart. International Union of Geological Sciences: International Commission on Stratigraphy, Paris, 2004

Jeletzky J.A. 1954. Tertiary rocks of Hesquiat-Nootka area, west coast of Vancouver Island, British Columbia; Geological Survey of Canada, Bulletin, 17 pp. 53-65.

Jicha, B.R., Singer, B.S., Brophy, J.G., Fournelle, J.H., Johnson, C.M., Beard, B.L., Lapen, T.J., and Mahlen, N.J. 2004, Variable impact of the subducted slab on Aleutian Island arc magma sources: Evidence from Sr, Nd, Pb, and Hf isotopes and trace element abundances: Journal of Petrology, v. 45, pp. 1845-1875.

Johnson, D.M., Hooper, P.R. & Conrey, R.M. 1999. XRF analysis of rocks and minerals for major and trace elements on a single low dilution Li-tetraborate fused bead. Advances in X-Ray Analysis v.41, pp. 843–867.

Kay, R.W. 1985. Island arc processes relevant to crustal and mantle evolution. Tectonophysics v. 112, pp. 1-15.

Kay, S.M. & Kay, R.W. 1985. Role of crystal cumulates and the oceanic crust in the formation of the lower crust of the Aleutian arc. Geology v. 13, pp. 461-464.

Kelemen, P.B., Yogodzinski, G.M., and Scholl, D.W. 2001. Along-strike Variations in Lavas of the Aleutian Island Arc: Implications for the Genesis of High Mg# Andesite and Continental Crust. AGU Monograph series, Unpublished

Kimura, J., Manton, W.I., Sun, C., Iizumi, S., Yoshida, T., and Stern, R.J. 2002. Chemical diversity of the Ueno Basalts, central Japan; identification of mantle and crustal contributions to arc basalts Journal of Petrology, v. 43(10), pp. 1923-1946.

Larocque, J. and Canil, D. 2009. The role of amphibole in the evolution of arc magmas and crust: the case from the Jurassic Bonanza arc section, Vancouver Island, Canada. Contributions to Mineralogy and Petrology, (doi:10.1007/s00410-009-0436-z)

Massey, N.W.D., and Friday, S.J. 1989. Geology of the Alberni – Nanaimo lakes area, Vancouver Island (91F/1W, 92F/2E and part of 92F/7). In Geological fieldwork, 1987. British Columbia Ministry of Energy, Mines and Petroleum Resources, Paper 1989-1, pp. 119-126.

Massey, N.W.D. 1992. Geology and Mineral Resources of the Alberni - Nanaimo Lakes Sheet; B.C. Ministry of Energy, Mines and Petroleum Resources, Paper 1992-2.

Massey, N.W.D. 1992. Geology and Mineral Resources of the Cowichan Lake Sheet; B.C. Ministry of Energy, Mines and Petroleum Resources, Paper 1992-3.

Monger, J.W.H., Price, R.A., and Tempelman-Kluit, D.J. 1982. Tectonic accretion and the origin of the two major metamorphic and plutonic welts in the Canadian Cordillera. Geology, v. 10, pp. 70–75.

Monger, J.W.H., Clowes, R.M., Cowan, D.S., Potter, C.J., Price, R.A., and Yorath, C.J., 1994. Continent-ocean transitions in western North America between latitudes 46 and 56 degrees: Transects B1, B2, B3, pp. 357-397. In Phanerozoic Evolution of the North American Continent-Ocean Transitions, Edited by Speed, R.C., Geological Society of America, DNAG, Continent-Ocean Transect volume.

Muller, J.E., and Carson D.J.T. 1969. Geology and mineral deposits of the Alberni area, British Columbia. Geological Survey of Canada, Paper 68-50.

Muller, J.E., Northcote, K.E., and Carlisle, D. 1974a. Geology and mineral deposits of Alert Bay – Cape Scott map area, Vancouver Island, British Columbia. Geological Survey of Canada, Paper 74-8.

Muller, J.E., Wanless, R.K., and Loveridge, W.D. 1974b. A Paleozoic zircon age of the Westcoast Crystalline Complex of Vancouver Island, British Columbia. Canadian Journal of Earth Sciences, v. 11. pp. 1717–1722.

Muller, J.E. 1977. Evolution of the Pacific Margin, Vancouver Island, and adjacent regions. Canadian Journal of Earth Sciences, v. 14, pp. 2062-2085.

Muller J.E., Cameron, B.E.B., and Northcote, K.E. 1981. Geology and mineral deposits of Nootka Sound map-area, Vancouver Island, British Columbia. Geological Survey of Canada, Paper 80-16.

Nixon, G.T., Hammack, J.L., Koyanagi, V.M., Payie, G.J., Massey, N.W.D., Hamilton J.V. and Haggart, J.W. 1994. Preliminary Geology of the Quatsino - Port McNeill Map Areas, Northern Vancouver Island (92L/12, 11); in Geological Fieldwork 1993, Grant, B. and Newell, J.M., Editors; B.C. Ministry of Energy, Mines and Petroleum Resources, Paper 1994-1, pp. 63-85.

Nixon, G.T., Hammack, J.L., Payie, G.J., Snyder, L.D., Archibald, D.A. and Barron, D. J. 1995. Quatsino - San Josef Map Area, Northern Vancouver Island (92L/12W, 102I/8, 9); in Geological Fieldwork 1994, Grant, B. and Newell, J.M., Editors; B.C. Ministry of Energy, Mines and Petroleum Resources, Paper 1995-1, pp. 9-21.

Nixon, G.T. and Orr, A.J. 2006. Recent revisions to the Early Mesozoic stratigraphy of northern Vancouver Island (NTS 102I; 092L) and metallogenic implications, British Columbia. In: Geologic Fieldwork 2006, British Columbia Ministry of Energy, Mines and Petroleum Resources, Paper 2007-1 and Geoscience BC, Report 2007-1, pp. 163-178.

Pacht, J.A. 1984. Petrologic evolution and paleogeography of the Late Cretaceous Nanaimo Basin, Washington and British Columbia: implications for Cretaceous tectonics; Geological Society of America Bulletin, v. 95, pp. 766-778.

Parrish, R.R., and McNicoll, V.J. 1992. U/Pb age determinations from the southern Vancouver Island area, British Columbia, in Radiogenic age and isotopic studies: Geological Survey of Canada, Paper 91-2, pp. 79–86.

Plafker, G., Nokleberg, W.J., and Lull, J.S. 1989. Bedrock geology an the tectonic evolution of the Wrangellia, Peninsular and Chugach terranes along the trans-Alaska crustal transect in the Chugach mountains and southern Copper River basin, Alaska. Journal of Geophysical Research, v. 94(B4), pp. 4255-4295.

Reymer, A. & Schubert, G. 1984. Phanerozoic addition rates to the continental crust and crustal growth. Tectonics v. 3(1), pp. 63-77.

Rollinson, H. 1993. Using Geochemical Data: Evaluation, Presentation, Interpretation, pp. 108–111, Addison-Wesley-Longman, Reading, Mass.

Rudnick, R.L. 1995. Making continental crust. Nature v. 378, pp. 571-577.

Rudnick, R.L. & Fountain, D.M. 1995. Nature and composition of the continental crust: a lower crustal perspective. Reviews of Geophysics v. 33(3), pp. 267-309.

Rüpke L., Morgan J., Hort M., Connolly J. 2002. Are the regional variations in Central American arc lavas due to differing basaltic versus peridotitic slab sources of fluids?: Geology, v. 30(11), pp. 1035– 1038.

Samson, S.D., Patchett, P.J., Gehrels, G.E., and Anderson, R.G. 1990. Nd and Sr isotopic characterization of the Wrangellia terrane and implications for crustal growth of the Canadian cordillera. Journal of Geology, v. 98, pp. 749-762.

Singer, B.S., Jicha, B.R., Leeman. W.P., Rogers, N.W., Thirwall, M.F., Ryan, J., Nicolaysen, K.E. 2007. Along-strike trace element and isotopic variation in Aleutian Island arc basalt: Subduction melts sediments and dehydrates serpentine. Journal of Geophysical Research 112:B06206.

Stern, R.J., Fouch, M.J., Klemperer, S.L. 2001. An Overview of the Izu-Bonin-Mariana Subduction Factory, unpublished

Straub, S., Layne, G., Schmidt, A. and Langmuir, C. 2004. Volcanic glasses at the Izu arc volcanic front: new perspectives on fluid and sediment melt recycling in subduction zones. Geochemistry, Geophysics, Geosystems 5, doi:10.1029/2002GC000408

Tipper, H.W. and Richards, T.A. 1976. Jurassic Stratigraphy and History of North-Central British Columbia, Geological Survey of Canada, Bulletin 270, pp. 73.

Tipper H.W. 1984. The allochthonous Jurassic-Cretaceous terranes of the Canadian Cordillera and their relation to correlative strata of the North American Craton. Geological Association of Canada Special paper 27, pp. 113-120.

van der Heyden, P. 1992. A middle Jurassic to early Tertiary Andean-Sierran arc model for the coast belt of British Columbia, Tectonics, v. 11(1), pp. 82–97.

Wanless, R.K., Stevens, R.D., Lachance, G.R., and Delabio, R.N.D. 1974. Age determinations and geological studies, K–Ar isotopic ages, Report 12. Geological Survey of Canada, Paper 74-2.

Workman, R.K. and Hart, S.R. 2005. Major and Trace Element Composition of the Depleted MORB Mantle (DMM), Earth and Planetary Science Letters, v. 231, pp. 53-72.

Yorath, C.J. 1991. Upper Jurassic to Paleogene assemblages: Chapter 9 in Geology of the Cordilleran Orogen of Canada: H. Gabrielse and C.J. Yorath (ed.): Geological Survey of Canada, no. 4, pp. 329-371 (also Geological Society of America, The Geology of North America, v. G-2).

Yorath, C.J., Sutherland Brown A., and Massey, N.W.D. 1999. LITHOPROBE, southern Vancouver Island, British Columbia: geology, Geological Survey of Canada Bulletin v. 498, pp. 145.

FIGURES

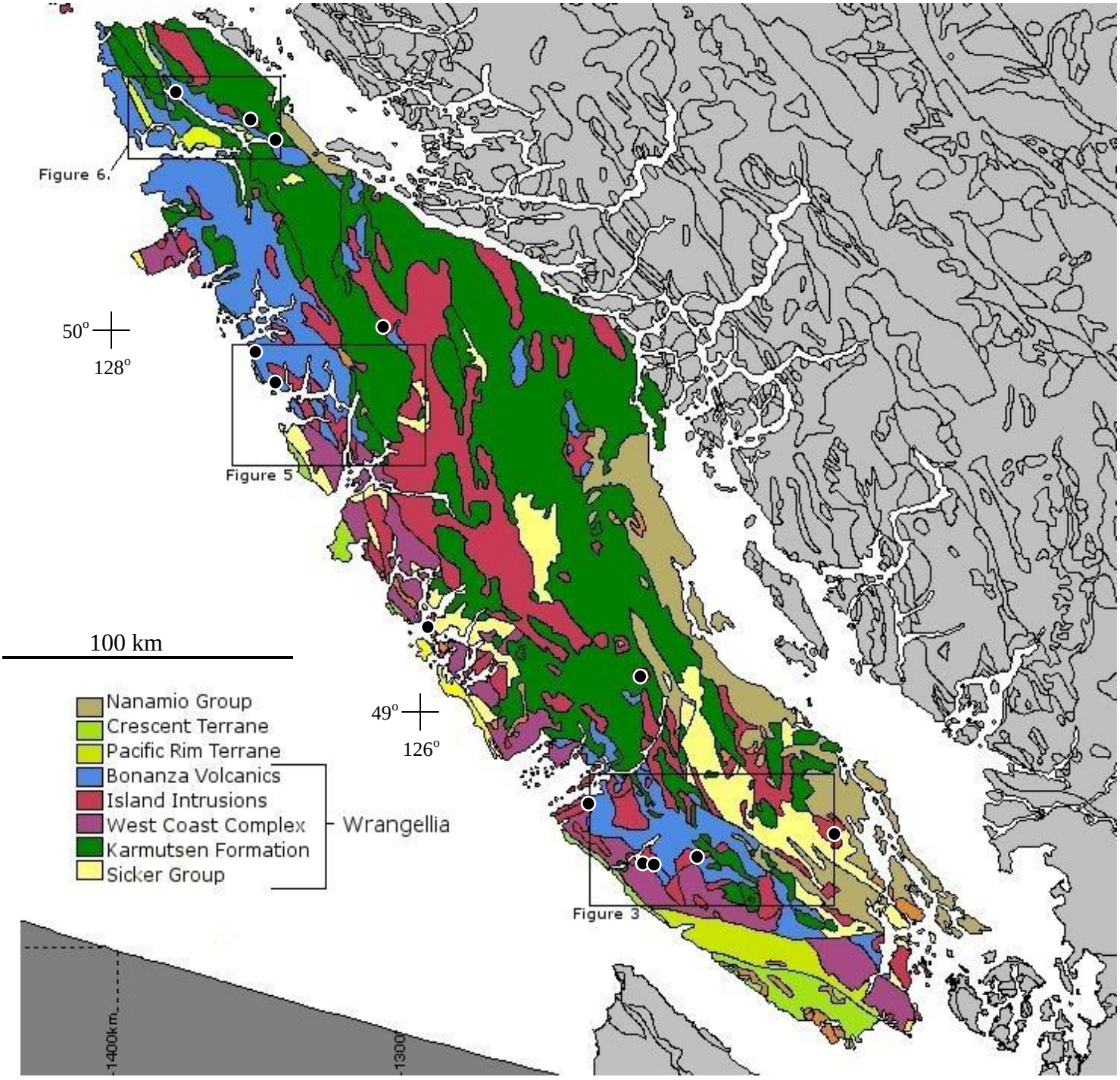

Figure 1. Geologic map of Vancouver Island showing the major geologic units and terranes. The Bonanza volcanics, Island Intrusions, Westcoast Crystalline Complex, Karmutsen Formation and the Sicker Group are all part of the Wrangellia Terrane. Black dots represent sampling localities for geochronology.

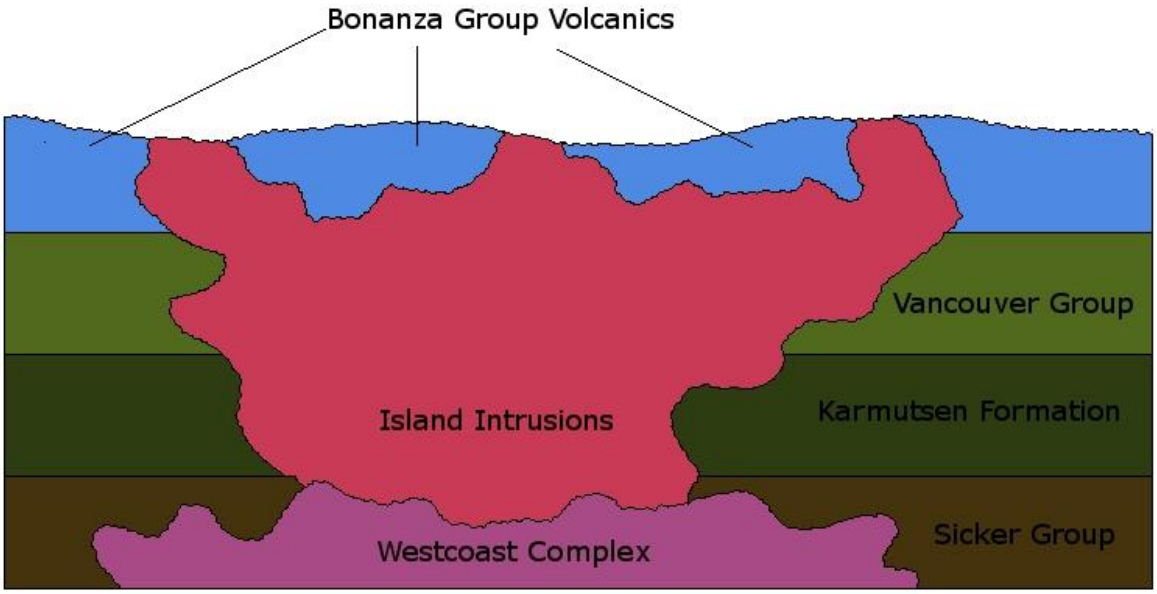

Figure 2. Schematic cross-section showing country rock and the different layers of the Bonanza Arc crust. The deepest level of magmatism represented by the Westcoast Crystalline Complex, the intermediate level represented by the Island Intrusions and the surficial level represented by Bonanza Group Volcanics.

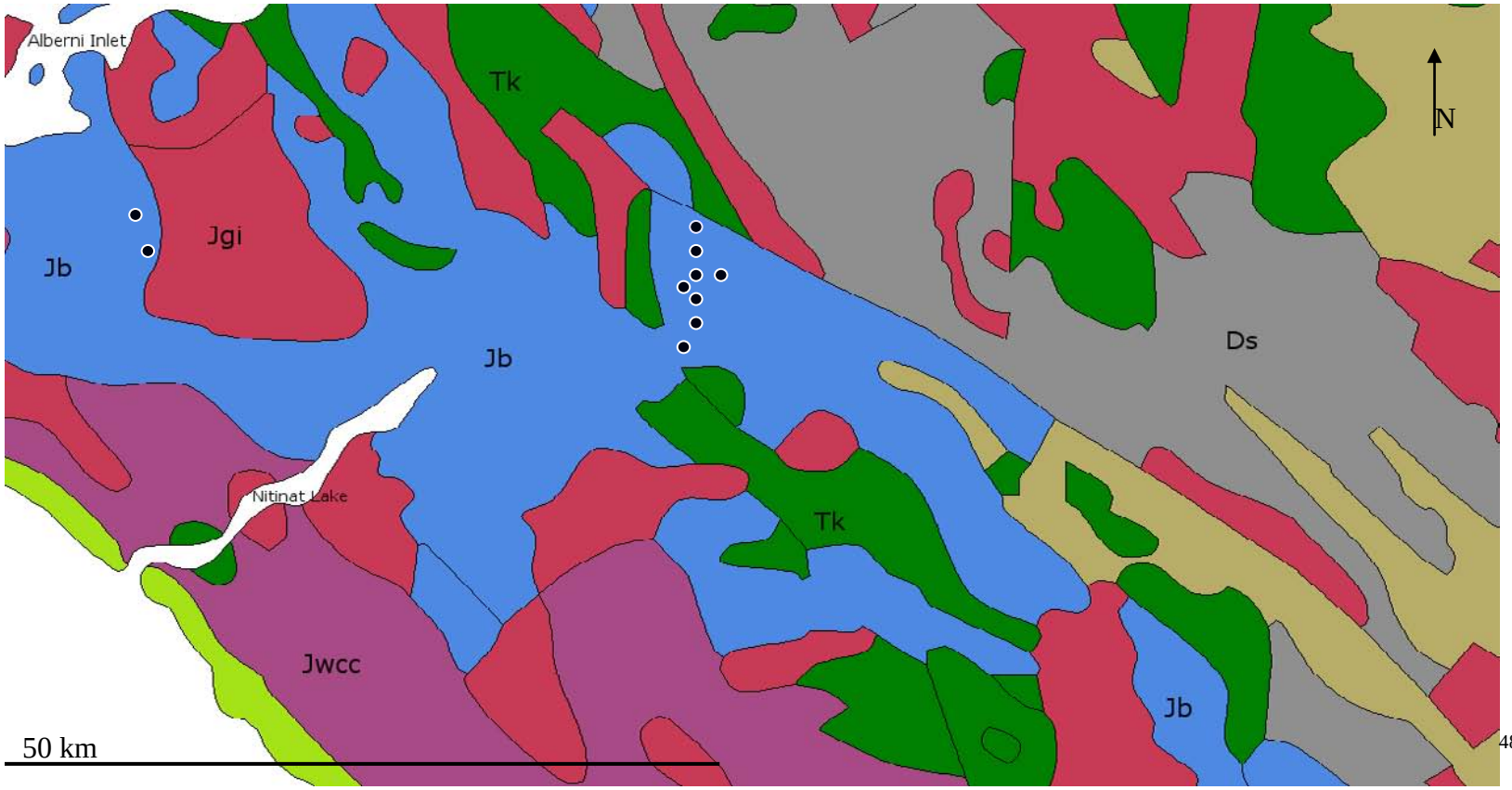

Figure 3. Geologic map of the Alberni Region, southern Vancouver Island. Black dots represent sampling localities. (Jb – Bonanza Volcanics, Jgi – Island Intrusions, Jwcc – Westcoast Crystalline Complex, Tk – Karmutsen Formation, Ds – Sicker Group).

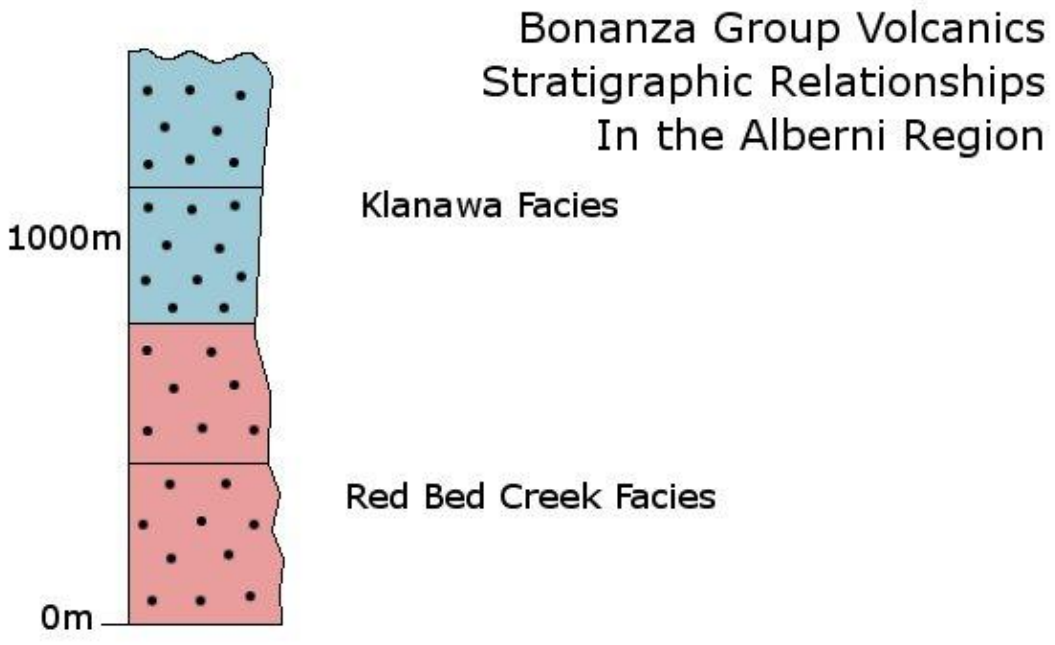

Figure 4. Schematic representation of the stratigraphic relationship between the Red Bed Creek facies and the Klanawa facies in the Alberni Region of Vancouver Island.

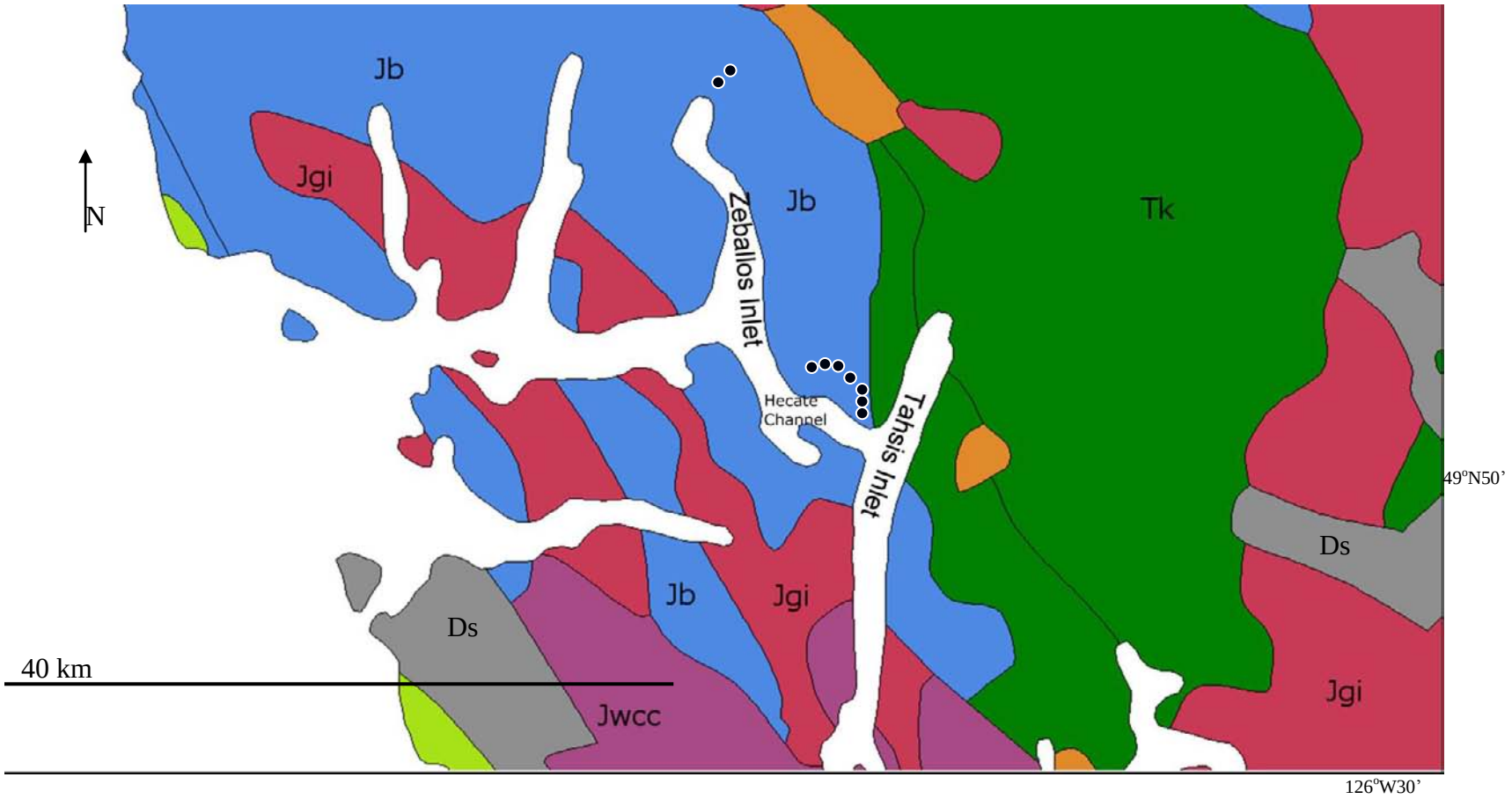

Figure 5. Geologic map of the Nootka Sound Region, Central Vancouver Island. Black dots represent sampling localities. (Jb – Bonanza volcanics, Jgi – Island Intrusions, Jwcc – Westcoast Crystalline Complex, Tk – Karmutsen Formation, Ds – Sicker Group).

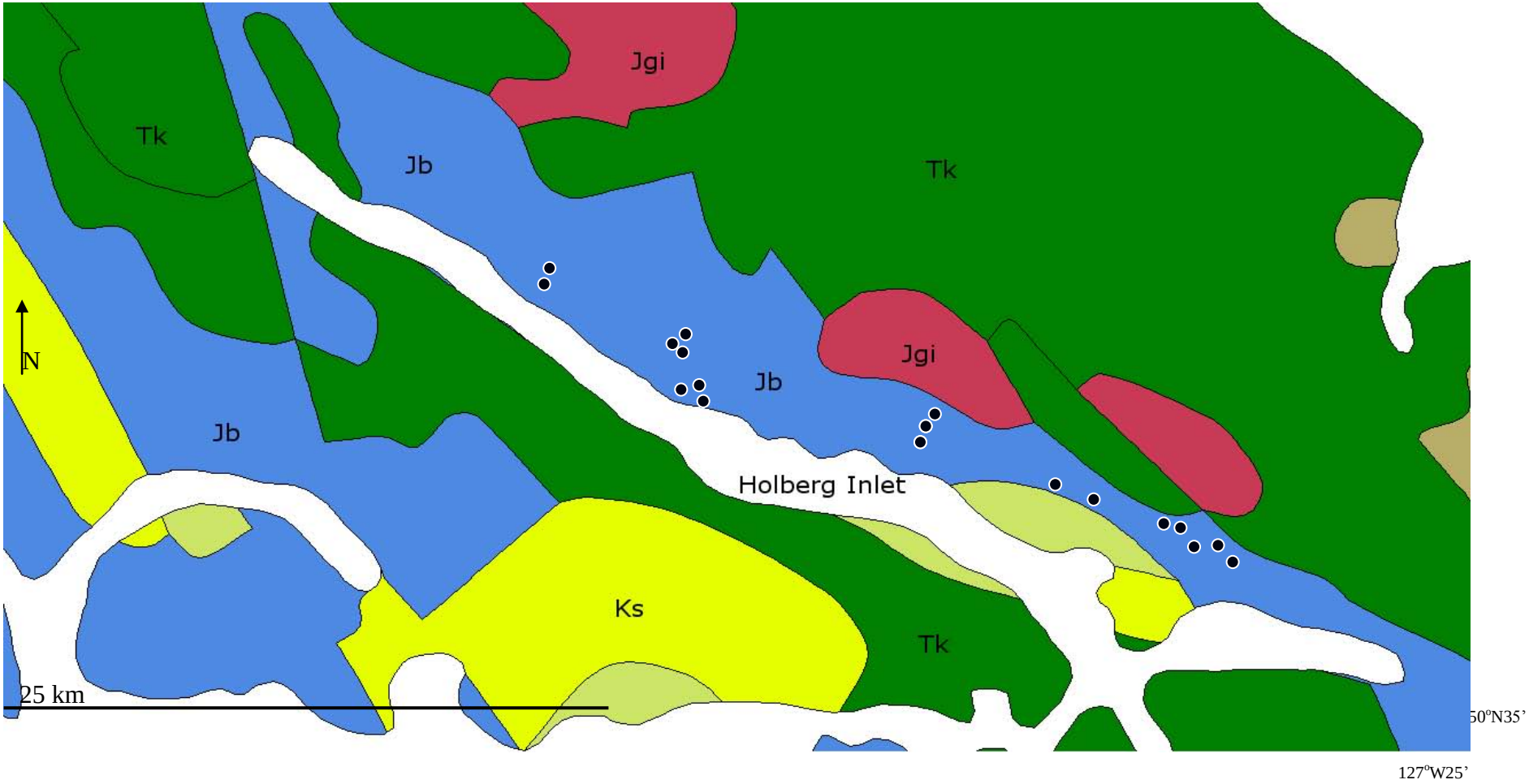

Figure 6. Geologic map of the Pemberton Hills Region, northern Vancouver Island. Black dots represent sampling localities. (Ks, Longram Formation Group Equivalent, Jb – Bonanza volcanics, Jgi – Island Intrusions, Jwcc – Westcoast Crystalline Complex, Tk – Karmutsen Formation).

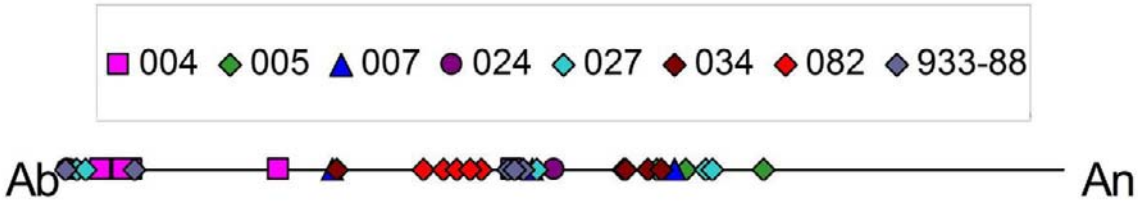

Figure 7. Line diagram showing the Anorthite contents of plagioclase feldspar based on analyses of samples from the Bonanza arc.

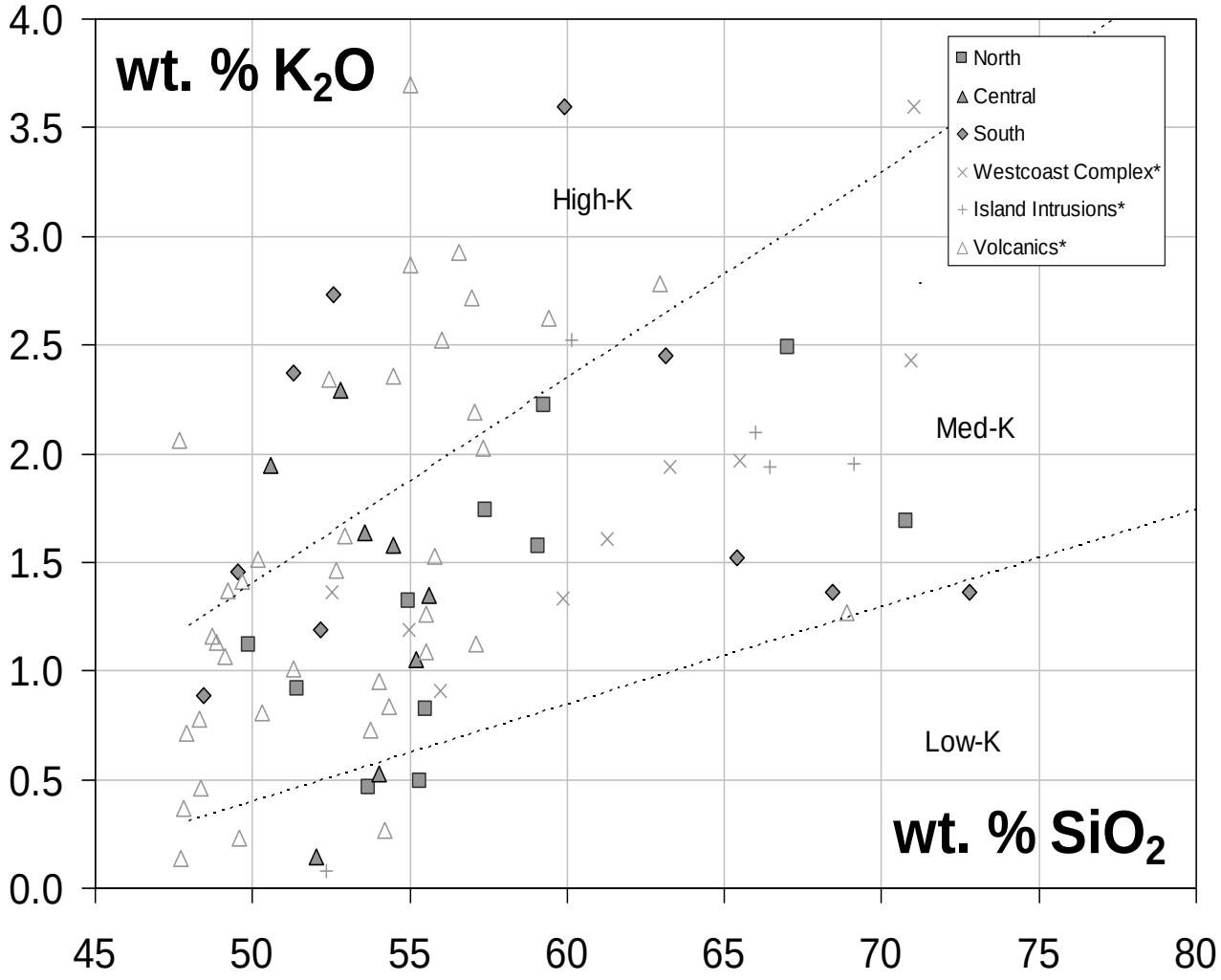

Figure 8. K-series classification of samples from the Bonanza arc based on wt.% SiO_2 and wt.% K_2O. North refers to Pemberton Hills region, Central refers to Nootka Sound region, and South refers to Alberni region.
*Data from DeBari et al., 1999

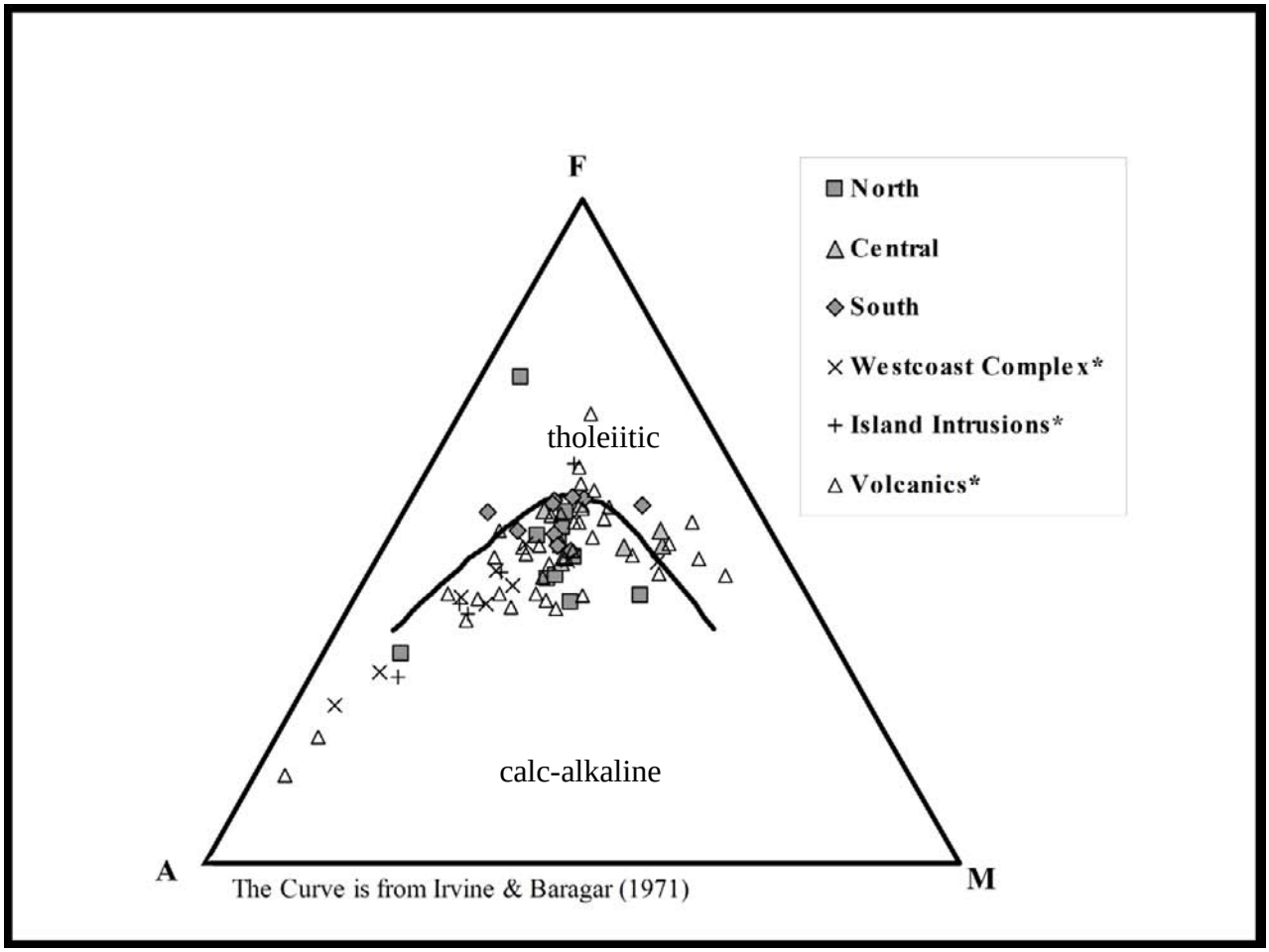

Figure 9. AFM ($A=Na_2O + K_2O$, F=FeOt and M=MgO) diagram of samples collected from the Bonanza arc. North refers to Pemberton Hills region, Central refers to Nootka Sound region, and South refers to Alberni region.
*Data from DeBari et al., 1999

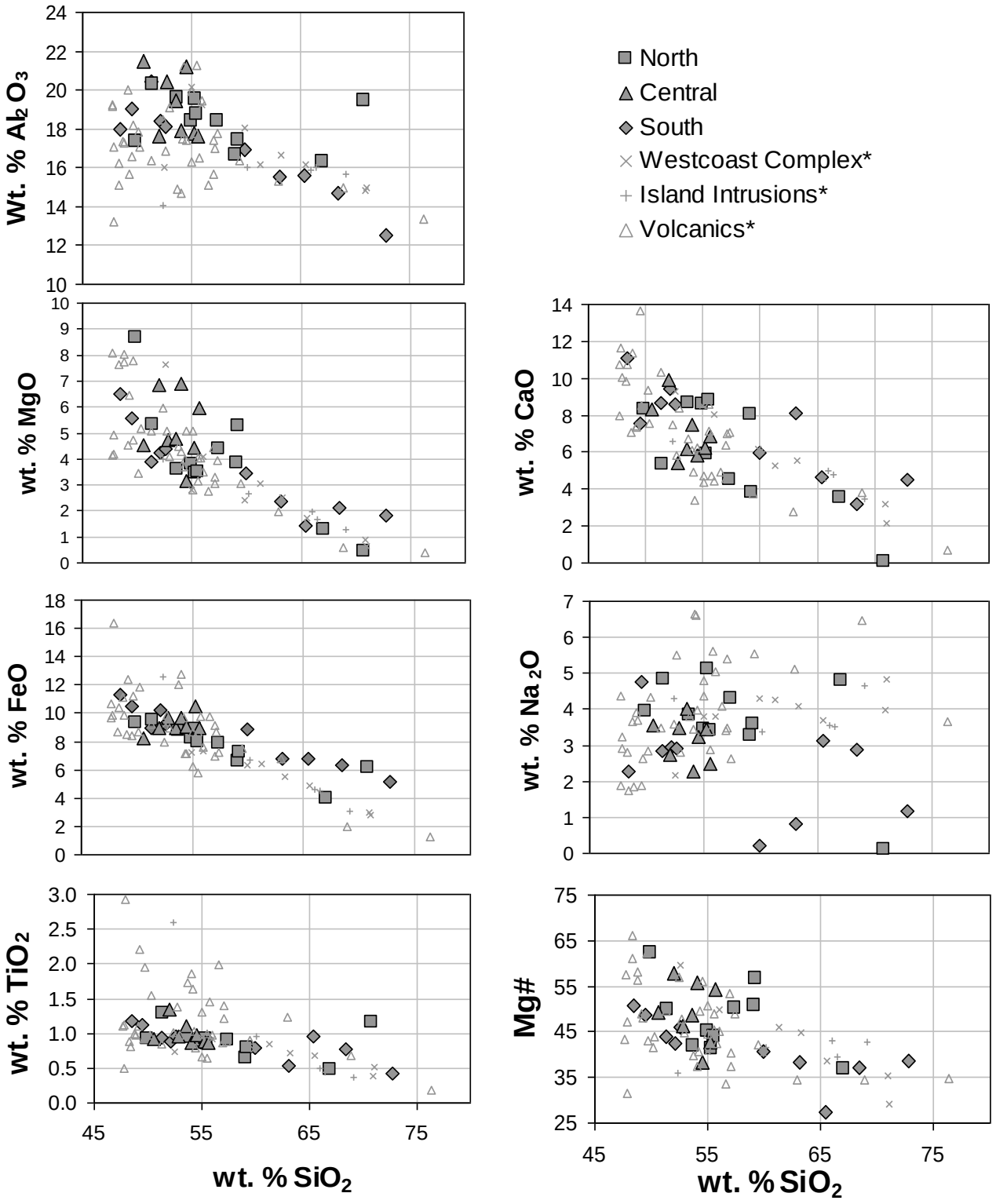

Figure 10. Harker diagrams of major elements (wt.%) based on analyses from the Bonanza arc. North refers to Pemberton Hills region, Central refers to Nootka Sound region, and South refers to Alberni region.
*data from DeBari et al., 1999

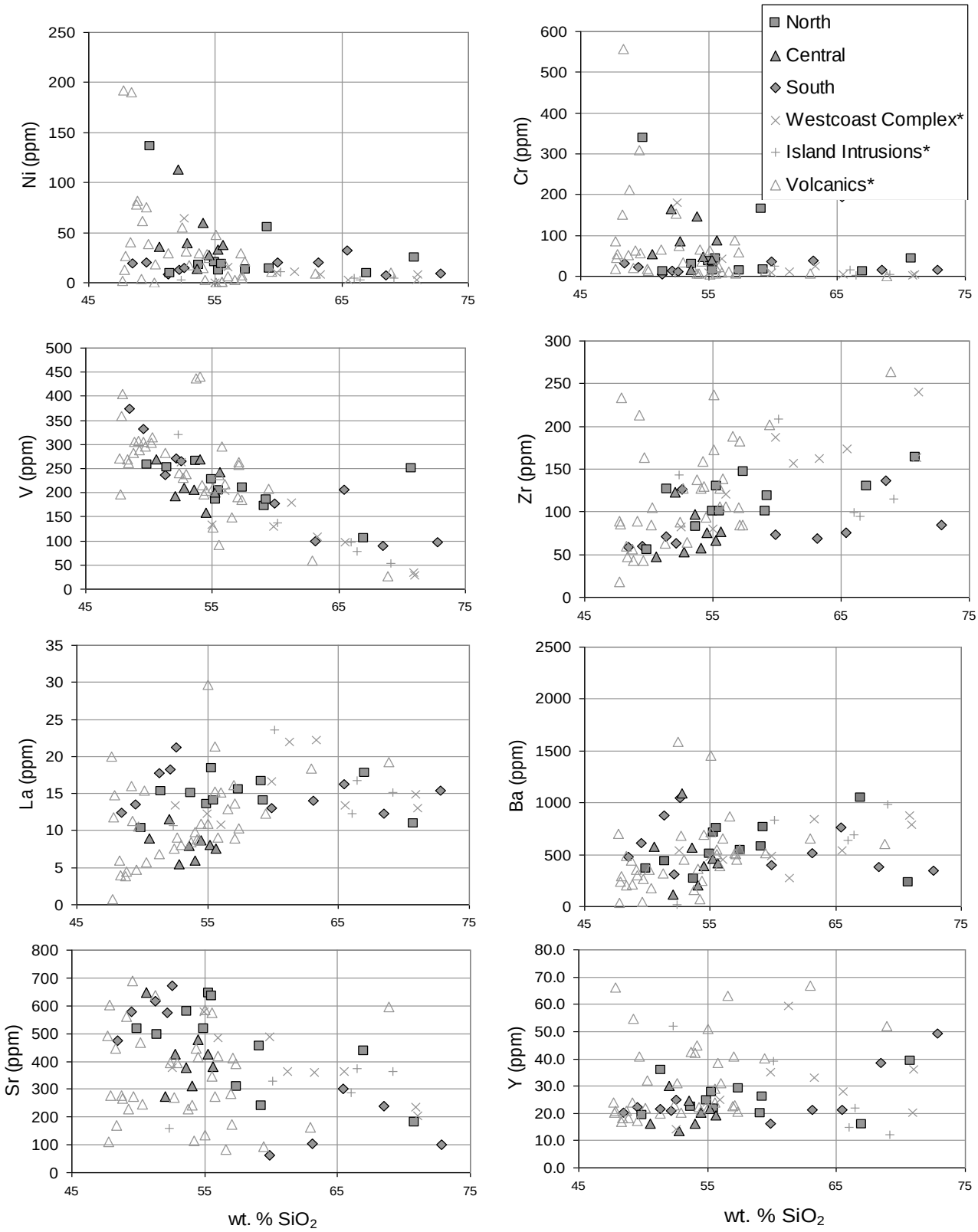

Figure 11. Harker diagrams of selected trace elements (ppm) based on analyses from the Bonanza arc. North refers to Pemberton Hills region, Central refers to Nootka Sound region, and South refers to Alberni region.
*data from DeBari et al., 1999

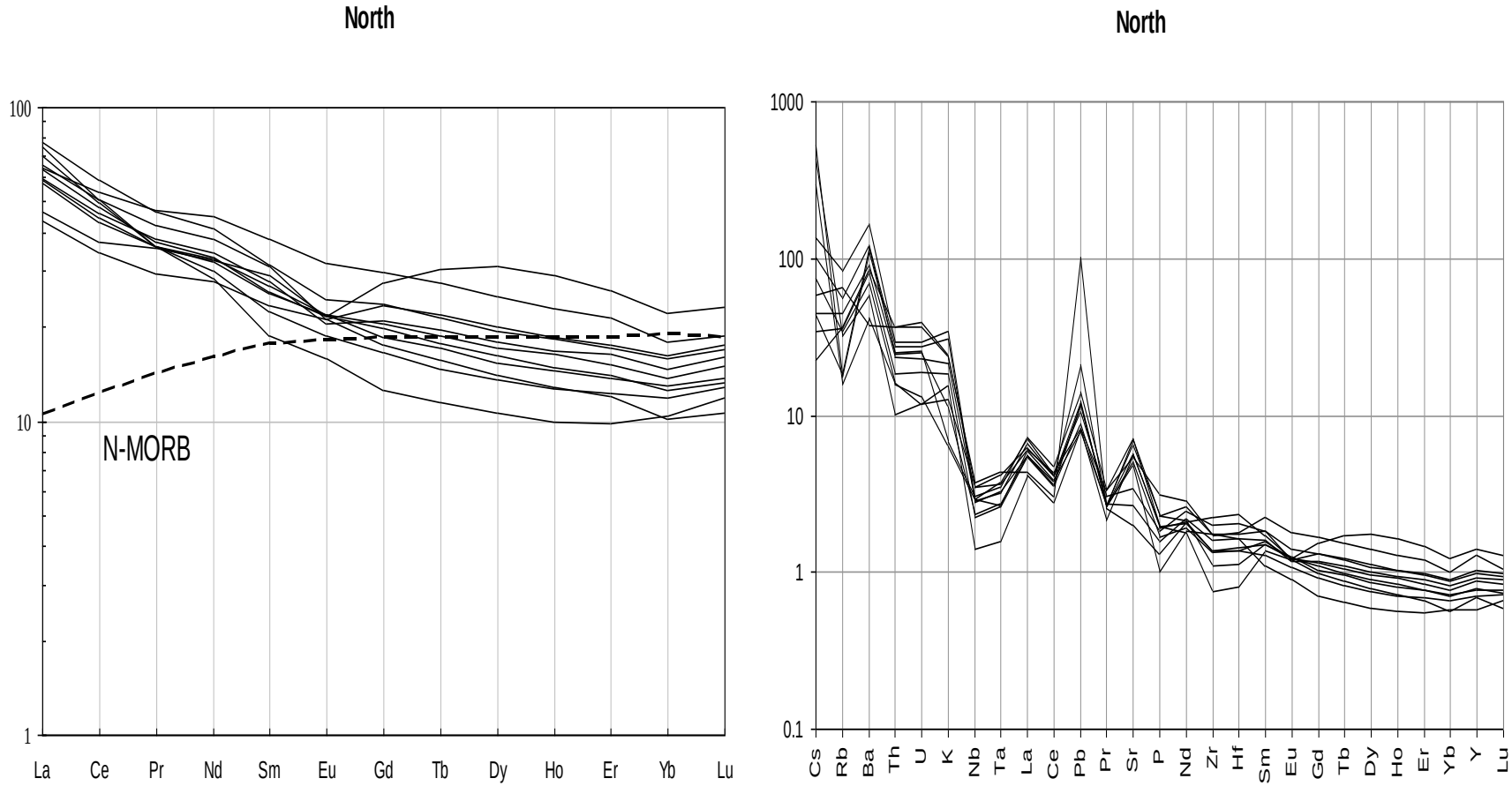

Figure 12. Chondrite-normalized rare earth element (REE) diagram (left) and multi-element, N-MORB normalized "spider diagrams" (right) of volcanic samples collected from the Bonanza arc. North refers to the Pemberton Hills region, Central refers to the Nootka Sound region, and South refers to the Alberni region of Vancouver Island (continued below).

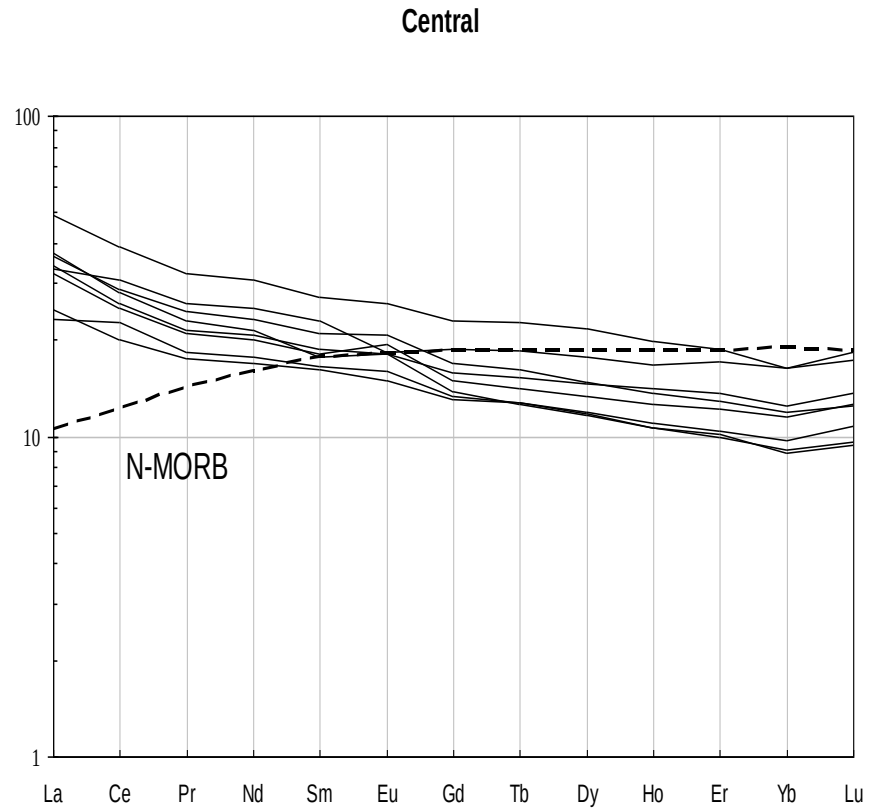

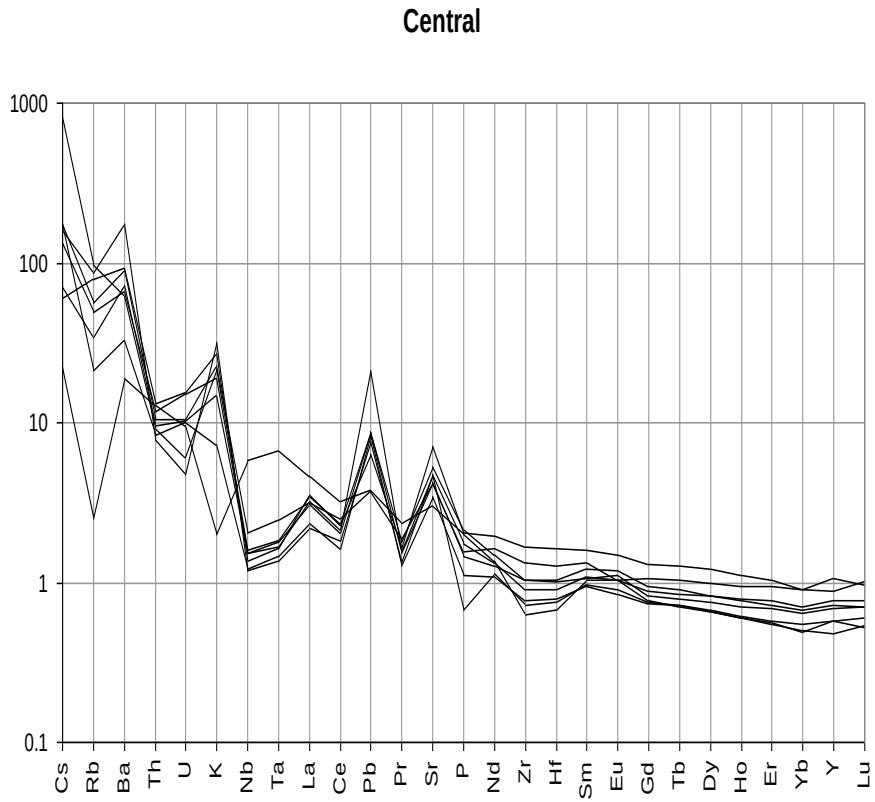

Figure 12. (Cont.)

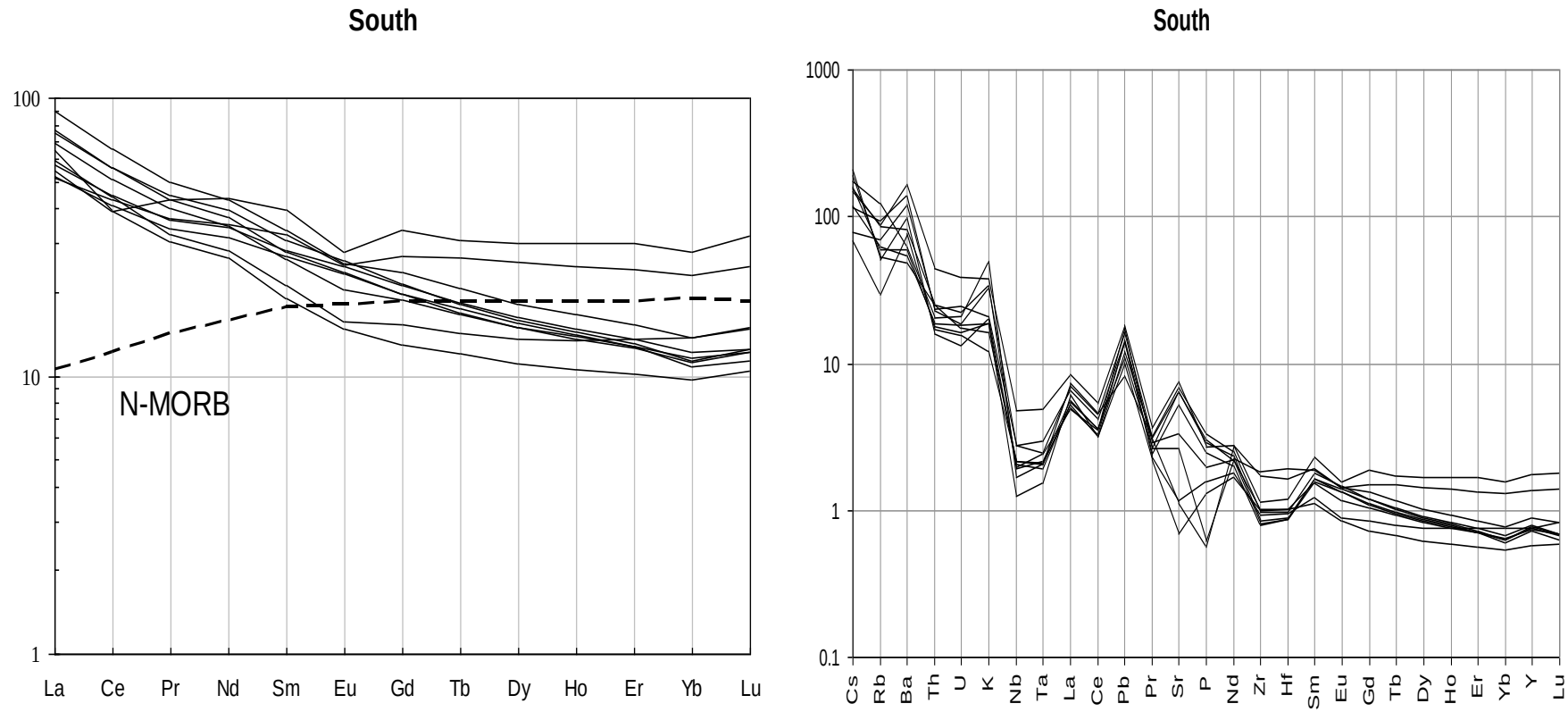

Figure 12. (Cont.)

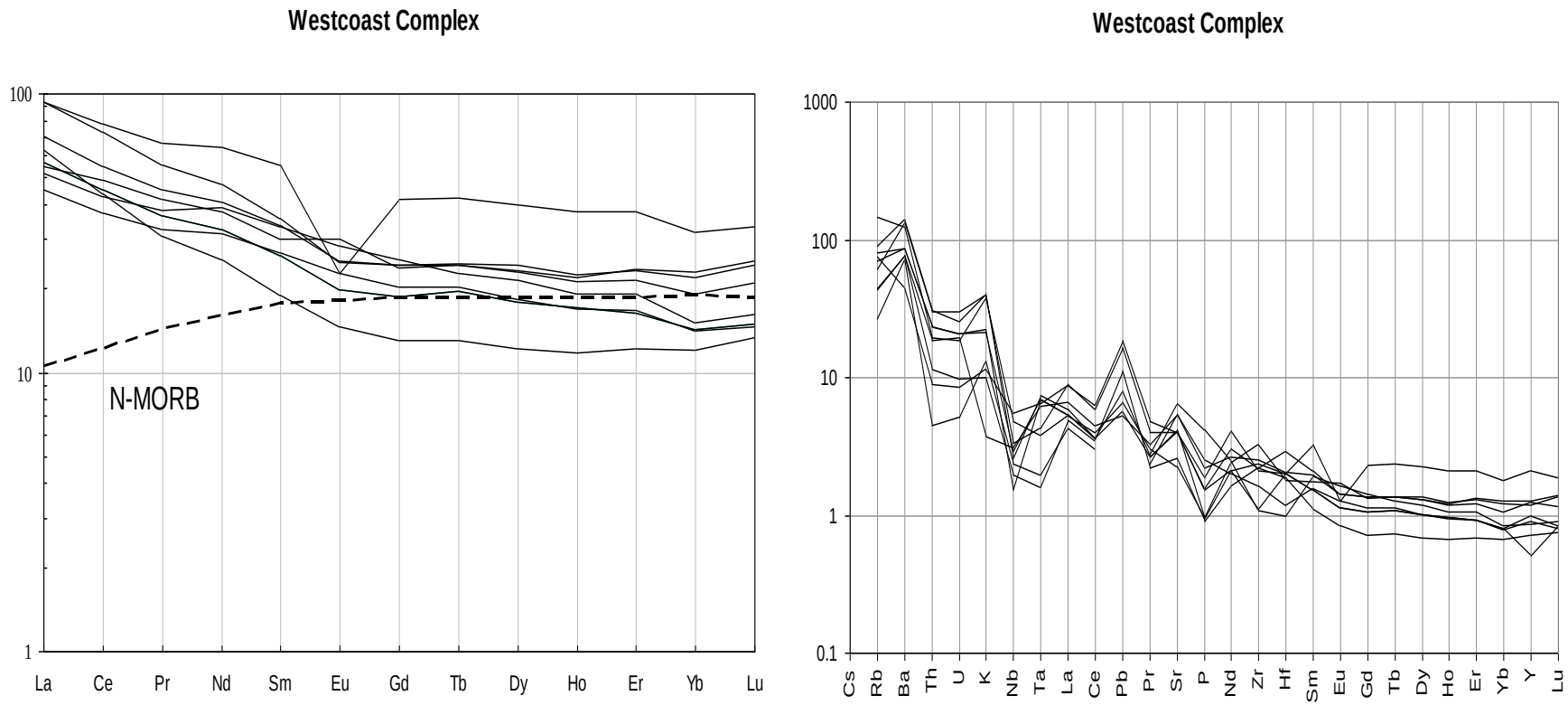

Figure 13. Chondrite-normalized rare earth element (REE) diagram (left) and multi-element, N-MORB normalized "spider diagrams" (right) of intrusive samples collected from the Bonanza arc. Data for intrusive samples is supplemented from DeBari et al., 1999. (continued below).

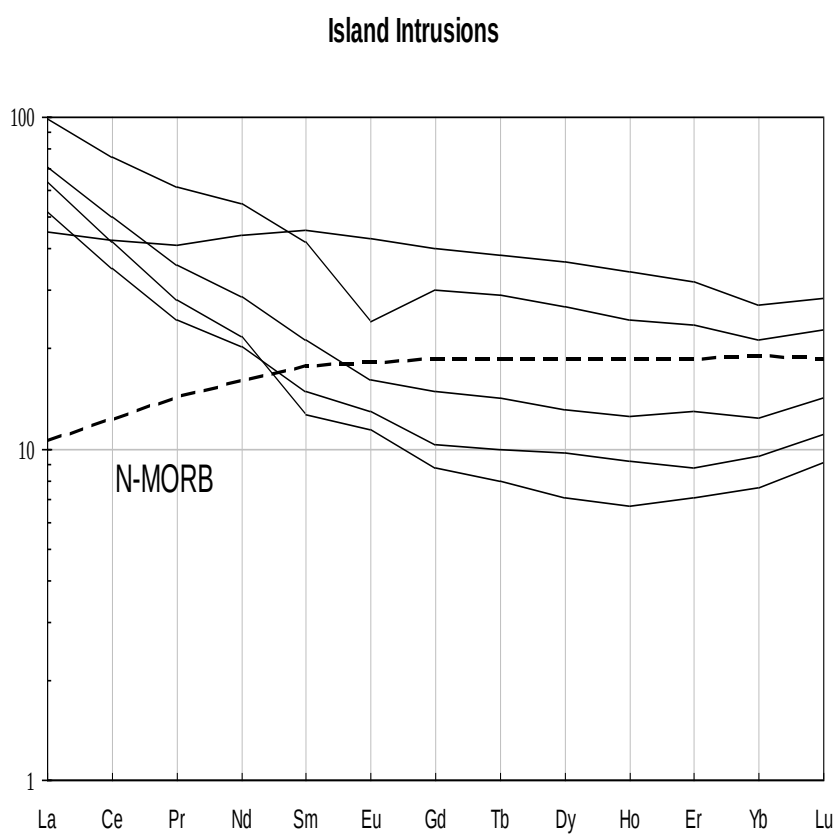

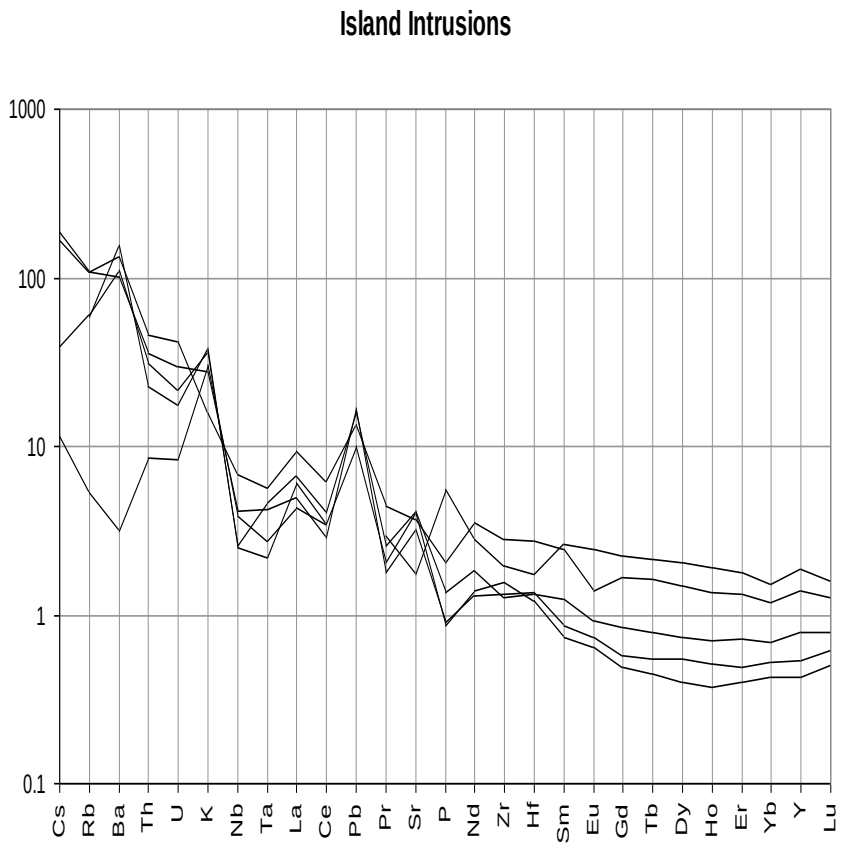

Figure 13. (Cont.)

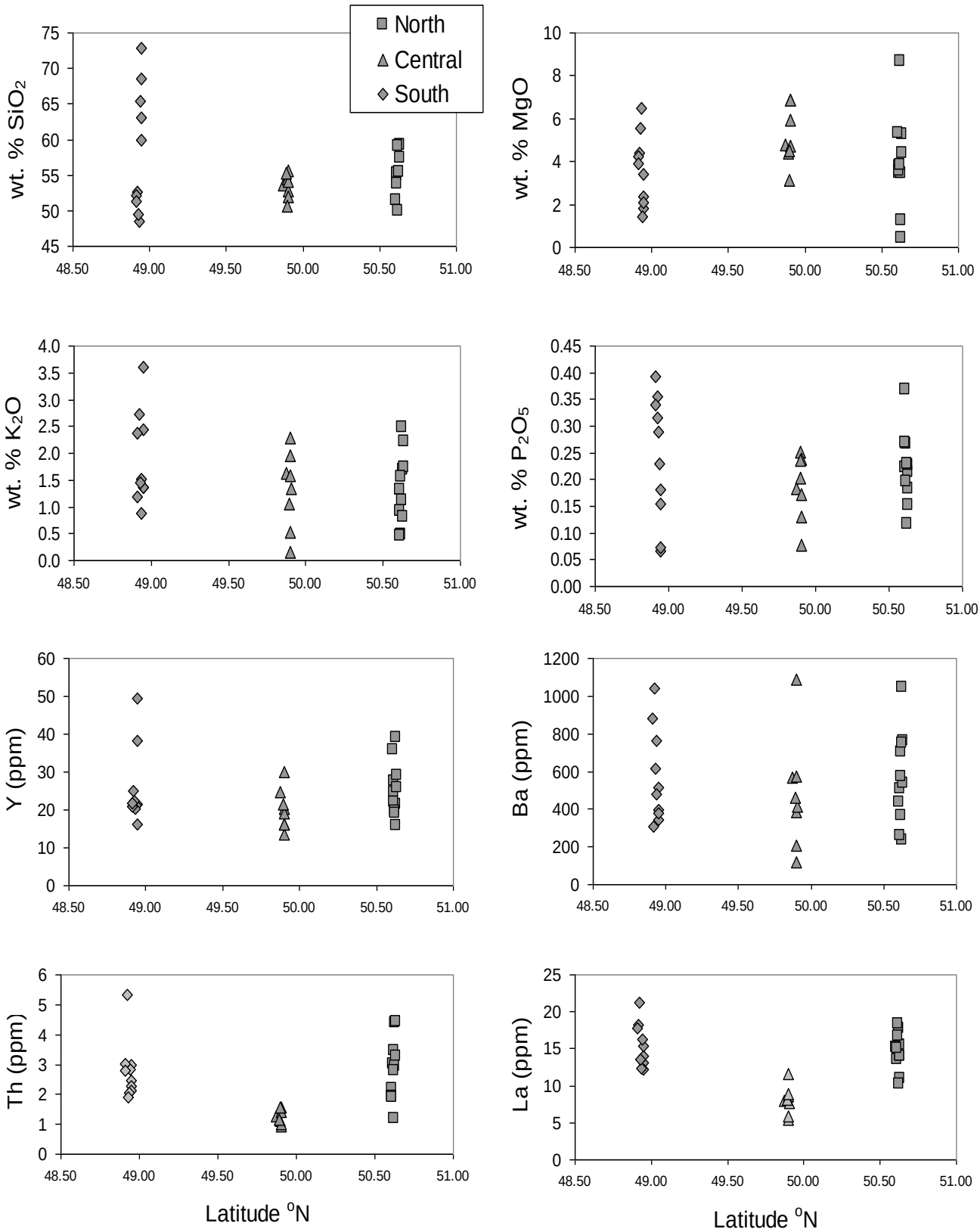

Figure 14. Select major and trace elements plotted against latitude of volcanic rocks from the Bonanza Arc to demonstrate along-strike variations within the Bonanza arc. North refers to the Pemberton Hills region, Central refers to the Nootka Sound region, and South refers to the Alberni region of Vancouver Island.

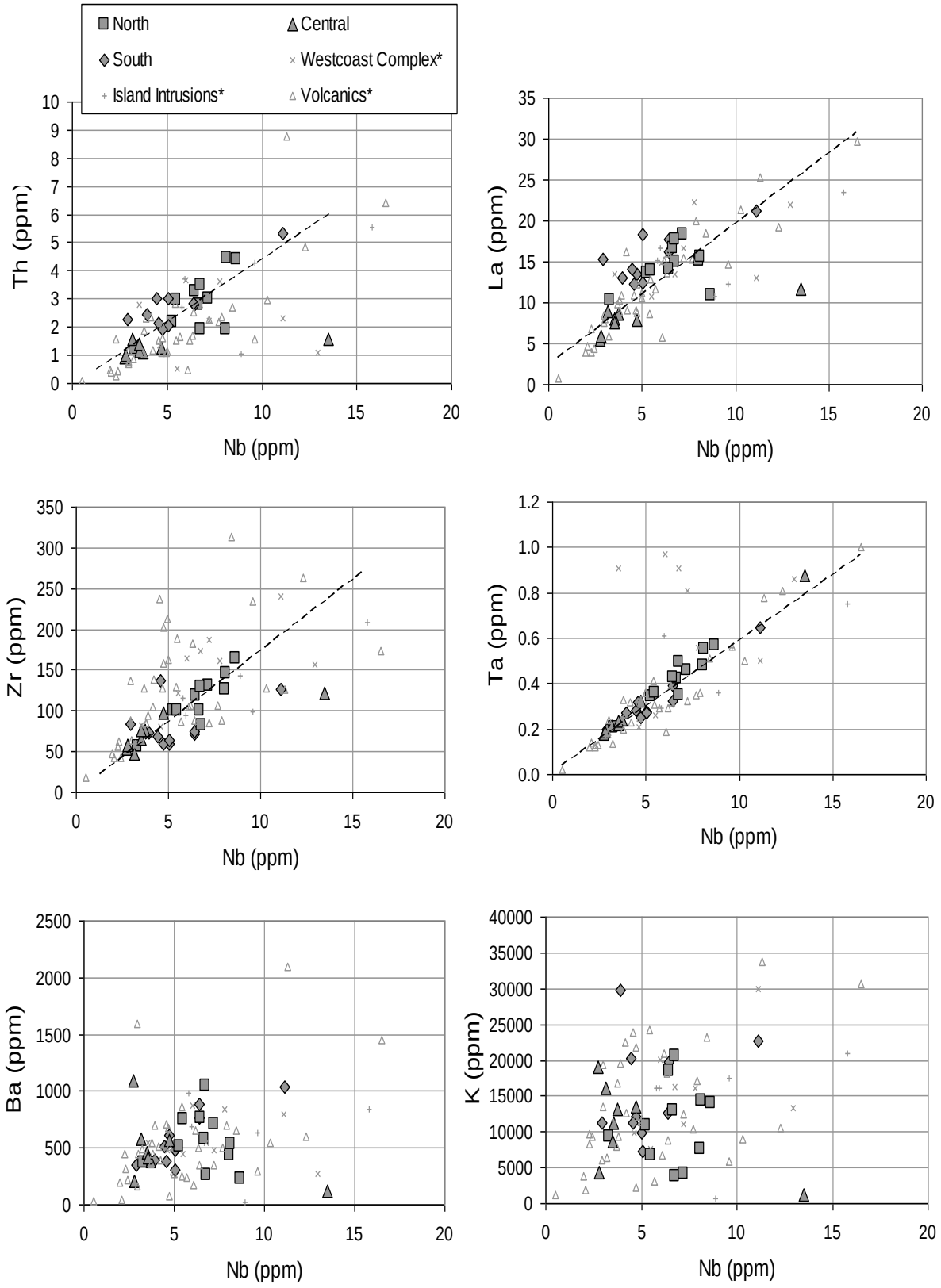

Figure 15. Select trace elements plotted against Nb of volcanic rocks from the Bonanza Arc to examine alteration. North refers to the Pemberton Hills region, Central refers to the Nootka Sound region, and South refers to the Alberni region of Vancouver Island. *data from DeBari et al., 1999

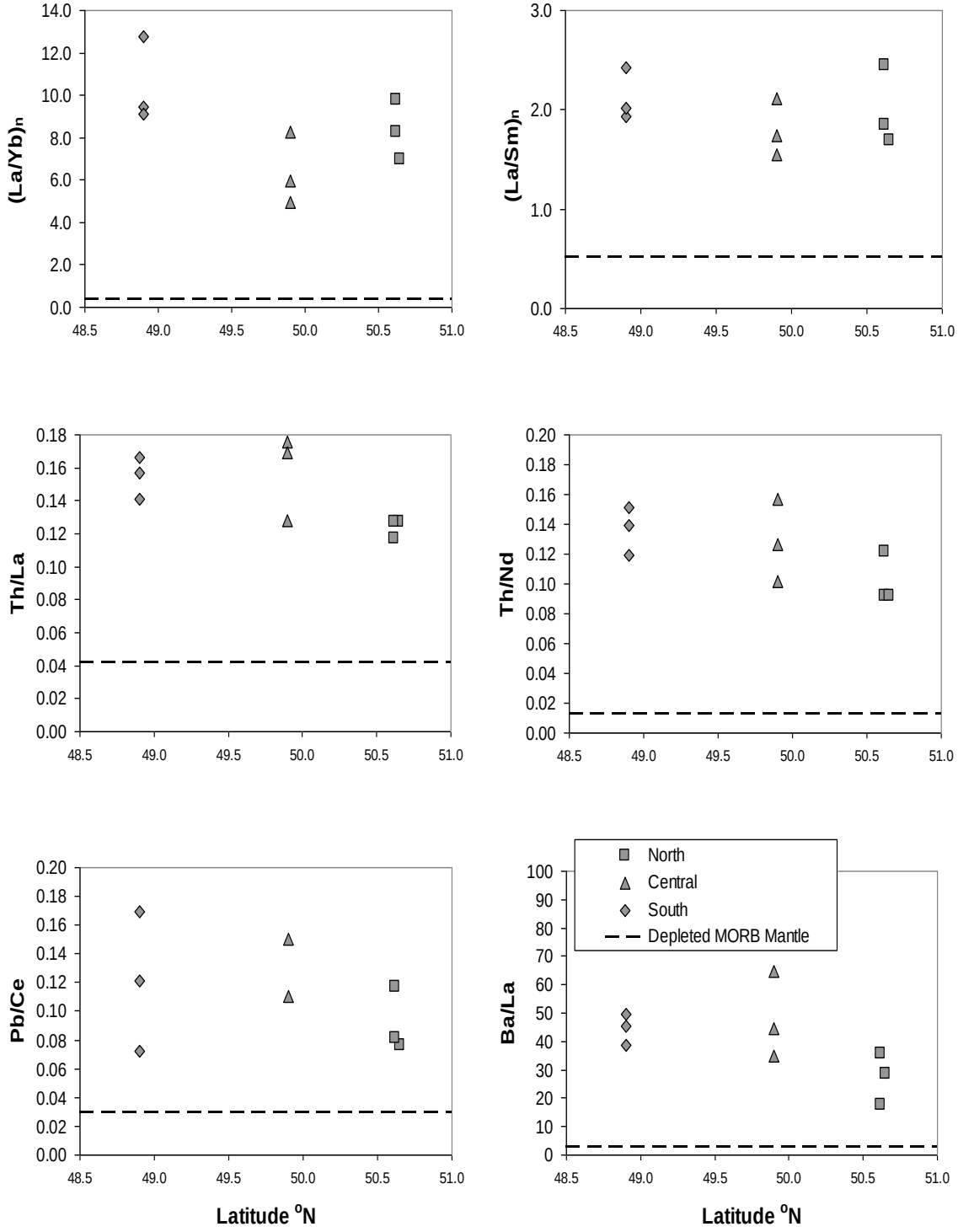

Figure 16. Select trace element ratios plotted against latitude of least altered, most mafic volcanic rocks from the Bonanza Arc. $(La/Yb)_n$ and $(La/Sm)_n$ are normalized to chondrite and show relative enrichment in REEs. Th/La and Th/Nd are indicators of sediment melt addition where Pb/Ce and Ba/La represent addition from the slab fluid. Dashed line represent depleted MORB mantle baseline. North refers to Pemberton Hills region, Central refers to Nootka Sound region, and South refers to Alberni region. *Data from DeBari et al., 1999

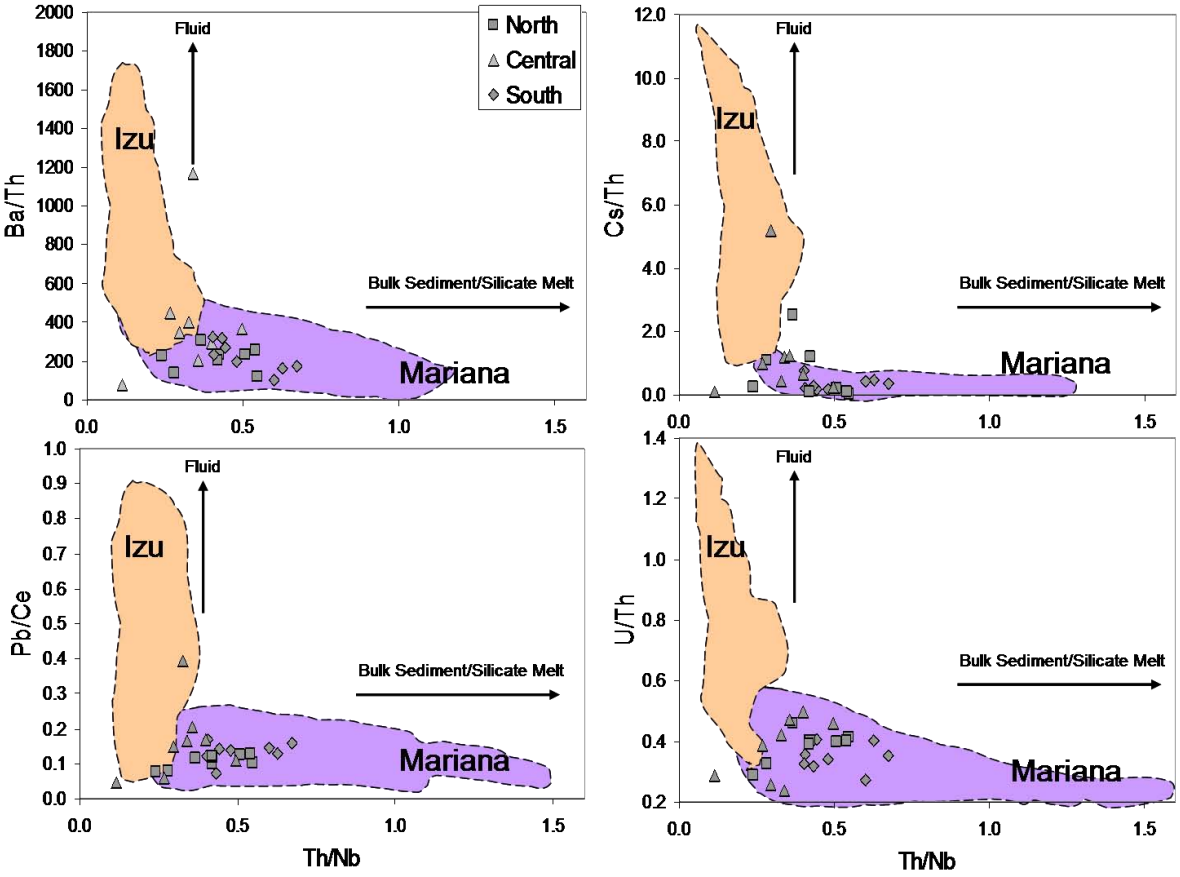

Figure 17. Variation of **s**elect trace element ratios of volcanic rocks with <58 wt.% SiO_2 from the Bonanza Arc indicating the relative amounts of sediment/silicate melt and/or slab fluid addition. Fields plotted for Izu and Mariana arc systems from Bryant et al., (2003) and references therein. North refers to Pemberton Hills region, Central refers to Nootka Sound region, and South refers to Alberni region.

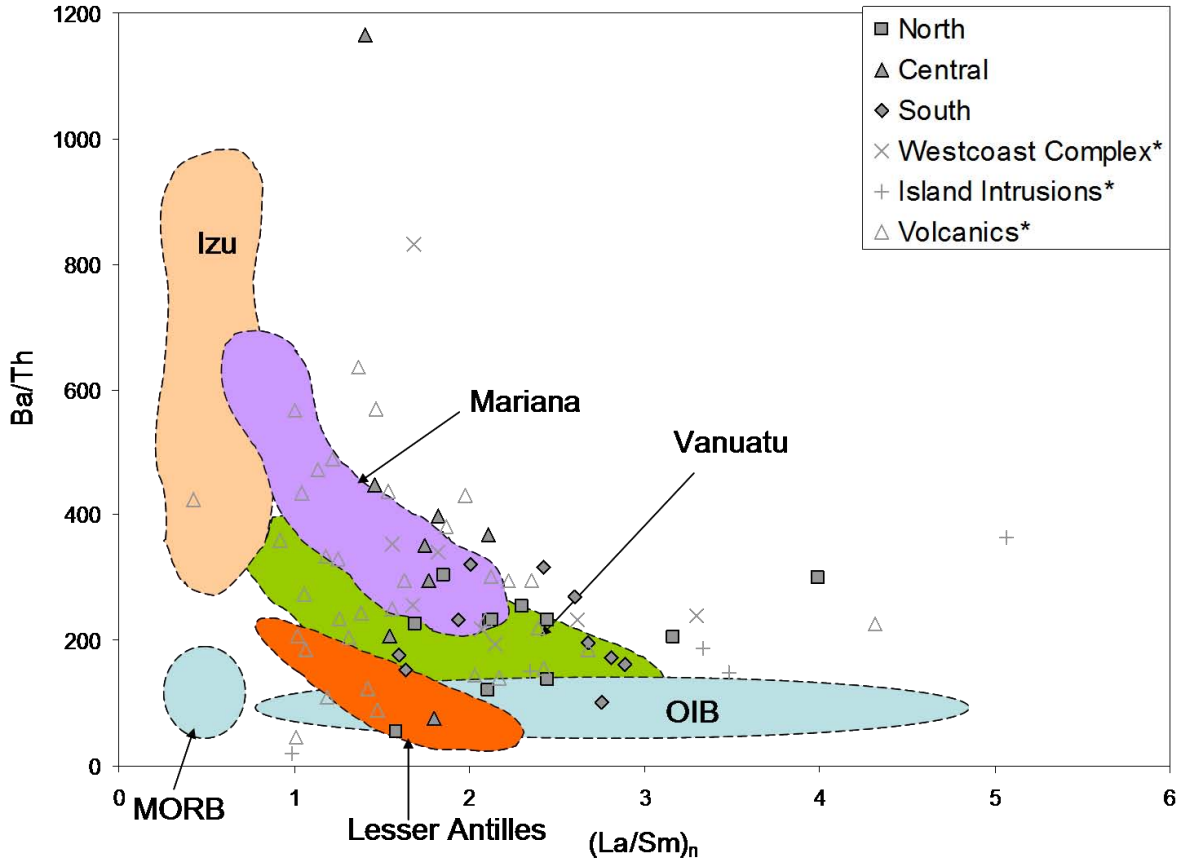

Figure 18. Plot of Ba/Th against $(La/Sm)_n$ normalized to chondrite of samples collected from the Bonanza arc. Enrichment of Ba/Th is interpreted to represent addition of slab fluids to arc magmas (Elliott 2003). Data for the regions of the various arcs, MORB and OIB are from Elliott 2003, and references therein. North refers to Pemberton Hills region, Central refers to Nootka Sound region, and South refers to Alberni region. *Data from DeBari et al., 1999

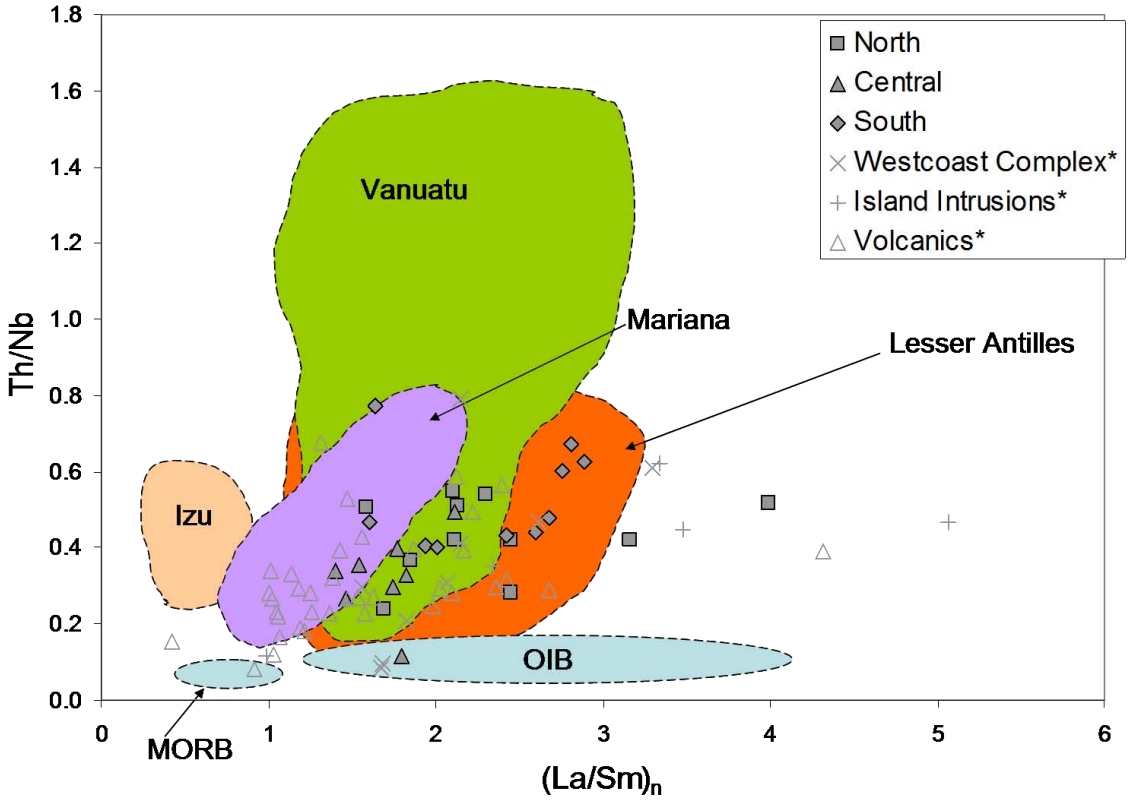

Figure 19. Plot of Th/Nb against $(La/Sm)_n$ normalized to chondrite of samples collected from the Bonanza arc. Enrichment of Th/Nb is interpreted to represent addition of sediment melt to arc magmas (Elliott 2003). Data for the regions of the various arcs, MORB and OIB are from Elliott (2003), and references therein. North refers to Pemberton Hills region, Central refers to Nootka Sound region, and South refers to Alberni region.
*Data from DeBari et al., 1999

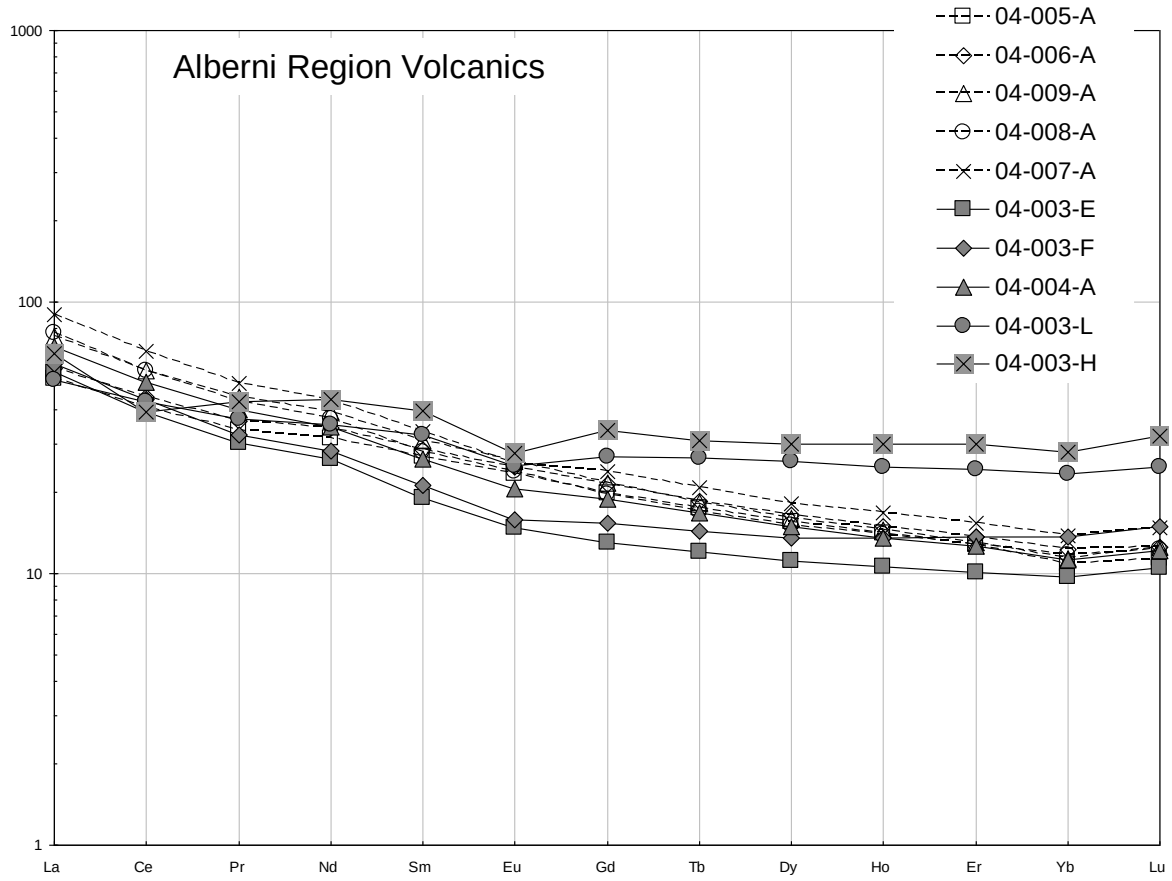

Figure 20. Chondrite-normalized rare earth element (REE) diagram for volcanic samples from the Alberni region of southern Vancouver Island. Samples from the Red Bed Creek facies are represented by solid lines with filled symbols, while samples from the Klanawa facies are represented by dashed lines with open symbols.

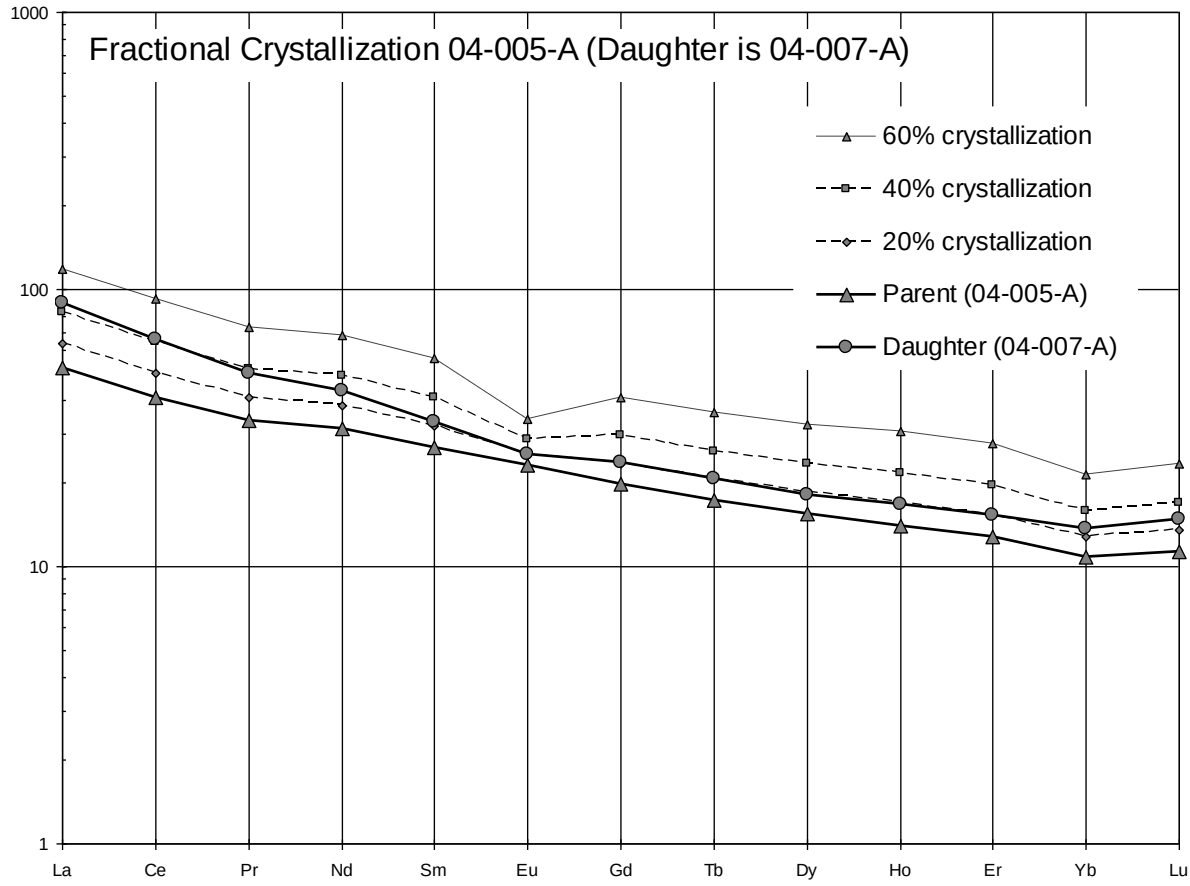

Figure 21. Chondrite-normalized rare earth element (REE) diagram of solutions to the Rayleigh fractionation equations from step 1. The parent rock is 04-005-A, the daughter is 04-007-A and crystallization is shown in a step-wise fashion with 20% increments of crystallization.

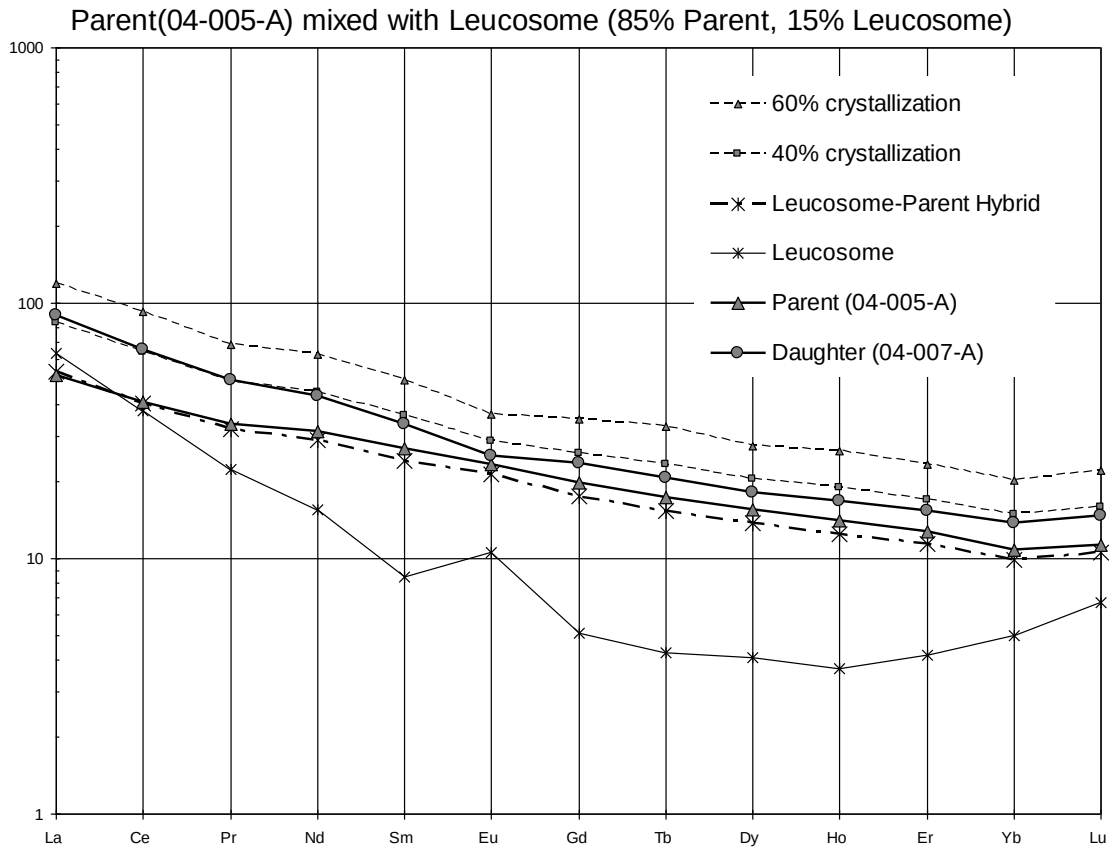

Figure 22. Chondrite-normalized rare earth element (REE) diagram of solutions to the Rayleigh fractionation equations of hybrid sample from step 1. The parent rock is 04-005-A, the daughter is 04-007-A and crystallization is shown for both 40% and 60% crystallization. The hybrid shown is a mixture of 85% of 04-005-A mixed with 15% of leucosome 91-039d.

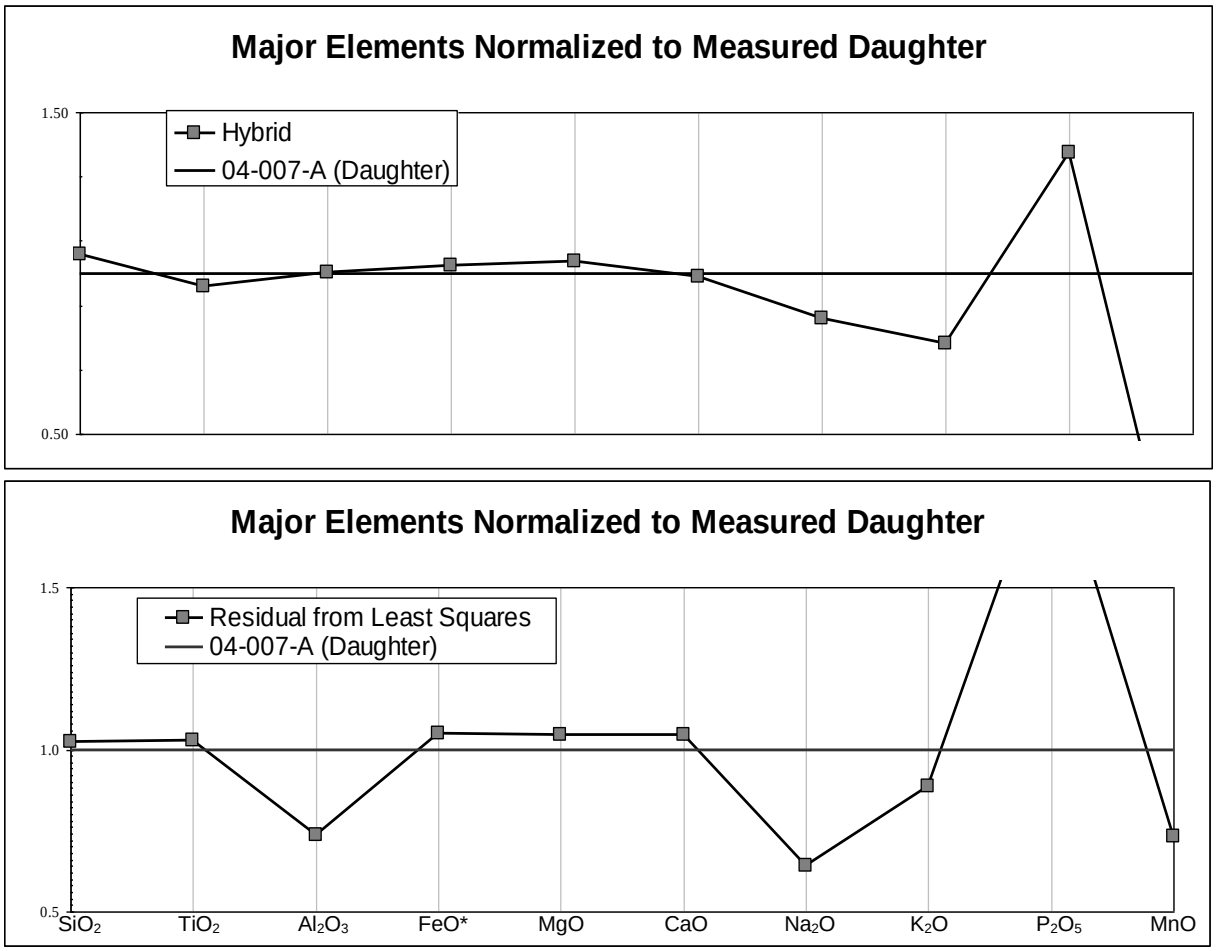

Figure 23. Line diagram comparing major elements of modeled samples to measured daughter sample 04-007-A. Top line represents the major elements of the hybrid magma mixed from 85% of sample 04-005-A and 15% of leucosome 91-039d normalized to the measured daughter sample 04-007-A. The bottom line shows the major elements of the residual magma calculated from least-squares regression normalized to the measured daughter sample (04-007-A).

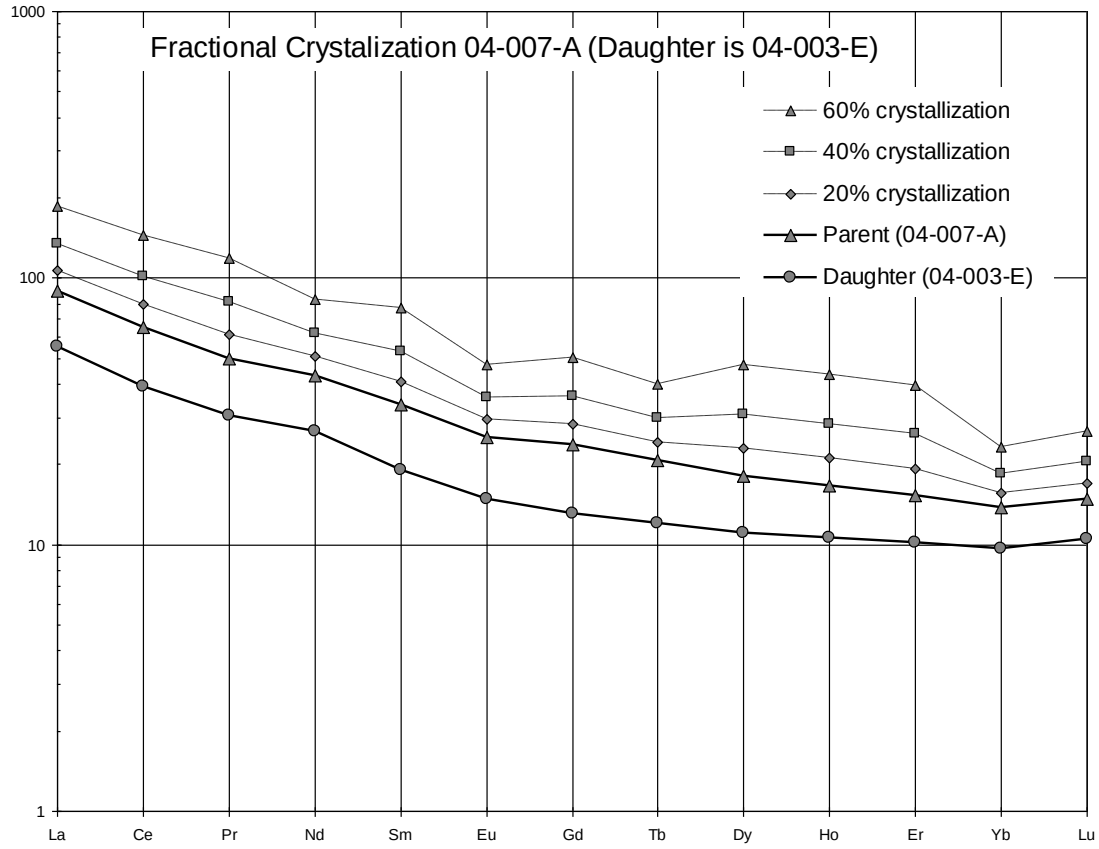

Figure 24. Chondrite-normalized rare earth element (REE) diagram of solutions to the Rayleigh fractionation equations for step 2. Parent is 04-007 and the daughter is 04-003-E crystallization is shown in a step-wise fashion with 20% increments of crystallization.

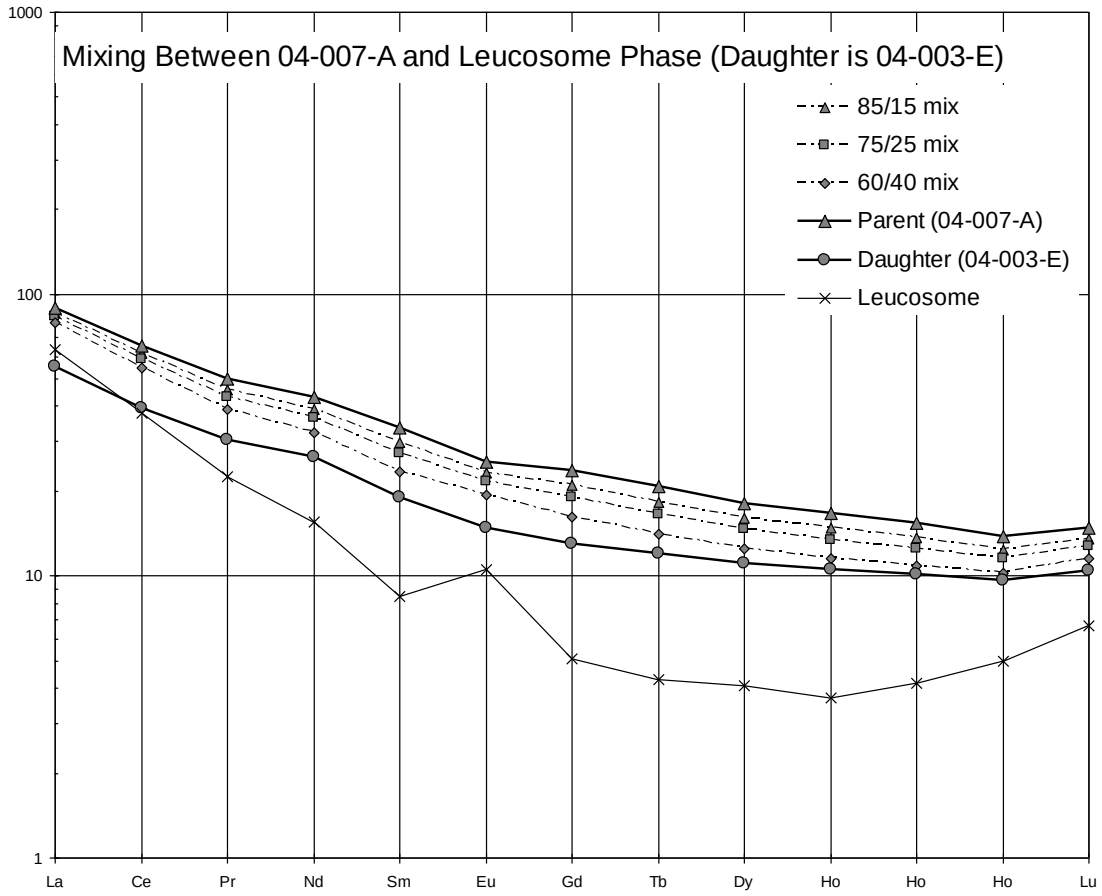

Figure 25. Chondrite-normalized rare earth element (REE) of mixing of different proportions between parent 04-007-A and leucosome 91-039d. Daughter sample is 04-003-E and mixing is shown at 85% parent - 15% leucosome, 75% parent – 25% leucosome, and 60% parent – 40% leucosome.

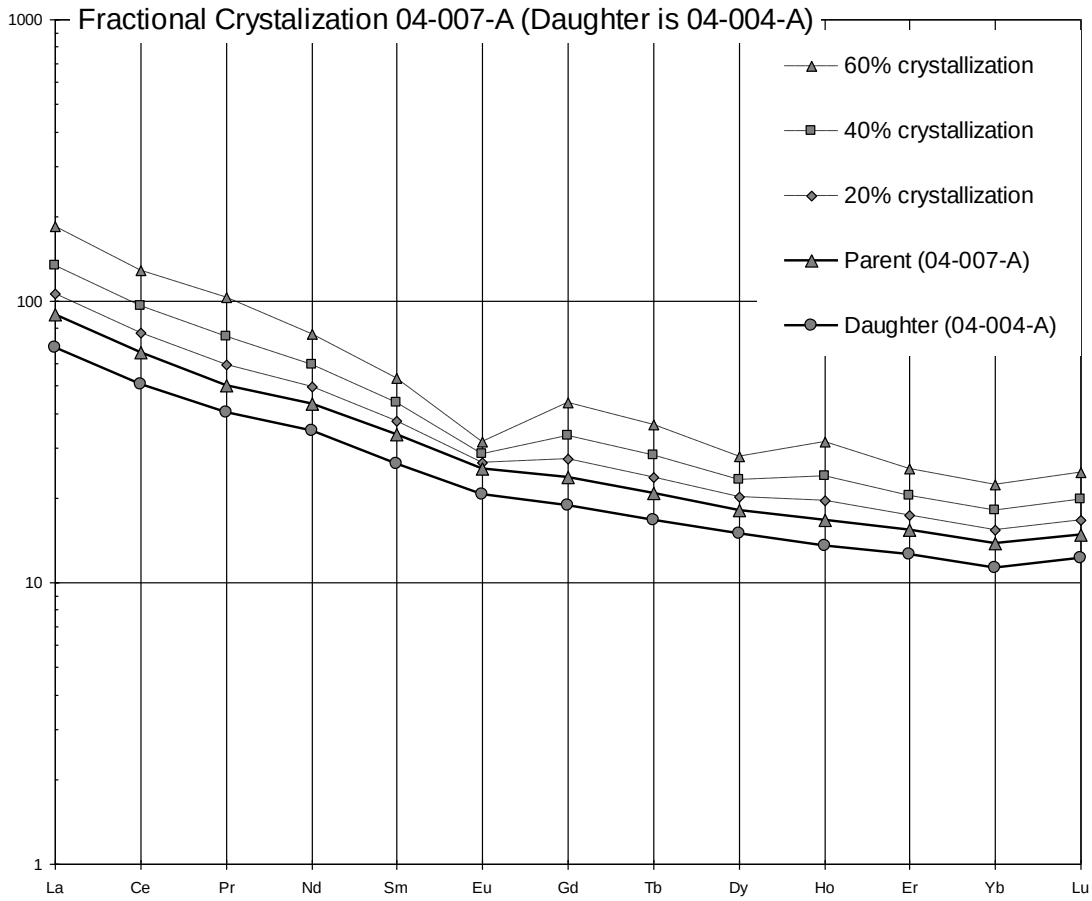

Figure 26. Chondrite-normalized rare earth element (REE) diagram of solutions to the Rayleigh fractionation equations for step 2, try 2. Parent is 04-007 and the daughter is 04-004 crystallization is shown in a step-wise fashion with 20% increments of crystallization.

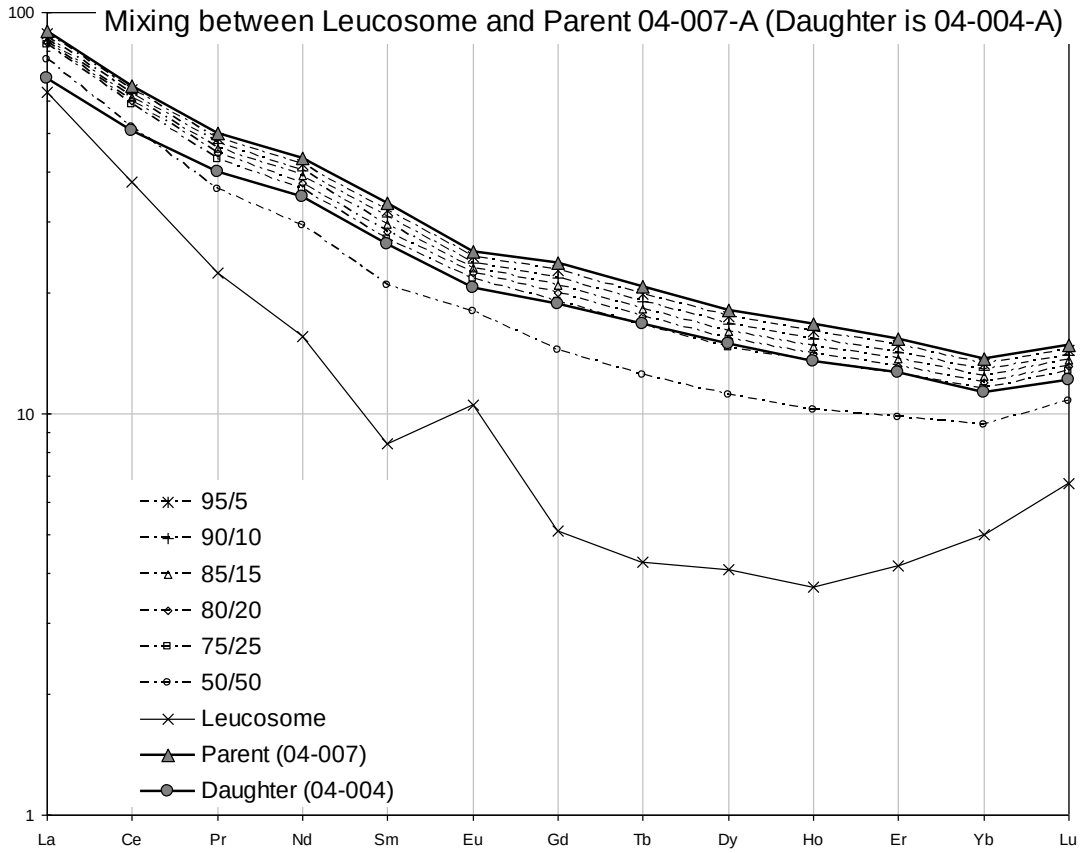

Figure 27. Chondrite-normalized rare earth element (REE) of mixing between the parent 04-007 and leucosome 91-039d to model daughter 04-004. Mixing occurs in various proportions ranging from 90% parent – 10% leucosome, 85% parent – 15% leucosome, 80% parent – 20% leucosome, 75% parent – 25% leucosome, and 50% parent – 50% leucosome.

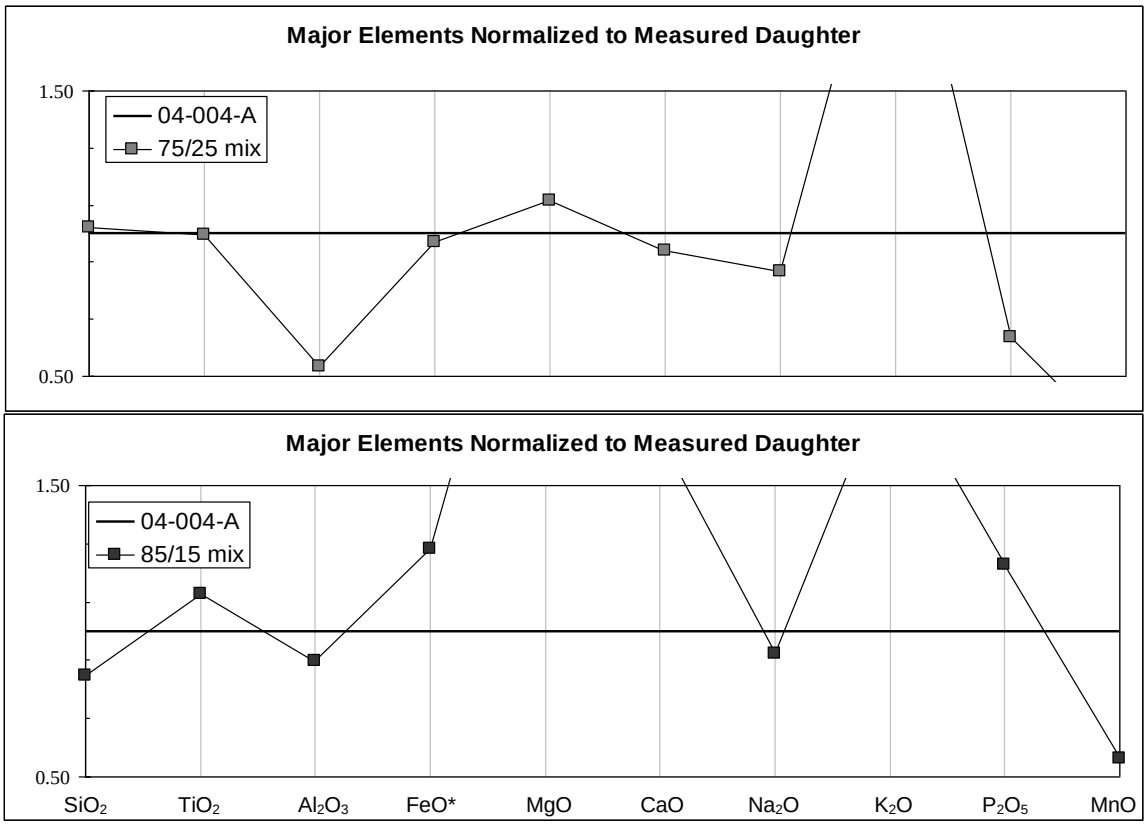

Figure 28. Line diagram comparing major elements of modeled samples to measured daughter sample 04-004-A. Top represents the major elements of the hybrid magma mixed from 85% of sample 04-007-A (parent) and 15% of leucosome 91-039d normalized to the measured daughter sample 04-004-A. Bottom represents the major elements of the hybrid magma mixed from 75% of sample 04-007-A (parent) and 25% of leucosome 91-039d normalized to the measured daughter sample 04-004-A.

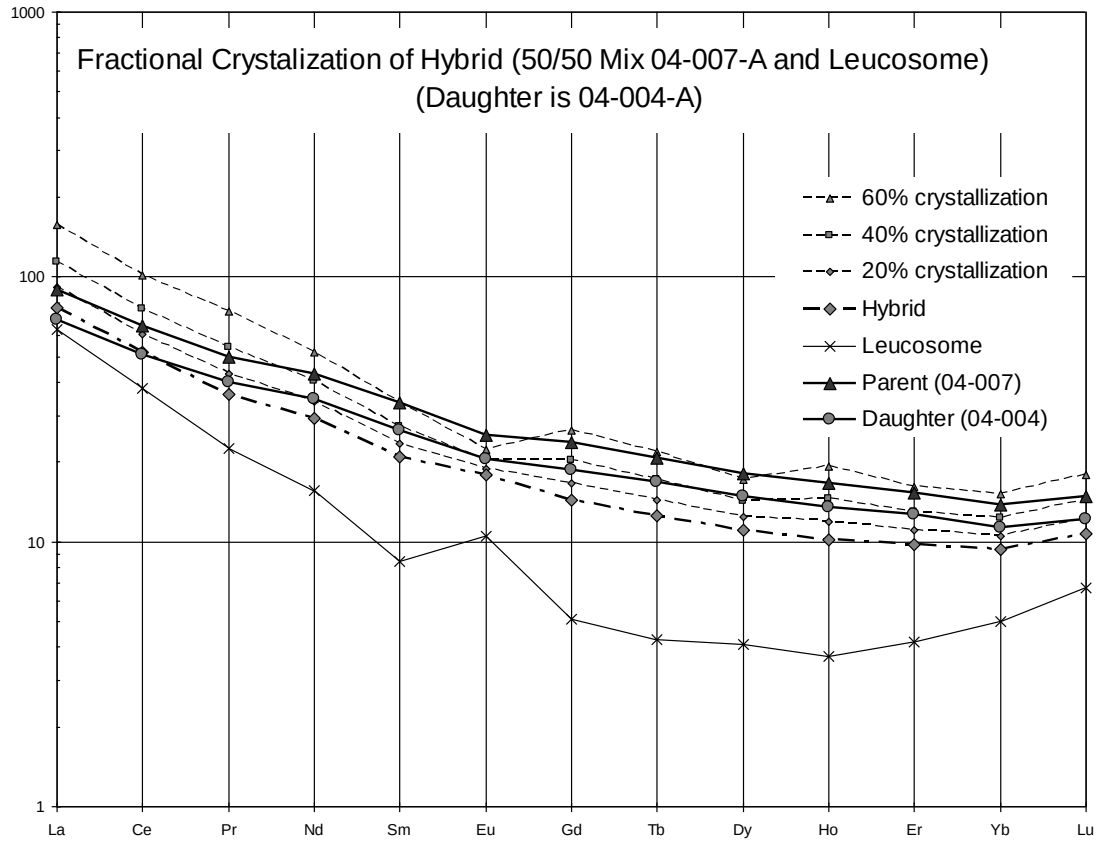

Figure 29. Chondrite-normalized rare earth element (REE) diagram of solutions to the Rayleigh fractionation equations for the hybrid magma mixed from 50% parent (04-007-A) and 50% leucosome (91-039d) crystallized at 20% increments.

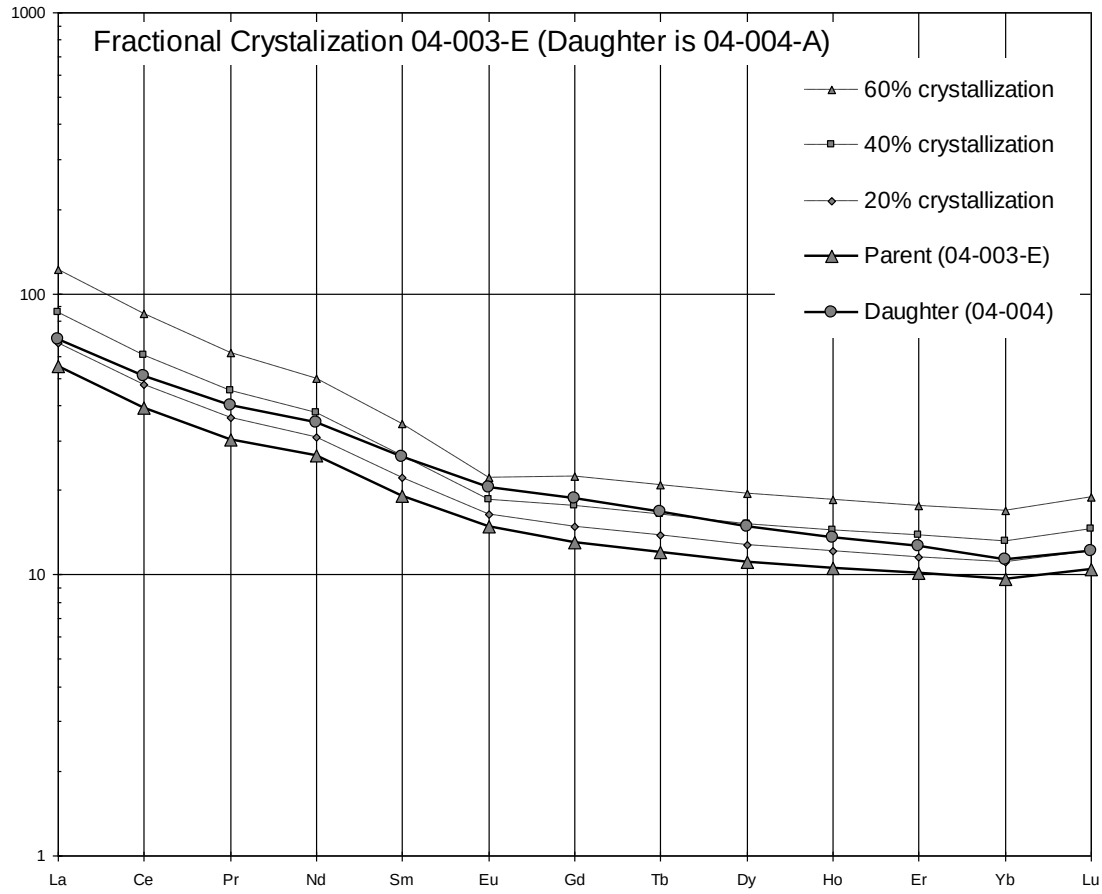

Figure 30. Chondrite-normalized rare earth element (REE) diagram of solutions to the Rayleigh fractionation equations for step 3. Parent is 04-003-E and the daughter is 04-004 crystallization is shown in a step-wise fashion with 20% increments of crystallization.

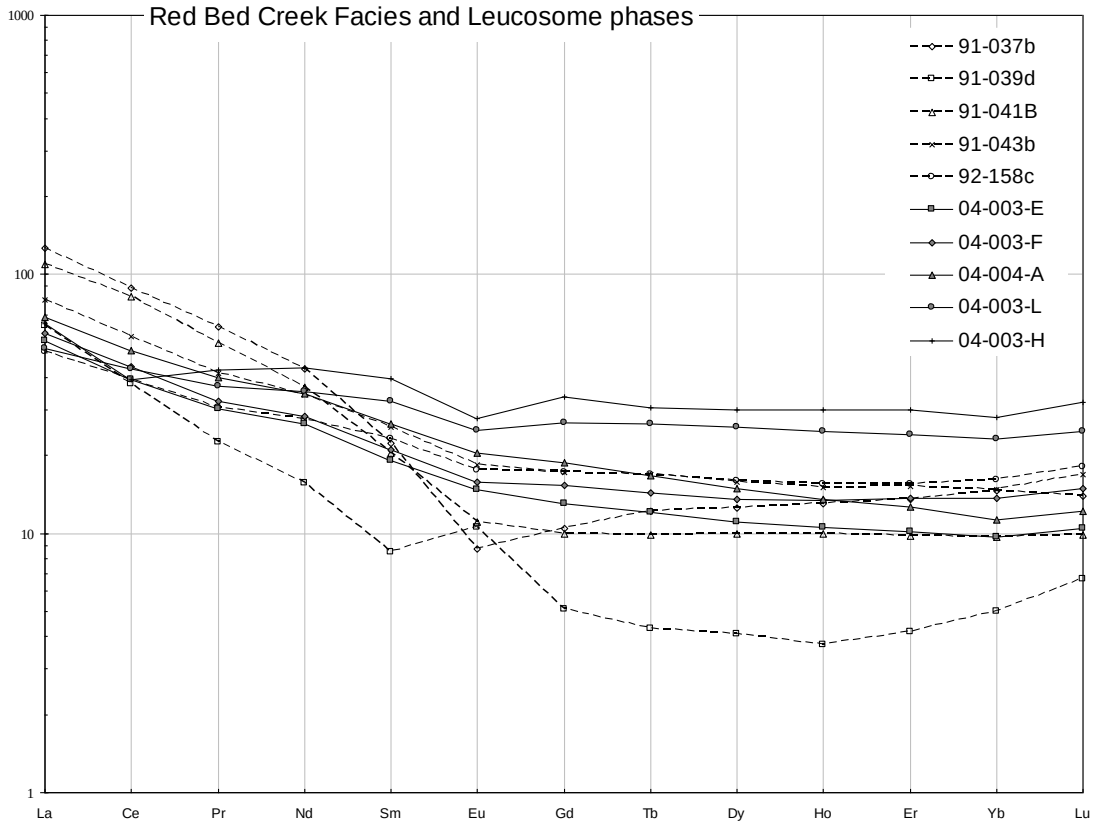

Figure 31. Chondrite-normalized rare earth element (REE) diagram of the Red Bed Creek facies of the Alberni region of Vancouver Island and selected leucosomes phases of the Westcoast Crystalline Complex.

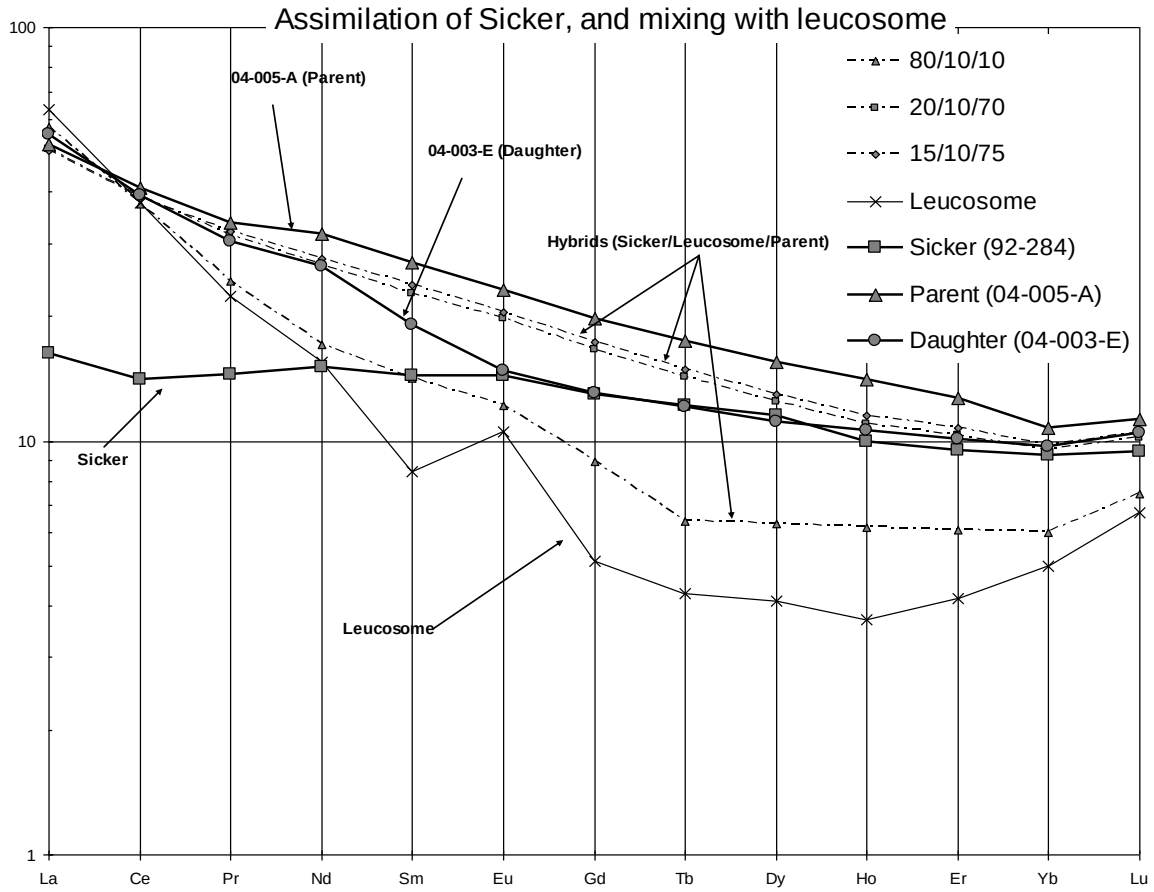

Figure 32. Chondrite-normalized rare earth element (REE) diagram of magma mixing between leucosome 91-039d and parent 04-005-A with assimilation of preexisting Sicker arc crust. Daughter is 04-003-E and hybrid magmas are mixtures of 80% leucosome - 10% Sicker crust (92-284) - 10% parent, 20% leucosome – 10% Sicker crust - 70% parent, and 15% leucosome – 10% Sicker crust - 75% parent.

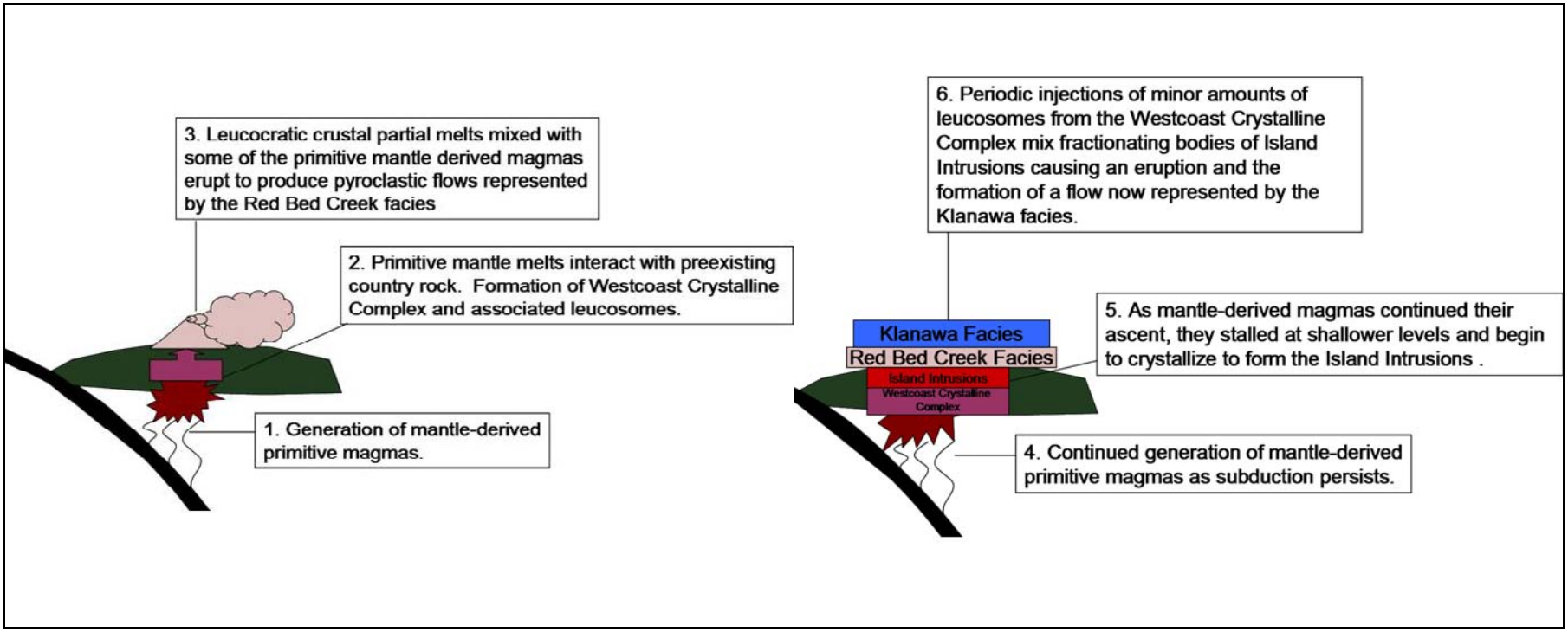

Figure 33. A time-integrated, petrogenetic model for the generation of the volcanic rocks in the Alberni region of Vancouver Island

TABLES

Table 1. Summary of Ages of the Bonanza Arc

Type	Location	Age (Ma)	Author
WCC			
U-Pb	Tofino	264±7	Muller et al. (1974b)
	Meares Island	180±4, 190±12	Isachsen (1987)
	Alberni Region, 48°42'06"N, 124°43'25"W	190.3±0.7	DeBari et al. (1999)
	Alberni Region, 48°34'20"N, 124°43'25"W	174.2±0.4	DeBari et al. (1999)
	Alberni Region, 48°50'55"N, 125°04'16"W	177.3±1.8	DeBari et al. (1999)
Rb-Sr	Black River	151±15, 169±3	Isachsen (1984)
K-Ar	Meares Island	172±6	Isachsen (1987)
		163±7, 115±5	Wanless et al. (1974)
Island Intrusions			
U-Pb	Southern Vancouver Island	168±2	Parrish and McNicoll (1992)
	Port Hardy	167±0.5, 168 +8/-2	Friedman and Nixon (1995)
	Port Alberni, 49°10'31"N, 124°46'09"W	175.7±2.6	DeBari et al. (1999)
	Alberni Region, 48°40'40"N, 124°06'15"W	170.3±0.9	DeBari et al. (1999)
	Nootka Sound Region, 50°12'45"N, 126°26'45"W	168.6±5.3	DeBari et al. (1999)
^{40}Ar-^{39}Ar	Port Hardy, Shore of Nahwitti Lake East end of Holberg Inlet	176, 166	Archibald and Nixon (1995)
K-Ar		181–152	Carson (1973); Muller (1977)
Bonanza Volcanics			
U-Pb	Port Hardy	202±3; 165; 169	Friedman and Nixon (1995)
Bivalves	Nootka Sound 49°53'35"N, 127°10'35"W	Pliensbachian	Muller et al. (1981)
Bivalves	Nootka Sound 49°53'50"N, 127°11'00"W	Pliensbachian	Muller et al. (1981)
Ammonites	Nootka Sound 49°53'50"N, 127°11'00"W	Late Pliensbachian	Muller et al. (1981)
Bivalves	Nootka Sound 49°55'35"N, 127°12'55"W	Lower Jurassic	Muller et al. (1981)

Table 2. Petrographic Summary of the Bonanza Volcanics

Lithology	Petrographic Characteristics	Phase Proportions		
Bonanza Volcanics		Phenocrysts		Size
Alberni Region (Red Bed Creek) 48-65% SiO_2 Alteration minerals: Chlorite, calcite, oxides	Typically massive, maroon-colored crystal lithic tuffs composed of fine lithic clasts, phenocrysts, and matrix. Euhedral to subhedral <1mm - 2 mm phenocrysts, angular lithic fragments and devitrified volcanic glass. The matrix is mostly ash with opaque disseminated hematite.	Plag. Pyroxene Biotite Oxides Qtz Lithics	10-15% 10-20% 0-10% 0-5% 0-5% 0-20%	<1 - 2mm <1 - 2mm <1mm <1mm <1mm 1-2mm
Alberni Region (Klanawa Facies) 60-73% SiO_2 Alteration minerals: Chlorite, calcite, oxides, zeolites	Plagioclase-phyric, basalts, basaltic andesite and andesite lava flows with 60-80% groundmass containing phenocrysts of plagioclase, pyroxene, and rare potassium feldspar. Angular lithic fragments, calcite filled amygdules, and semi-opaque devitrified glass is also present.	Plag. Pyroxene Amphibole Oxides Qtz	10-25% 5-10% 0-10% 0-5% 0-5%	0.3-1.5 mm <1 - 2mm <1 - 1mm <1mm <1mm
Nootka Sound Region 51-56% SiO_2 Alteration minerals: Chlorite, sericite, zeolites, clay and calcite	Basalts, basaltic andesites, and andesite porphyries, crystal lithic tuffs, lapilli tuffs, and block and ash flows. Phenocrysts in the porphyries are dominated by plagioclase and less pyroxene, with rare amphibole, +/- biotite, quartz, and potassium feldspar.	Plag. Pyroxene Biotite Amphibole Qtz/K-spar	10-25% 5-15% 0-5% 0-10% 0-5%	1 - 8mm 1 - 2mm <1mm <1 - 1.5 mm <1mm
Pemberton Hills Region 50-71% SiO_2 Alteration minerals: Chlorite, sericite, zeolites, clay and calcite	Flows of basalt, basaltic andesite, andesite and rhyolite as well as air-fall tuffs, lapilli tuffs and block and ash flows. Phenocrysts are 20-50% (by volume) of the lava flows. Lithic fragments in the block and ash flows and the lithic tuffs are typically plagioclase-rich, sub-rounded to sub-angular, 1mm to 2mm clasts that can reach up to 4cm in the block and ash flows.	Plag. Pyroxene Amphibole Oxides Qtz/K-spar	10-30% 0-10% 0-10% 0-10% 0-15%	<1 - 1.5mm <1 -1.2 mm <1mm <1mm <1 - 1.5mm

Table 3. Electron microprobe analyses (Pyroxene)

Clinopyroxene	SiO_2	TiO_2	Al_2O_3	FeO	MnO	MgO	CaO	Na_2O	Total	Mg #
Volcanic										
005CPX2	51.35	0.51	2.91	8.55	0.31	15.04	21.11	0.30	100.06	75.82
007CPX1	52.10	0.62	2.76	9.18	0.29	14.52	21.14	0.35	100.95	73.82
007CPX2	50.84	0.58	2.87	9.23	0.30	14.71	21.10	0.34	99.98	73.96
007CPX3	52.04	0.62	2.84	7.99	0.22	14.84	21.73	0.31	100.60	76.80
Plutonic										
933-88cpx1	53.06	0.38	2.23	19.60	1.60	17.16	2.71	0.46	97.22	60.95
933-88cpx2	51.40	0.49	3.37	16.53	1.56	13.90	9.53	0.78	97.57	59.98
933-88cpx3	52.56	0.44	2.24	19.89	1.54	17.12	2.68	0.50	97.00	60.54
933-88cpx4	53.05	0.26	1.55	22.53	2.46	15.85	1.40	0.34	97.43	55.64
933-88cpx5	51.80	0.36	2.13	21.19	1.71	16.53	2.62	0.39	96.75	58.17
933-88cpx6	52.78	0.23	1.62	22.50	2.64	15.69	1.49	0.35	97.32	55.42

Table 4. Electron microprobe analyses (Plagioclase)

Plagioclase	SiO_2	Al_2O_3	FeO	CaO	Na_2O	K_2O	SrO	Total	An
Volcanic									
004pl1	65.63	20.77	0.12	0.81	10.68	0.31	0.11	98.43	6.78
004pl2	73.11	17.44	0.20	0.99	8.66	0.30	0.08	100.77	9.89
004pl3	67.15	20.76	0.08	0.72	10.79	0.33	0.11	99.94	6.01
004pl4	65.20	21.01	2.14	1.10	10.13	0.19	0.16	99.92	9.46
004pl5	63.32	23.46	1.01	1.15	9.02	1.35	0.12	99.45	10.93
004pl6	60.44	20.63	2.00	4.48	9.05	0.72	0.16	97.46	32.25
004pl7	60.13	25.04	0.21	6.85	4.66	0.06	0.10	97.06	58.65
004pl8	65.83	21.14	0.05	1.18	10.70	0.20	0.45	99.55	9.60
005pl1	55.15	28.49	0.66	11.27	4.92	0.51	0.17	101.18	68.80
005pl2	49.81	29.90	0.95	14.79	3.50	0.22	0.15	99.32	80.29
005pl3	52.76	29.63	0.88	12.85	4.33	0.27	0.13	100.86	74.07
007pl1	53.83	29.24	0.64	11.72	4.15	0.80	0.15	100.53	73.13
007pl2	59.15	24.72	0.77	4.94	7.53	1.25	0.18	98.54	38.70
007pl3	56.60	27.37	0.60	9.25	5.82	0.62	0.15	100.42	60.48
024pl1	56.47	27.09	0.82	9.62	5.55	0.44	0.17	100.16	62.53
024pl3	69.48	19.70	0.13	0.16	11.31	0.12	0.08	100.99	1.38
024pl4	69.47	19.45	0.08	0.05	11.66	0.05	0.01	100.77	0.38
027pl1	52.76	29.34	1.03	12.86	3.97	0.20	0.09	100.25	75.74
027pl2	52.03	29.38	0.88	13.16	3.94	0.18	0.11	99.68	76.28
027pl3	54.05	28.20	1.02	11.69	4.45	0.30	0.12	99.84	71.66
027pl4	56.79	26.22	1.17	9.31	5.76	0.53	0.11	99.89	60.88
027pl5	68.95	19.65	0.08	0.24	11.39	0.05	0.03	100.39	1.98
027pl6	68.65	19.85	0.08	0.45	11.47	0.05	0.07	100.61	3.61
034pl1	47.19	21.13	8.79	3.45	5.12	0.24	0.04	85.95	39.35
034pl2	53.47	28.55	0.67	11.66	4.61	0.25	0.11	99.33	70.92
034pl3	53.12	28.03	0.66	11.28	4.88	0.27	0.11	98.36	69.02
034pl4	54.96	25.10	2.12	7.71	6.26	0.52	0.13	96.81	54.29
034pl5	52.84	29.00	0.73	11.75	4.37	0.38	0.09	99.16	72.15
Plutonic									
082pl1	58.02	27.11	0.38	5.89	5.85	2.20	0.01	99.46	49.24
082pl2	57.16	24.49	0.16	7.32	6.64	0.31	0.09	96.17	51.52
082pl3	58.43	25.88	0.19	7.90	6.75	0.37	0.10	99.62	53.00
082pl4	57.86	26.28	0.18	8.39	6.48	0.37	0.10	99.66	55.48
082pl5	57.71	26.04	0.11	8.16	6.64	0.32	0.12	99.08	54.19
933-88pl1	57.47	26.32	0.21	8.99	6.27	0.26	0.12	99.64	58.00
933-88pl2	56.35	26.77	0.25	9.29	6.06	0.28	0.12	99.11	59.61
933-88pl4	56.85	26.77	0.25	9.08	6.14	0.30	0.13	99.52	58.74

Table 5. Electron microprobe analyses (Amphibole)

Amphibole	SiO_2	TiO_2	Al_2O_3	FeO	MnO	MgO	CaO	Na_2O	K_2O	Total	Mg #
Volcanic											
005amph1	49.70	0.87	5.44	9.26	0.26	13.43	21.27	0.42	-	100.65	72.11
005amph2	47.86	0.83	6.63	8.03	0.18	13.57	22.45	0.26	-	99.86	75.08
Plutonic											
082amph1	45.82	0.99	6.28	13.87	0.65	12.67	13.33	0.87	-	94.48	61.95
082amph2	48.02	1.13	6.64	14.52	0.68	13.36	11.66	0.90	-	96.94	62.12
082amph3	48.38	0.91	5.84	13.89	0.70	13.89	11.65	0.93	-	96.18	64.06
082amph4	48.72	1.02	6.27	14.03	0.71	13.64	11.54	0.87	-	96.81	63.41
1-1 h-q*	47.91	0.36	4.14	14.38	0.76	12.42	10.63	0.73	0.31	91.62	60.62
1-5 h-q*	46.53	0.70	6.97	16.48	0.88	11.61	10.30	1.30	0.39	95.16	55.65
2-1 h-q*	48.07	1.30	6.81	14.18	0.34	13.12	10.81	1.22	0.39	96.23	62.25
92b h-q*	47.13	1.20	6.26	16.77	0.73	11.90	10.91	1.35	0.64	96.88	55.84
92b-4 h-q*	47.46	1.27	6.04	15.02	0.58	13.41	10.88	1.39	0.63	96.69	61.41
90-5 h-q*	44.32	1.78	7.13	20.23	0.81	9.38	10.80	1.79	0.74	96.97	45.26
92-275-1*	48.59	0.89	7.17	15.00	0.67	12.69	11.39	1.17	0.50	98.06	60.14
92-275-1 r*	46.59	0.85	7.07	15.51	0.71	12.69	11.56	1.19	0.52	96.69	59.31
92-190-1 r*	49.39	1.65	7.31	12.78	0.53	14.33	11.00	1.36	0.39	98.74	66.66

* Amphibole data supplemented from DeBari S.M. unpublished data

Table 6. Whole-rock analyses of igneous rocks of the Bonanza arc

Sample	04-005-A	04-006-A	04-009-A	04-008-A	04-007-A	04-003-E	04-003-F	04-004-A
UTM E	388690	388208	387375	388044	387915	389281	389281	388900
UTM N	5421250	5420444	5418785	5418871	5419920	5422789	5422789	5421833
Lithology	Alb. Volc	Alb. Volc	Alb. Volc	Alb. Volc	Alb. Volc	Alb. Volc	Alb. Volc	Alb. Volc
Major Elements (wt.%)								
SiO_2	48.45	49.52	51.32	52.16	52.58	59.91	63.11	65.41
TiO_2	1.18	1.13	0.93	0.88	0.95	0.79	0.54	0.97
Al_2O_3	17.97	19.03	20.46	18.43	18.10	16.92	15.55	15.59
FeO*	11.27	10.46	8.95	10.18	9.21	8.86	6.75	6.78
MnO	0.14	0.20	0.19	0.19	0.19	0.17	0.15	0.30
MgO	6.49	5.56	3.91	4.24	4.40	3.43	2.36	1.43
CaO	11.05	7.54	8.64	9.43	8.60	5.98	8.09	4.65
Na_2O	2.27	4.76	2.84	2.96	2.92	0.20	0.81	3.12
K_2O	0.89	1.46	2.37	1.19	2.73	3.59	2.45	1.52
P_2O_5	0.29	0.35	0.39	0.34	0.32	0.15	0.18	0.23
Mg#	50.7	48.7	43.8	42.6	46.0	40.8	38.4	27.4
Minor Elements (ppm)								
Ni	19.5	20.4	8.7	12.7	14.6	20.3	19.9	32.5
Cr	32.0	23.4	5.5	13.8	10.4	36.7	39.4	194
Sc	36.2	27.7	18.2	22.2	26.4	20.9	15.9	23.4
V	375	331	237	271	264	178	100	205
Sr	476	578	616	574	673	62	105	300
Zr	58.9	60.1	71.4	63.4	126	73.7	68.4	75.3
Ba	478	615	881	309	1040	396	517	765
Ga	18.8	20.5	20.8	19.0	17.2	15.0	13.1	15.4
Cu	59.7	52.4	95.6	3.7	70.9	7.2	45.6	38.5
Zn	90.0	98.4	88.9	100	87.1	84.4	79.3	71.5
Trace Elements (ppm)								
La	12.4	13.6	17.8	18.3	21.2	13.1	14.1	16.3
Ce	25.0	27.4	34.3	34.3	40.2	24.0	26.9	31.1
Pr	3.20	3.47	4.22	4.08	4.75	2.88	3.06	3.82
Nd	14.7	16.0	18.4	17.3	20.2	12.4	13.2	16.2
Sm	4.13	4.35	4.73	4.28	5.11	2.92	3.23	4.04
Eu	1.35	1.44	1.51	1.38	1.47	0.86	0.91	1.19
Gd	4.06	4.37	4.41	4.03	4.87	2.67	3.15	3.85
Tb	0.65	0.69	0.68	0.63	0.77	0.45	0.54	0.63
Dy	3.94	4.16	4.04	3.82	4.60	2.82	3.43	3.78
Ho	0.80	0.84	0.82	0.79	0.95	0.60	0.76	0.76
Er	2.11	2.26	2.16	2.11	2.54	1.68	2.26	2.09
Yb	1.83	2.08	1.94	1.98	2.34	1.65	2.33	1.92
Lu	0.29	0.32	0.32	0.31	0.38	0.27	0.38	0.31
Th	2.05	1.91	2.78	3.03	5.33	2.46	2.99	2.84
Nb	5.06	4.74	6.42	5.05	11.1	3.92	4.44	6.42
Y	20.3	22.3	21.7	20.9	25.1	16.1	21.4	21.2
Hf	1.79	1.77	1.98	1.80	3.40	2.07	1.94	2.11
Ta	0.28	0.25	0.32	0.27	0.64	0.27	0.28	0.39
U	0.73	0.62	0.89	0.83	1.83	0.99	1.05	1.15
Pb	4.23	3.31	2.49	4.94	5.54	3.07	4.31	4.41
Rb	16.4	28.2	52.3	29.7	49.3	68.5	48.4	38.7
Cs	0.48	1.46	0.80	1.32	1.02	1.21	1.07	0.55
Sr	476	578	616	574	673	62	105	300

***Alb. Volc is Alberni region volcanics**

Table 6. Whole-rock analyses of igneous rocks of the Bonanza arc (cont.)

Sample	04-003-L	04-003-H	04-036-A	04-027-A	04-034-A	04-014-A	04-015-A	04-029-B
UTM E	389281	389281	603434	587698	603982	598980	597333	582657
UTM N	5422789	5422789	5608859	5606783	5607644	5607611	5608006	5609098
Lithology	Alb. Volc	Alb. Volc	Pem. Volc	Pem. Volc	Pem. Volc	Pem. Volc	Pem. Volc	Pem. Volc
Major Elements (wt.%)								
SiO_2	68.46	72.81	49.91	51.44	53.71	54.96	55.32	55.51
TiO_2	0.78	0.42	0.92	1.29	0.94	0.89	0.92	0.84
Al_2O_3	14.69	12.54	17.35	20.29	19.61	18.38	19.53	18.78
FeO*	6.35	5.16	9.32	9.46	8.80	8.21	8.84	7.93
MnO	0.10	0.15	0.19	0.78	0.17	0.19	0.20	0.20
MgO	2.10	1.83	8.67	5.31	3.57	3.79	3.47	3.48
CaO	3.20	4.48	8.34	5.35	8.63	8.58	5.86	8.78
Na_2O	2.88	1.19	3.95	4.82	3.84	3.45	5.10	3.43
K_2O	1.36	1.36	1.12	0.91	0.46	1.32	0.49	0.82
P_2O_5	0.07	0.07	0.23	0.37	0.27	0.22	0.27	0.23
Mg#	37.1	38.7	62.4	50.0	42.0	45.2	41.2	43.9
Minor Elements (ppm)								
Ni	7.4	9.4	136	9.4	17.8	19.8	11.6	18.3
Cr	15.5	15.0	338	10.2	28.8	35.2	12.8	43.1
Sc	25.4	19.0	33.0	30.4	28.3	26.8	23.1	24.8
V	91	98	258	252	264	227	185	205
Sr	239	101	516	494	578	515	644	634
Zr	137	84.1	55.8	126	81.8	101	130	101
Ba	377	344	367	437	262	509	706	752
Ga	16.6	12.0	15.4	19.8	19.6	17.6	13.6	18.7
Cu	22.4	57.9	53.0	41.2	40.7	21.8	44.6	44.7
Zn	77.5	61.4	75.8	101	82.7	69.3	78.2	81.0
Trace Elements (ppm)								
La	12.2	15.4	10.3	15.2	15.0	13.6	18.3	14.0
Ce	26.4	24.0	21.0	32.9	29.3	26.4	35.9	27.4
Pr	3.52	4.07	2.81	4.44	3.52	3.42	4.41	3.43
Nd	16.5	20.4	13.1	21.0	15.6	15.3	19.1	15.0
Sm	4.94	6.06	3.59	5.82	3.95	4.13	4.83	3.92
Eu	1.45	1.61	1.23	1.84	1.26	1.26	1.42	1.27
Gd	5.51	6.92	3.59	6.10	4.08	4.21	4.84	3.79
Tb	1.00	1.15	0.59	1.03	0.66	0.70	0.80	0.64
Dy	6.55	7.60	3.55	6.35	4.13	4.37	4.93	3.89
Ho	1.40	1.70	0.73	1.29	0.84	0.93	1.03	0.82
Er	4.00	4.97	1.98	3.56	2.31	2.51	2.83	2.28
Yb	3.94	4.77	1.73	3.04	2.14	2.34	2.69	2.20
Lu	0.63	0.81	0.27	0.48	0.34	0.38	0.43	0.35
Th	2.13	2.26	1.20	1.93	1.90	2.20	3.03	2.95
Nb	4.56	2.92	3.29	8.07	6.77	5.25	7.18	5.46
Y	38.3	49.4	19.2	35.9	22.1	24.6	27.8	21.6
Hf	3.91	2.44	1.65	3.69	2.30	2.82	3.62	2.93
Ta	0.32	0.20	0.21	0.48	0.35	0.34	0.46	0.36
U	0.77	0.86	0.56	0.56	0.62	0.88	1.22	1.19
Pb	5.25	3.65	2.47	2.50	2.37	2.66	4.28	3.53
Rb	33.6	35.2	18.1	19.2	8.8	20.1	9.8	10.4
Cs	1.11	0.83	3.02	0.52	2.08	0.24	3.68	0.31
Sr	239	101	516	494	578	515	644	634

***Pem. Volc is Pemberton Hills region volcanics**

Table 6. Whole-rock analyses of igneous rocks of the Bonanza arc (cont.)

Sample	04-023-A	04-035-A	04-024-A	04-013-B	04-022-A	92-269	04-042-B	04-040-A
UTM E	586798	602448	586834	601026	587139	-	665586	664372
UTM N	5609782	5608449	5609642	5609019	5609118	-	5530216	5530130
Lithology	Pem. Volc	Pem. Volc	Pem. Volc	Pem. Volc	Pem. Volc	Noot. Volc	Noot. Volc	Noot. Volc
Major Elements (wt.%)								
SiO_2	57.40	59.11	59.27	67.01	70.78	50.58	52.03	52.79
TiO_2	0.91	0.64	0.80	0.48	1.16	0.93	1.34	0.97
Al_2O_3	18.38	16.64	17.44	16.27	19.48	21.47	17.66	20.43
FeO*	7.84	6.59	7.21	3.94	6.12	8.27	8.92	9.70
MnO	0.28	0.16	0.18	0.10	0.00	0.17	0.16	0.15
MgO	4.40	3.82	5.28	1.28	0.46	4.51	6.86	4.72
CaO	4.52	8.01	3.81	3.51	0.05	8.35	9.91	5.37
Na_2O	4.31	3.27	3.60	4.78	0.11	3.54	2.72	3.50
K_2O	1.74	1.57	2.22	2.49	1.69	1.95	0.14	2.29
P_2O_5	0.21	0.20	0.18	0.12	0.15	0.24	0.24	0.08
Mg#	50.0	50.8	56.6	36.7	11.7	49.3	57.8	46.4
Minor Elements (ppm)								
Ni	12.5	54.9	13.9	9.2	25.1	36.0	113	39.8
Cr	14.3	165	15.7	10.5	42.8	53.6	165	85.3
Sc	26.3	23.4	23.2	11.8	23.7	30.7	30.0	35.4
V	209	171	185	106	251	269	193	209
Sr	308	454	239	438	179	646	272	427
Zr	147	100	118	130	164	47	122	53
Ba	537	575	764	1050	234	575	118	1090
Ga	20.1	15.3	16.2	15.4	26.0	20.5	19.1	19.3
Cu	67.0	31.7	57.0	25.9	175	80.9	61.0	69.0
Zn	77.6	62.2	62.0	56.9	33.4	72.5	76.3	88.9
Trace Elements (ppm)								
La	15.5	16.7	14.0	17.8	11.0	8.9	11.6	5.5
Ce	31.2	30.4	28.3	31.0	22.8	17.2	23.9	13.8
Pr	4.02	3.42	3.61	3.44	3.37	2.17	3.07	1.74
Nd	17.7	14.0	16.0	13.3	15.2	10.0	14.3	8.25
Sm	4.77	3.40	4.25	2.88	4.48	2.72	4.17	2.52
Eu	1.22	1.09	1.19	0.92	1.26	1.05	1.50	0.93
Gd	4.81	3.39	4.30	2.58	5.67	2.83	4.75	2.75
Tb	0.82	0.55	0.73	0.43	1.14	0.47	0.85	0.48
Dy	5.08	3.43	4.57	2.70	7.91	2.97	5.49	3.01
Ho	1.05	0.72	0.95	0.56	1.66	0.60	1.12	0.60
Er	2.91	2.04	2.70	1.63	4.33	1.68	3.10	1.64
Yb	2.76	2.01	2.50	1.77	3.75	1.50	2.77	1.54
Lu	0.44	0.33	0.41	0.30	0.59	0.24	0.44	0.24
Th	4.44	2.80	3.28	3.48	4.39	1.56	1.55	0.93
Nb	8.11	6.66	6.45	6.74	8.65	3.15	13.5	2.74
Y	29.0	19.8	25.9	16.0	39.0	16.1	30.0	13.4
Hf	4.22	2.78	3.37	3.39	4.79	1.37	3.31	1.53
Ta	0.55	0.42	0.43	0.49	0.57	0.21	0.88	0.18
U	1.83	1.09	1.30	1.38	1.74	0.72	0.45	0.22
Pb	3.16	3.69	3.55	6.31	30.5	1.91	1.14	2.28
Rb	20.5	25.0	31.1	46.5	36.9	44.4	1.41	48.2
Cs	0.16	0.31	0.71	0.96	0.41	0.42	0.15	1.12
Sr	308	454	239	438	179	646	272	427

***Noot. Volc is Nootka Sound region volcanic**

Table 6. Whole-rock analyses of igneous rocks of the Bonanza arc (cont.)

Sample	04-038-A	04-041-A	04-039-A	04-044-A	04-043-A	93-417	93-412B	92-270b
UTM E	667221	665275	664149	666285	666045	-	-	-
UTM N	5527071	5530184	5529999	5529439	5530439	-	-	-
Lithology	Noot. Volc	Noot. Volc	Noot. Volc	Noot. Volc	Noot. Volc	volcanic	volcanic	volcanic
Major Elements (wt.%)								
SiO_2	53.57	54.04	54.50	55.22	55.62	47.69	47.82	47.89
TiO_2	1.10	0.87	0.97	0.88	0.87	1.11	1.12	2.94
Al_2O_3	19.48	17.93	21.23	17.78	17.66	19.25	17.04	13.25
FeO*	8.96	9.71	9.08	10.53	8.91	9.67	9.90	16.33
MnO	0.15	0.14	0.16	0.23	0.12	0.23	0.20	0.26
MgO	4.77	6.89	3.16	4.41	5.94	4.16	4.95	4.21
CaO	6.14	7.49	5.83	6.25	6.87	7.97	11.65	10.03
Na_2O	4.02	2.27	3.24	3.44	2.49	4.36	3.22	2.92
K_2O	1.63	0.53	1.58	1.05	1.35	2.06	0.37	0.71
P_2O_5	0.18	0.13	0.25	0.20	0.17	0.43	0.26	0.53
Mg#	48.7	55.9	38.3	42.7	54.3	43.4	47.1	31.5
Minor Elements (ppm)								
Ni	14.1	59.7	27.7	33.4	37.9	2	13	27
Cr	15.2	146.9	46.3	41.4	88.0	18	44	55
Sc	27.4	39.4	28.5	27.9	32.8	23	40	26
V	205	269	158	201	242	271	359	404
Sr	376	313	479	427	380	491	603	278
Zr	97.3	57.4	75.9	66.2	76.8	89	86	234
Ba	568	206	387	458	416	696	241	296
Ga	18.9	15.6	20.0	14.3	16.1	19	16	22
Cu	113	57.2	74.5	34.1	49.8	55	55	87
Zn	77.1	80.2	98.9	69.3	75.8	105	89	137
Trace Elements (ppm)								
La	7.9	5.9	8.7	8.1	7.6	20.0	11.7	14.7
Ce	18.8	12.3	17.6	16.0	15.3	39.4	22.6	36.2
Pr	2.48	1.67	2.35	2.04	1.99	4.90	2.93	5.31
Nd	11.8	7.88	10.9	9.74	9.35	21.7	13.2	27.0
Sm	3.51	2.47	3.20	2.86	2.78	5.47	3.73	8.92
Eu	1.06	0.87	1.20	1.05	1.12	1.71	1.25	2.94
Gd	3.86	2.69	3.48	3.27	3.06	5.06	3.58	10.7
Tb	0.69	0.48	0.61	0.57	0.53	0.77	0.63	1.89
Dy	4.51	3.03	3.74	3.71	3.39	4.55	3.91	12.1
Ho	0.95	0.63	0.77	0.79	0.71	0.90	0.77	2.59
Er	2.83	1.72	2.15	2.26	2.03	2.41	2.25	7.07
Yb	2.78	1.66	2.03	2.13	1.96	2.13	1.93	6.50
Lu	0.46	0.27	0.32	0.35	0.32	0.34	0.32	1.03
Th	1.27	1.00	1.11	1.15	1.41	2.36	1.68	1.59
Nb	4.72	2.80	3.73	3.51	3.53	7.90	5.70	9.60
Y	24.8	16.2	20.3	21.6	19.2	24.0	21.0	66.0
Hf	2.62	1.62	2.11	1.84	2.10	2.01	1.68	6.14
Ta	0.33	0.19	0.24	0.22	0.24	0.36	0.29	0.57
U	0.49	0.47	0.28	0.49	0.70	0.67	0.56	0.93
Pb	1.10	2.51	2.64	6.28	2.61	0.00	0.00	4.00
Rb	31.5	11.7	53.8	19.0	27.6	41.0	5.0	13.0
Cs	1.23	1.23	5.76	0.49	0.94	0.00	0.00	0.25
Sr	376	313	479	427	380	491	603	278

*****volcanic is from DeBari et al., 1999 volcanics

Table 6. Whole-rock analyses of igneous rocks of the Bonanza arc (cont.)

Sample	93-409	93-411	93-419	92-158B	93-342	93-329	93-406	93-421
Lithology	volcanic	volcanic	volcanic	volcanic	volcanic	volcanic	volcanic	volcanic
Major Elements (wt.%)								
SiO_2	48.29	49.14	50.16	50.29	51.29	52.67	54.47	55.04
TiO_2	0.89	1.10	0.97	1.54	0.84	1.39	0.79	0.67
Al_2O_3	16.26	20.01	17.87	17.07	16.36	16.86	17.44	19.97
FeO*	8.66	8.48	8.64	11.81	9.26	9.86	7.11	6.24
MnO	0.19	0.23	0.18	0.21	0.19	0.23	0.17	0.16
MgO	7.63	4.55	3.45	5.19	5.08	5.05	5.07	2.80
CaO	9.84	7.33	9.38	7.54	10.35	5.79	6.26	4.74
Na_2O	2.79	3.90	2.83	4.33	3.49	5.50	3.99	4.37
K_2O	0.78	1.07	1.51	0.81	1.01	1.46	2.36	3.70
P_2O_5	0.15	0.33	0.27	0.22	0.28	0.27	0.20	0.27
Mg#	61.1	48.9	41.6	43.9	49.4	47.7	56.0	44.4
Minor Elements (ppm)								
Ni	40	4	-	18	29	31	25	-
Cr	152	20	17	14	66	74	35	4
Sc	30	21	26	31	38	34	21	12
V	269	308	303	314	282	230	205	127
Sr	448	561	468	247	636	270	415	584
Zr	60	89	85	105	63	128	94	173
Ba	486	353	351	176	319	681	694	1460
Ga	12	22	19	22	16	21	15	17
Cu	92	37	37	41	55	48	64	-
Zn	70	116	89	103	79	138	72	88
Trace Elements (ppm)								
La	5.90	16.0	15.4	5.73	6.87	9.11	10.9	29.7
Ce	13.0	31.5	29.5	14.1	14.3	20.4	21.9	52.4
Pr	1.90	3.93	3.60	2.19	2.15	2.82	2.83	5.57
Nd	9.11	18.0	15.5	11.9	10.5	13.8	12.6	21.8
Sm	2.59	4.77	4.10	4.03	3.38	4.30	3.31	4.44
Eu	0.97	1.53	1.34	1.52	1.13	1.65	1.08	1.45
Gd	2.96	4.68	4.06	4.83	3.57	5.16	3.55	4.17
Tb	0.49	0.76	0.65	0.88	0.58	0.96	0.60	0.66
Dy	3.11	4.58	3.91	5.67	3.63	6.00	3.81	3.86
Ho	0.65	0.95	0.81	1.18	0.77	1.22	0.81	0.79
Er	1.78	2.63	2.24	3.32	2.12	3.68	2.18	2.18
Yb	1.63	2.38	2.07	2.93	1.88	3.12	2.14	2.19
Lu	0.26	0.38	0.34	0.46	0.30	0.51	0.33	0.35
Th	0.85	2.52	2.27	0.49	1.56	1.07	2.30	6.44
Nb	3.20	6.40	7.20	6.10	2.30	4.70	3.90	16.5
Y	17	24	22	32	20	31	21	22
Hf	1.27	2.02	1.93	2.50	1.28	3.02	2.49	3.85
Ta	0.14	0.32	0.32	0.19	0.13	0.25	0.27	1.00
U	0.36	0.85	0.73	0.19	0.35	0.42	0.94	2.48
Pb	-	5	2	-	1	10	3	1
Rb	21.0	21.0	33.0	16.0	22.0	24.0	66.0	85.0
Cs	-	-	-	0.73	0.00	0.22	-	-
Sr	448	561	468	247	636	270	415	584

Table 6. Whole-rock analyses of igneous rocks of the Bonanza arc (cont.)

Sample	93-414A	93-416A	93-341	93-344	93-400	92-153A	92-145a	92-169-A
Lithology	volcanic	volcanic	volcanic	volcanic	volcanic	volcanic	volcanic	volcanic
Major Elements (wt.%)								
SiO_2	55.53	55.53	56.00	68.87	76.35	47.74	48.36	48.74
TiO_2	0.64	0.99	0.98	0.68	0.18	0.50	0.81	1.00
Al_2O_3	21.27	17.77	19.48	14.97	13.36	19.18	15.11	17.34
FeO*	5.79	8.65	7.58	1.96	1.24	10.64	10.37	11.13
MnO	0.19	0.18	0.16	0.06	0.04	0.19	0.20	0.17
MgO	3.13	4.02	3.51	0.58	0.37	8.08	11.36	8.02
CaO	7.15	8.62	4.41	3.79	0.68	10.72	10.75	7.10
Na_2O	3.40	2.88	5.06	6.47	3.67	1.87	1.74	3.67
K_2O	1.09	1.26	2.52	1.27	4.07	0.14	0.46	1.16
P_2O_5	0.45	0.27	0.30	0.14	0.04	0.04	0.14	0.17
Mg#	49.1	45.3	45.2	34.5	34.7	57.5	66.1	56.2
Minor Elements (ppm)								
Ni	1	1	6	10	7	192	190	78.0
Cr	6	20	8	1	5	85.6	557	51.1
Sc	14	30	24	9	2	-	-	0.0
V	91	237	217	27	7	196	261	283
Sr	575	347	420	594	217	110	169	277
Zr	128	106	106	264	126	18.5	47.6	56.4
Ba	550	506	658	602	2100	34	200	443
Ga	17	21	17	19	11	-	-	0.0
Cu	13	71	143	0.0	6	87.8	39.0	80.4
Zn	101	86	77	70	28	45.8	106	154
Trace Elements (ppm)								
La	21.3	15.3	15.1	19.3	25.4	0.79	4	3.9
Ce	42.2	30.9	31.0	48.4	39.9	1.8	9.4	9.0
Pr	5.11	3.80	3.95	6.85	3.80	0.35	1.43	1.37
Nd	21.5	16.5	18.1	31.4	12.9	2.16	7.24	7.13
Sm	5.13	4.70	4.94	8.75	2.07	1.20	2.47	2.44
Eu	1.65	1.37	1.49	2.59	0.47	0.58	0.94	0.97
Gd	4.50	4.60	4.92	9.07	2.05	2.01	2.85	2.84
Tb	0.76	0.84	0.85	1.58	0.32	0.46	0.54	0.55
Dy	4.60	5.19	5.50	10.2	2.01	3.31	3.59	3.54
Ho	0.97	1.07	1.12	2.18	0.43	0.77	0.73	0.74
Er	2.81	3.20	3.21	6.16	1.32	2.48	2.12	2.21
Yb	2.63	2.70	2.91	6.16	1.62	2.35	1.82	1.76
Lu	0.42	0.44	0.46	0.98	0.30	0.39	0.29	0.29
Th	2.97	2.17	1.53	4.86	8.78	0.08	0.46	0.27
Nb	10.3	7.70	6.20	12.3	11.3	0.52	1.97	2.28
Y	24.0	29.0	31.0	52.0	15.0	20.3	18.2	21.0
Hf	2.76	2.44	2.44	7.54	3.61	0.63	1.34	1.21
Ta	0.50	0.35	0.29	0.81	0.78	0.02	0.12	0.12
U	0.81	0.60	0.46	2.67	3.38	0.02	0.17	0.11
Pb	2	5	0	10	5	1.77	1.68	1.95
Rb	26	19	50	14	88	3.06	6.86	22.3
Cs	-	-	-	-	-	0.22	0.38	0.46
Sr	575	347	420	594	217	110	169	277

Table 6. Whole-rock analyses of igneous rocks of the Bonanza arc (cont.)

Sample	92-249a	92-170	92-252	92-177	92-272	92-189	92-244	92-256
Lithology	volcanic	volcanic	volcanic	volcanic	volcanic	volcanic	volcanic	volcanic
Major Elements (wt.%)								
SiO_2	48.84	49.23	49.68	52.42	52.95	53.74	54.04	54.21
TiO_2	0.98	2.20	1.95	1.01	0.98	1.73	1.86	1.64
Al_2O_3	17.25	15.67	18.19	18.49	19.08	14.93	14.69	17.48
FeO*	9.89	12.42	11.20	7.99	8.97	12.01	12.75	9.68
MnO	0.25	0.21	0.18	0.32	0.16	0.22	0.24	0.13
MgO	7.75	6.46	4.74	5.96	4.09	4.46	4.27	3.71
CaO	11.39	7.42	8.53	7.49	8.36	6.74	6.11	4.92
Na_2O	1.83	3.69	2.63	3.58	2.81	3.80	3.45	6.65
K_2O	1.13	1.37	1.42	2.34	1.62	0.73	0.95	0.27
P_2O_5	0.15	0.37	0.33	0.20	0.22	0.27	0.32	0.47
Mg#	58.3	48.1	43.0	57.1	44.8	39.8	37.4	40.6
Minor Elements (ppm)								
Ni	81.6	61.4	38.8	54.8	17.2	29.5	14.6	2.8
Cr	211	62.3	55.6	154	33.8	18.1	6.2	6.7
Sc	-	-	-	-	-	-	-	-
V	306	288	296	241	239	437	441	216
Sr	265	229	274	393	395	229	244	113
Zr	42.9	214	163	87.6	64.5	138	127	159
Ba	215	300	270	1590	453	163	364	74.0
Ga	-	-	-	-	-	-	-	-
Cu	54.3	87.2	168	62.5	10.5	119	18.4	11.1
Zn	108	135	115	141	78.2	103	130	81.9
Trace Elements (ppm)								
La	4.43	11.3	10.6	7.61	8.06	8.50	9.81	8.79
Ce	9.76	26.8	24.4	16.4	15.5	20.9	22.0	21.6
Pr	1.41	3.91	3.50	2.24	2.11	3.07	3.19	3.17
Nd	7.10	20.5	17.5	10.7	9.62	15.6	16.3	16.8
Sm	2.35	6.87	5.42	3.11	2.78	5.39	5.35	5.61
Eu	0.97	2.14	1.82	1.13	1.00	1.66	1.78	1.75
Gd	2.79	7.78	6.08	3.51	3.00	6.04	6.12	6.39
Tb	0.53	1.47	1.16	0.65	0.57	1.17	1.17	1.19
Dy	3.32	9.44	7.25	4.19	3.53	7.54	7.44	7.93
Ho	0.69	1.99	1.54	0.86	0.75	1.61	1.57	1.70
Er	2.04	5.81	4.58	2.47	2.12	4.70	4.82	5.16
Yb	1.73	5.03	3.87	2.11	1.87	4.06	4.08	4.50
Lu	0.27	0.81	0.60	0.34	0.31	0.63	0.64	0.73
Th	0.44	1.10	1.15	0.68	1.19	0.79	1.09	1.62
Nb	2.42	4.97	5.00	2.97	2.99	2.95	3.71	4.74
Y	18.1	54.7	40.9	22.9	20.2	42.6	42.3	44.9
Hf	1.23	4.85	3.63	2.07	1.59	3.30	3.33	3.88
Ta	0.13	0.36	0.36	0.18	0.24	0.19	0.24	0.32
U	0.18	0.55	0.41	0.27	0.47	0.33	0.50	0.63
Pb	1.78	3.39	3.85	35.3	2.96	1.80	2.60	2.22
Rb	31.6	34.6	23.4	63.9	34.7	13.7	24.1	6.04
Cs	0.77	0.36	0.55	1.78	0.92	0.62	0.35	0.33
Sr	265	229	274	393	395	229	244	113

Table 6. Whole-rock analyses of igneous rocks of the Bonanza arc (cont.)

Sample	92-265b	92-187	92-258	92-185	92-259	92-241	92-230a	92-270a
Lithology	volcanic	volcanic	volcanic	volcanic	volcanic	volcanic	volcanic	volcanic
Major Elements (wt.%)								
SiO_2	54.33	55.04	55.77	56.56	56.99	57.06	57.10	57.35
TiO_2	1.03	1.30	1.46	1.99	0.87	1.40	1.22	0.88
Al_2O_3	21.24	16.30	16.48	15.11	17.45	15.67	17.01	17.75
FeO*	7.18	8.70	9.73	9.77	6.94	9.09	8.66	7.27
MnO	0.18	0.26	0.18	0.33	0.11	0.23	0.15	0.15
MgO	3.98	5.05	4.04	2.76	4.44	3.05	3.28	3.93
CaO	3.43	4.38	4.72	4.91	6.36	4.60	7.03	7.04
Na_2O	6.60	4.80	5.61	4.10	3.40	5.40	3.50	2.62
K_2O	0.84	2.87	1.53	2.93	2.72	2.19	1.13	2.03
P_2O_5	0.26	0.19	0.29	0.58	0.21	0.33	0.28	0.22
Mg#	49.7	50.8	42.5	33.4	53.3	37.4	40.3	49.1
Minor Elements (ppm)								
Ni	28.5	48.2	18.4	3.0	29.8	7.1	4.7	21.2
Cr	65.6	64.1	21.8	11.5	89.0	7.4	9.9	59.1
Sc	-	-	-	-	-	-	-	-
V	197	210	296	149	191	263	257	186
Sr	447	136	272	82.9	284	172	414	393
Zr	129	237	139	188	104	182	84.7	84.8
Ba	251	714	393	866	514	507	451	550
Ga	-	-	-	-	-	-	-	-
Cu	39.7	87.0	13.3	5.0	8.9	47.7	31.6	55.9
Zn	102	200	118	219	61.9	121	91.1	72.3
Trace Elements (ppm)								
La	8.71	11.0	9.04	12.9	16.2	13.7	8.98	10.3
Ce	19.7	26.7	20.4	31.9	30.7	28.9	19.3	19.1
Pr	2.79	3.88	2.90	4.76	3.80	3.90	2.63	2.46
Nd	13.3	19.8	14.4	25.4	16.9	18.6	13.0	11.2
Sm	3.82	6.25	4.67	8.27	4.36	5.40	3.78	3.00
Eu	1.24	1.66	1.42	3.10	1.28	1.40	1.33	0.99
Gd	3.68	6.97	5.26	9.6	4.40	5.85	3.83	3.14
Tb	0.68	1.34	1.04	1.80	0.72	1.08	0.69	0.56
Dy	4.15	8.78	6.59	11.3	4.11	7.02	4.07	3.55
Ho	0.83	1.86	1.40	2.33	0.83	1.47	0.83	0.74
Er	2.35	5.71	4.29	6.80	2.36	4.43	2.47	2.13
Yb	2.08	5.05	3.67	5.71	2.00	3.80	2.14	1.95
Lu	0.34	0.78	0.58	0.89	0.32	0.60	0.34	0.33
Th	2.86	1.51	1.19	1.53	2.34	1.72	1.03	1.86
Nb	5.42	4.55	4.23	5.45	4.14	6.32	3.81	3.77
Y	22.4	50.9	38.6	63.0	22.6	40.7	22.9	20.6
Hf	2.98	5.66	3.20	4.57	2.68	4.14	2.14	1.90
Ta	0.41	0.31	0.23	0.31	0.32	0.39	0.20	0.33
U	1.08	0.60	0.47	0.58	0.92	0.66	0.40	0.69
Pb	1.55	24.2	2.60	1.83	2.14	3.18	1.68	2.33
Rb	22.4	59.6	29.0	59.2	58.8	53.1	28.8	47.9
Cs	0.48	1.01	0.39	0.44	0.76	0.32	0.87	0.73
Sr	447	136	272	83	284	172	414	393

Table 6. Whole-rock analyses of igneous rocks of the Bonanza arc (cont.)

Sample	92-261	92-235	91-079A	93-392A	93-350	91-082	91-135D	93-348B
Lithology	volcanic	volcanic	WCC	WCC	WCC	WCC	WCC	WCC
Major Elements (wt.%)								
SiO_2	59.44	62.94	52.54	54.97	55.98	59.88	61.27	63.27
TiO_2	0.90	1.23	0.73	0.94	0.93	0.78	0.85	0.72
Al_2O_3	16.34	15.29	16.04	20.15	19.27	18.06	16.15	16.63
FeO*	7.46	6.77	9.22	7.21	7.36	6.31	6.39	5.49
MnO	0.23	0.21	0.16	0.17	0.15	0.13	0.15	0.17
MgO	3.06	2.00	7.62	2.79	4.11	2.40	3.05	2.51
CaO	3.71	2.78	9.27	8.51	8.07	6.18	5.28	5.52
Na_2O	5.56	5.11	2.15	3.79	3.81	4.30	4.27	4.10
K_2O	2.63	2.79	1.36	1.19	0.91	1.34	1.61	1.94
P_2O_5	0.20	0.43	0.11	0.49	0.30	0.26	0.22	0.18
Mg#	42.2	34.5	59.6	40.8	49.9	40.4	46.0	44.9
Minor Elements (ppm)								
Ni	10.9	9.4	64.5	0.0	16.0	10.0	11.2	8.0
Cr	13.8	7.8	181	8.0	42.0	8.8	11.2	24.0
Sc	-	-	-	-	-	-	-	-
V	207	58.3	264	133	204	129	179	109
Sr	91.9	163	376	579	484	487	363	359
Zr	202	313	82.2	80.0	121	187	157	162
Ba	510	660	545	483	449	484	278	846
Ga	-	-	-	-	-	-	-	-
Cu	49.0	7.4	46.8	24.0	71.0	28.2	14.0	34.0
Zn	126	94.4	86.0	81.0	72.0	62.5	124.8	78.0
Trace Elements (ppm)								
La	12.3	18.4	13.5	12.3	10.7	16.6	22.0	22.2
Ce	27.5	41.7	27.6	26.3	22.8	33.5	47.7	44.5
Pr	3.64	5.82	3.46	3.64	3.10	4.29	6.35	5.25
Nd	16.8	28.4	15.2	18.2	14.8	19.2	30.1	22.2
Sm	5.08	8.60	4.04	5.11	4.11	5.17	8.50	5.48
Eu	1.34	2.53	1.15	1.66	1.31	1.46	1.31	1.44
Gd	5.52	9.46	3.87	5.23	4.17	5.02	8.59	4.99
Tb	1.03	1.79	0.73	0.85	0.76	0.91	1.59	0.92
Dy	6.75	11.4	4.56	5.44	4.63	5.86	10.2	6.16
Ho	1.44	2.40	0.97	1.08	0.96	1.20	2.14	1.27
Er	4.42	7.01	2.71	3.17	2.77	3.57	6.22	3.83
Yb	4.03	6.13	2.44	2.58	2.40	3.26	5.45	3.72
Lu	0.65	0.98	0.38	0.41	0.37	0.53	0.85	0.62
Th	2.04	2.70	2.80	1.37	0.54	2.23	1.08	3.64
Nb	4.74	8.43	3.53	4.60	5.50	7.21	12.94	7.80
Y	40.0	67.0	14.2	24.0	25.0	35.0	59.4	33.0
Hf	4.75	6.97	4.15	2.01	2.45	4.21	4.14	5.95
Ta	0.33	0.51	0.91	0.21	0.26	0.81	0.86	0.56
U	0.81	1.01	0.97	0.46	0.24	0.91	0.40	1.41
Pb	1.6	2.8	1.7	-	-	1.5	5.6	5.0
Rb	49.8	62.7	39.0	25.0	15.0	24.2	41.7	34.0
Cs	0.45	0.45	-	-	-	-	-	-
Sr	92	163	376	579	484	487	363	359

*WCC is from DeBari et al., 1999 Westcoast Crystalline Complex

Table 6. Whole-rock analyses of igneous rocks of the Bonanza arc (cont.)

Sample	91-092b	91-083	93-346	92-158a	92-276	92-274	91-003B	93-388
Lithology	WCC	WCC	WCC	Is. Intrus	Is. Intrus	Is. Intrus	Is. Intrus	Is. Intrus
Major Elements (wt.%)								
SiO_2	65.49	70.92	71.02	52.33	60.14	66.00	66.44	69.13
TiO_2	0.68	0.39	0.52	2.59	0.95	0.50	0.45	0.36
Al_2O_3	16.18	14.81	14.96	14.09	16.02	15.88	15.99	15.68
FeO*	4.92	2.98	2.82	12.60	6.65	4.60	4.56	3.08
MnO	0.10	0.08	0.07	0.23	0.13	0.10	0.12	0.09
MgO	1.73	0.91	0.65	3.98	2.64	1.96	1.67	1.29
CaO	4.55	3.16	2.15	6.61	6.02	4.99	4.75	3.46
Na_2O	3.69	4.00	4.82	4.29	3.38	3.57	3.52	4.67
K_2O	1.97	2.43	3.60	0.08	2.52	2.10	1.94	1.95
P_2O_5	0.18	0.11	0.11	0.65	0.24	0.11	0.16	0.10
Mg#	38.5	35.2	29.1	36.0	41.4	43.2	39.5	42.7
Minor Elements (ppm)								
Ni	2.5	3.2	8.0	3.0	11.0	5.0	2.5	5.0
Cr	4.5	3.0	4.0	7.0	24.0	15.0	3.0	5.0
Sc	-	-	-	-	-	-	-	-
V	96.8	35.2	29.0	321.0	137.0	98.0	78.6	53.0
Sr	363	235	205	158	330	289	374	365
Zr	174	164	240	143	209	99.0	94.9	115
Ba	545	875	792	20	837	636	693	982
Ga	-	-	-	-	-	-	-	-
Cu	10.7	4.2	4.0	17.0	62.0	22.0	7.8	8.0
Zn	56.5	40.1	28.0	87.0	64.0	42.0	56.9	39.0
Trace Elements (ppm)								
La	13.5	14.9	13.1	10.7	23.5	12.2	16.7	15.2
Ce	27.6	26.9	29.8	26.0	46.1	21.4	30.5	25.7
Pr	3.46	2.94	3.99	3.91	5.83	2.33	3.42	2.68
Nd	15.2	11.9	17.6	20.7	25.6	9.5	13.4	10.1
Sm	4.04	2.91	4.63	6.97	6.47	2.27	3.24	1.93
Eu	1.15	0.85	1.74	2.49	1.41	0.75	0.94	0.66
Gd	3.87	2.67	4.90	8.30	6.19	2.12	3.07	1.79
Tb	0.73	0.49	0.91	1.43	1.09	0.37	0.53	0.30
Dy	4.56	3.09	5.89	9.27	6.78	2.47	3.34	1.80
Ho	0.97	0.67	1.24	1.94	1.38	0.52	0.71	0.38
Er	2.71	2.02	3.91	5.26	3.93	1.45	2.14	1.18
Yb	2.44	2.05	3.89	4.63	3.60	1.61	2.10	1.30
Lu	0.38	0.34	0.64	0.72	0.58	0.28	0.36	0.23
Th	2.80	3.67	2.32	1.03	5.54	4.30	3.71	2.70
Nb	6.76	6.01	11.1	8.90	15.8	9.60	5.95	5.80
Y	27.9	20.3	36.0	52.0	39.0	15.0	21.9	12.0
Hf	4.15	3.84	3.70	3.61	5.60	2.78	2.70	2.48
Ta	0.91	0.97	0.50	0.36	0.75	0.56	0.61	0.29
U	0.97	1.20	0.87	0.39	1.98	1.39	1.01	0.83
Pb	2.37	3.39	2.0	0.00	4.0	5.0	4.81	3.0
Rb	45.0	50.2	81.0	3.0	61.0	60.0	33.7	33.0
Cs	0.0	0.0	0.0	0.1	1.2	1.3	0.3	0.0
Sr	363	235	205	158	330	289	374	365

*Is. Intrus is from DeBari et al., 1999 Island Intrusions

***Table 7**. Least-squares fractional crystallization solutions step 1*

Sample		Proportion		SiO_2	Al_2O_3	TiO_2	FeO*	MnO	CaO	MgO	Na_2O	Mg#
Parent												
04-005-A				48.45	17.97	1.18	11.27	0.14	11.05	6.49	2.27	50.7
Daughter												
04-007-A		53.29%	crystallized	52.58	18.10	0.95	9.21	0.19	8.60	4.40	2.92	46.0
Fractionated minerals												
005CPX2	**cpx**	17.18%		51.35	2.91	0.51	8.55	0.31	21.11	15.04	0.30	75.8
005ox3	**sp**	9.40%		0.16	1.79	15.63	73.93	0.08	0.00	0.00	0.00	0.0
005pl2	**plag**	54.82%		49.81	29.90	0.00	0.95	0.00	14.79	0.00	3.50	0.0
Ol	**ol**	13.45%		38.14	0.00	0.02	24.98	0.52	0.03	36.42	0.00	72.2
005amph2	**Amph**	5.15%		47.86	6.63	0.83	8.03	0.18	22.45	13.57	0.26	75.1
	Calculated composition			48.45	17.98	1.04	11.30	0.14	11.05	6.47	2.09	50.5
	Parent			48.45	17.97	1.18	11.27	0.14	11.05	6.49	2.27	50.7
	Difference			0.01	0.01	-0.14	0.03	0.00	0.00	-0.03	-0.18	
	% of oxide (daughter)			0.01	0.06	-14.90	0.32	0.00	-0.04	-0.61	-6.08	
	$\sum R^2$			0.0535						**% crystallized**		53.29
	Kd (Fe/Mg) cpx/liq (parent)			0.33						**% melt**		46.71

*Total Fe as FeO, cpx = Pyroxene, plag = Plagioclase, sp = Spinel, ol = Olivine, Amph = Amphibole

***Table 8**. Least-squares fractional crystallization solutions step 2*

Sample		Proportion		SiO_2	Al_2O_3	TiO_2	FeO*	MnO	CaO	MgO	Na_2O	Mg#
Parent												
04-007-A				52.58	18.10	0.95	9.21	0.19	8.60	4.40	2.92	46.0
Daughter												
04-003-E		79.06%	crystallized	59.90	16.90	0.73	8.86	0.17	5.98	3.42	0.20	40.8
Fractionated minerals												
007CPX2	**cpx**	-12.14%		52.10	2.76	0.62	9.18	0.29	21.14	14.52	0.35	73.8
007ox3	**sp**	5.00%		0.13	3.91	15.46	71.59	0.51	0.00	0.01	0.00	0.0
007pl1	**plag**	55.27%		53.83	29.24	0.00	0.64	0.00	11.72	0.00	4.15	0.0
082amph2	**Amph**	51.87%		48.38	5.84	0.91	13.89	0.70	11.65	13.89	0.93	64.1
	Calculated composition			54.40	18.60	0.92	9.47	0.33	9.46	4.59	3.85	46.4
	Parent			52.58	18.10	0.95	9.21	0.19	8.60	4.40	2.92	46.0
	Difference			0.00	-0.02	-0.16	0.04	-0.14	0.01	-0.02	0.10	
	% of oxide (daughter)			0.00	-0.10	-16.54	0.54	-47.49	0.22	-1.39	3.26	
	$\sum R^2$			0.05860						**% crystallized**		79.06
	Kd (Fe/Mg) cpx/liq (parent)			0.30						**% melt**		20.94

*Total Fe as FeO, cpx = Pyroxene, plag = Plagioclase, sp = Spinel, Amph = Amphibole

Table 9. *Least-squares fractional crystallization solutions step 2, try 2.*

Sample		Proportion		SiO_2	Al_2O_3	TiO_2	FeO*	MnO	CaO	MgO	Na_2O	Mg#
Parent												
04-007-A				52.58	18.10	0.95	9.21	0.19	8.60	4.40	2.92	46.0
Daughter												
04-004-A		79.45%	crystallized	65.41	15.59	0.97	6.78	0.30	4.65	1.43	3.12	27.3
Fractionated minerals												
007CPX2	**cpx**	9.16%		49.70	5.44	0.87	9.26	0.26	21.27	13.43	0.42	72.1
007ox3	**sp**	5.33%		0.16	1.79	15.63	73.93	0.08	0.00	0.00	0.00	0.0
007pl1	**plag**	62.09%		49.81	29.90	0.00	0.95	0.00	14.79	0.00	3.50	0.0
933-88amph2	**Amph**	23.42%		51.80	2.13	0.36	21.19	1.71	2.62	16.53	0.39	58.2
	Calculated composition			52.57	18.09	0.96	9.21	-0.03	8.59	4.43	3.10	46.2
	Parent			52.58	18.10	0.95	9.21	0.19	8.60	4.40	2.92	46.0
	Difference			0.00	-0.01	0.00	0.00	-0.22	-0.01	0.04	0.18	
	% of oxide (daughter)			-0.01	-0.07	0.49	0.02	-73.17	-0.26	2.47	5.62	
	$\sum R^2$			0.08130						**% crystallized**		79.45
	Kd (Fe/Mg) cpx/liq (parent)			0.30						**% melt**		20.55

*Total Fe as FeO, cpx = Pyroxene, plag = Plagioclase, sp = Spinel, Amph = Amphibole

***Table 10**. Least-squares fractional crystallization solutions step 3*

Sample		Proportion		SiO_2	Al_2O_3	TiO_2	FeO*	MnO	CaO	MgO	Na_2O	Mg#
Parent												
04-003-E				59.90	16.90	0.73	8.86	0.17	5.98	3.42	0.20	40.8
Daughter												
04-004-A		43.28%	crystallized	65.41	15.59	0.97	6.78	0.30	4.65	1.43	3.12	27.3
Fractionated minerals												
933-88cpx6	**cpx**	36.71%		52.78	1.62	0.23	22.50	2.64	1.49	15.69	0.35	55.4
005ox6	**sp**	3.47%		0.14	5.68	11.66	72.81	0.11	0.00	0.04	0.00	0.1
007pl1	**plag**	57.03%		53.83	29.24	0.00	0.64	0.00	11.72	0.00	4.15	0.0
005amph1	**Amph**	2.80%		49.70	5.44	0.87	9.26	0.26	21.27	13.43	0.00	72.1
	Calculated composition			59.97	17.19	0.75	8.83	-0.26	5.86	3.33	-2.48	27.4
	Parent			59.90	16.90	0.73	8.86	0.17	5.98	3.42	0.20	27.9
	Difference			0.07	0.29	0.02	-0.03	-0.43	-0.12	-0.09	-2.68	
	% of oxide (daughter)			0.11	1.89	1.98	-0.38	-143.61	-2.51	-6.53	-85.81	
	$\sum R^2$			7.47000						**% crystallized**		43.28
	Kd (Fe/Mg) cpx/liq (parent)			0.56						**% melt**		56.72

*Total Fe as FeO, cpx = Pyroxene, plag = Plagioclase, sp = Spinel, Amph = Amphibole

APPENDIX

Field Work

During the summer of 2004, 106 samples from 49 sample locations were collected for petrography and major, minor and trace element geochemistry. Field localities on Vancouver Island were restricted to the volcanic sequence of the Bonanza Arc in the south (Alberni region), the central (Nootka Sound region), and the north (Pemberton Hills) along the strike of the Bonanza arc.

An attempt to sample, describe, and measure stratigraphic sections at 3 localities on Vancouver Island was made, but stratigraphic reconstruction was hindered due to poor exposure as a result of thick vegetation. Exposures were best in road-cuts along logging roads, rock quarries, in higher elevation areas, and along stream beds. In light of these difficulties, stratigraphic reconstruction is not as detailed as originally planned, but in each locality, samples from the basal units were collected so stratigraphic control was still obtainable.

Alberni Region

Samples collected from the southern portion of Vancouver Island were restricted to the areas near Red Bed Creek and southwest of Sarita Lake. Access was gained following South Shore Rd west out of the town of Lake Cowichan, to Tuck Main Logging Rd. Exposure was best in stream beds with over 325 meters of continuous exposure along Red Bed Creek where the conformable contact of the Red Bed Creek facies of the Jurassic Bonanza formation was visible with the Triassic, fossiliferous reefoid limestones of the Sutton formation. The Red Bed Creek facies are moderately

dipping (~142/52), medium bedded, fine-grained, maroon to green ash fall and lapilli tuffs (Figure 34). Bedding is massive with minor cross-stratification and laminations locally, cross-cut by aphanitic and phenocryst-rich basalt and basaltic andesite dykes.

South of Red Bed Creek, intermittent exposures in the form of road cuts along Tuck Main logging road permitted sampling of the over-lying Klanawa facies of the Bonanza volcanics. The Klanawa facies are dominated by plagioclase-phyric, medium-bedded, medium to light gray, basaltic andesites to andesites. Thin beds of lapilli and crystal-lithic tuffs are intercalated within the Klanawa facies. Rare, sub-angular and blocky pyroclasts occur and can be up to 20 cm in diameter. Additional sampling of the Klanawa facies was done south-southwest of Sarita Lake and the rocks there exhibit similar characteristic as described above.

Nootka Sound Region

Sample localities in the Nootka Sound region were restricted to intermittent exposures along logging roads south west of the town of Tahsis and north of the town of Zeballos. South of Tahsis, along the Extravagant Main Line logging road provided the best exposure of the Bonanza formation with additional samples collected from the Barr Creek Main Line logging road further to the west and north. Additional samples collected just north of Zeballos, along Zeballos Main Line Logging road, in combination with samples collected by DeBari, S.M. in 1993 supplemented the collection done in the Nootka Sound region.

Typical lithology of the Bonanza volcanics in this region are dominated by medium bedded, greenish-gray to medium gray, basaltic to andesitic lithic tuff, lapilli tuff, tuff breccia, and volcanic breccia. Lithic clasts range up to 20 cm, are greenish gray,

plagioclase-phyric, sub-angular to angular in shape and display alteration rinds. Rare, dark gray to black, aphanitic basalt flows (04-045) and plagioclase and pyroxene-phyric light to medium gray andesite (04-046) flows were intercalated within the volcaniclastic sequence.

Pemberton Hills

North of the Holberg Inlet, west of the town of Coal Harbor lies the area of the Pemberton hills. Relying heavily on the mapping and stratigraphic construction done by Nixon et al. (1993), samples from 4 distinct, local stratigraphic units of the Bonanza formation were collected. Exposure was best along road-cuts, quarries, minor drainages, and in the less-vegetated, higher elevations areas of the Pemberton hills. Lithology of the Bonanza formation varied widely in this region including Mafic to intermediate flows, felsic flows and tuffs, mafic to intermediate tuff and minor associated flows, and mafic to intermediate tuffs and associated siltstones (Nixon, et al., 1993).

Access to the Pemberton Hills was gained by heading west from the town of Coal Harbor along Wanokano Main Line logging road and subsequent secondary logging roads. Samples were also collected from the northern shore of the Holberg Inlet.

Previous investigations of Vancouver Island and the Bonanza Group Volcanics

Over the last century there have been numerous geologic investigations of Vancouver Island and the Bonanza Group Volcanics. The previous workers mapped out the location of the Bonanza Group Volcanics and provided preliminary stratigraphic insights. Gunning (1930, 1932) was the first to distinguish the strata of the Bonanza Group from those of the Sicker Group and the Karmutsen Formation. Subsequent mapping by Hordley (1953) and Jeletzky (1954) provided more detail and a better understanding of the general geology of Vancouver Island and the stratigraphy of the Bonanza Group volcanics. Muller and Carson (1969) and Muller et al. (1981) measured and described the stratigraphy of the Bonanza Volcanics as well as the associated plutonic rocks of the Westcoast Crystalline Complex and the Island Intrusions in the Nootka Sound area in central Vancouver Island. The LITHOPROBE 1 project and regional mapping at 1:50,000-scale was initiated by the Geological Survey of Canada in the late 1980's through the late 1990's and brought a wealth of new information concerning the geology of Vancouver Island (Yorath et al., 1999). Massey and Friday (1989) and Massey (1992) mapped in detail the geology of the Alberni and Nanaimo Lakes area. In northern Vancouver Island Nixon et al. (1994) and Nixon et al. (1995) mapped in the Quatsino – Port McNeill areas. Detailed work by Nixon et al. (1994) in the Pemberton Hills on the Bonanza Group provided excellent stratigraphic insights. Yorath et al. (1999) mapped in Southern Vancouver Island as part of the LITHOPROBE 1 project and provided measured stratigraphy of the Bonanza volcanics as well as facies divisions. Recent work by DeBari et al. (1999) provided new insights on the

geochemistry of the plutonic and volcanic rocks of the Bonanza arc as well as new radiometric age constraints

Appendix Figures

Figure 34. Typical exposure and bedding in the Red Bed Creek Facies in the Alberni region of Vancouver Island, Canada. Geologist in lower-left is ~2m tall for scale.

Appendix Tables

Table 11.

Basalt and Basaltic Andesite Kd's from Rollinson

	cpx	sp	ol	plag	amph
Ba	0.026	0.001	0.001	0.230	0.042
La	0.056	0.010	0.007	0.19	0.25
Ce	0.092	0.010	0.006	0.111	0.32
Pr	0.277	0.010	0.006	0.17	0.35
Nd	0.23	0.010	0.006	0.09	1.3395
Sm	0.445	0.010	0.007	0.072	1.8035
Eu	0.474	0.010	0.007	0.443	1.557
Gd	0.556	0.010	0.010	0.071	2.0165
Tb	0.57	0.010	0.010	0.026	1.29
Dy	0.582	0.010	0.013	0.063	2.0235
Ho	0.440	0.010	0.011	0.011	1.1
Er	0.583	0.010	0.026	0.057	1.74
Yb	0.542	0.010	0.049	0.056	1.642
Lu	0.506	0.010	0.045	0.053	1.562
Ni	4.4	3.000	13.930	0.000	16
Sr	0.06	0.010	0.014	1.83	1.02
Rb	0.031	0.010	0.010	0.071	1.9
Zr	0.1	0.010	0.005	0.0480	1.2

Andesite Kd's from Rollinson

	cpx	sp	ol	plag	amph
Ba	0.040	0.001	0.001	0.151	0.730
La	0.047	0.010	0.007	0.190	0.500
Ce	0.250	0.010	0.006	0.111	0.230
Pr	0.450	0.010	0.006	0.100	0.100
Nd	0.645	0.010	0.006	0.090	0.600
Sm	0.750	0.010	0.007	0.072	1.200
Eu	0.800	0.010	0.007	0.443	0.360
Gd	0.950	0.010	0.010	0.071	0.490
Tb	0.950	0.010	0.010	0.066	0.700
Dy	0.960	0.010	0.010	0.063	0.075
Ho	0.970	0.010	0.011	0.060	1.500
Er	0.980	0.010	0.011	0.057	0.090
Yb	0.900	0.010	0.014	0.056	0.980
Lu	0.840	0.010	0.016	0.053	0.820
Ni	3.483	3.000	13.930	0.000	7.200
Sr	0.100	0.010	0.010	1.360	0.190
Rb	0.001	0.010	0.001	0.0294	0.300
Zr	0.13	0.010	0.005	0.0094	0.001

Arth (1976); Fujikami et al.(1984); Irving and Frey (1978); Green and Pearson (1985a); Green et al., (1989); Pearce and Norry (1979)

cpx = Pyroxene, plag = Plagioclase, sp = Spinel, ol = Olivine, amph = Amphibole